Construction and Building Materials 286 (2021) 122815

Contents lists available at ScienceDirect

Construction and Building Materials

journal homepage: www.elsevier.com/locate/conbuildmat

Progress in silica aerogel-containing materials for buildings' thermal insulation

Alyne Lamy-Mendes [a], Ana Dora Rodrigues Pontinha [a], Patrícia Alves [a], Paulo Santos [b], Luisa Durães [a,*]

[a] University of Coimbra, CIEPQPF, Department of Chemical Engineering, Rua Silvio Lima, 3030-790 Coimbra, Portugal
[b] University of Coimbra, ISISE, Department of Civil Engineering, Rua Luís Reis Santos, 3030-788 Coimbra, Portugal

HIGHLIGHTS

- Recent years progress on silica aerogel-containing building materials.
- Silica aerogel benefit as lightweight, thermal insulating and translucent material.
- Thermal insulation panels and blankets based on silica aerogels.
- Silica aerogels incorporation in cement, mortars and concrete composites.
- Allying translucence and insulation features for glazing & solar collector systems.

GRAPHICAL ABSTRACT

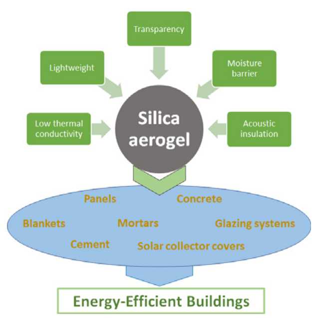

ARTICLE INFO

Article history:
Received 22 November 2020
Received in revised form 30 January 2021
Accepted 19 February 2021
Available online 17 March 2021

Keywords:
Silica aerogels
Composites
Buildings
Thermal insulation
Glazing

ABSTRACT

Silica aerogels hold remarkable properties, particularly their translucence/transparency and extremely low thermal conductivity and density, for buildings thermal insulation purpose. Incorporated in composites or framing systems, they reduce the overall weight of the building envelope while increasing its thermal resistance, being especially valuable for energy-efficient retrofitting solutions, spanning from covering façades to window panes. This review presents the production process of silica aerogels in brief, their relevant properties regarding building's needs, and a full survey of last years' scientific achievements on silica aerogel-containing materials for buildings, such as panels, blankets, cement, mortars, concrete, glazing systems, solar collector covers, among others.

1. Introduction

In recent years, the overall energy consumption worldwide has changed the construction of buildings [1]. In 2016, the global building sector was responsible for consuming around 30% of total final energy use and contributed with 28% of global energy-related to CO_2 emissions [2]. The thermal performance of building's envelope (floor, roof and walls) is a prime factor, since it influences the amount of energy required for indoor thermal comfort. A common passive strategy for the reduction in energy consumption is the incorporation of thermal insulation materials in walls and roof. This is recognized as one of the most effective ways to ensure energy savings, being capable of mitigating outward heat losses. Superinsulating materials are still the main tool for improving the energy behaviour of a building, even after thirty years of the introduction of thermal insulation in most countries [3–5].

* Corresponding author.
E-mail addresses: alyne@eq.uc.pt (A. Lamy-Mendes), dpontinha@eq.uc.pt (A.D.R. Pontinha), palves@eq.uc.pt (P. Alves), pfsantos@dec.uc.pt (P. Santos), luisa@eq.uc.pt (L. Durães).

https://doi.org/10.1016/j.conbuildmat.2021.122815
0950-0618/

Nearly zero energy buildings, as well as Passivhaus requirements, are not achievable without highly insulated building envelopes [6]. New thermal insulation solutions are needed to fulfil the thermal behaviour and energy performance requirements [7]. Besides very low thermal conductivity, other properties are crucial to assess the suitability of an insulating material for this purpose. Sought properties may include site adaptability, mechanical strength, opacity or transparency, durability and resilience to weathering, fire protection, low environmental and human health hazard, and low cost. Moreover, in order to ensure building's sustainability [8], the new insulation materials are now increasingly being evaluated taking into account a life cycle assessment (LCA) and cost (LCC) perspective, which includes the environmental impacts [9] along with cost [10]. Regarding the economic aspects, the return of investment (ROI) [7] and the discounted pay-back period (DPBP) [11] are two related parameters often used.

There are several new superinsulating materials being developed for high performance buildings [7], such as vacuum insulating panels (VIPs) [12], low-emissivity films for glazed openings [13], foam perlite with a triple-hierarchical porous structure [14] and aerogel enhanced blankets [15].

Aerogels represent a state-of-the-art thermal insulation material, and may be the one with highest potential at the moment [16–20]. While in some applications aerogels can be used as a bulk material [21], in buildings they are usually applied as aerogel glazing [22,23] and blankets [24,25], but can also be employed in the building structure, inside bricks [26], or incorporated in cement/plaster composites [27,28].

Although aerogels may have several compositions, silica aerogels are the most known due to their thermal superinsulation feature, easy production and cost-effectiveness [29]. They were first produced, in the 1930s, by Samuel Stephen Kistler [30], but did not have significant development for several decades. The interest in this material, and especially in its very low thermal conductivity, re-emerged in the 1980s when energy savings became more important.

Silica aerogels consist of a pearl necklace-like internal structure of SiO_2 linked chains with a large number of air-filled pores (porosity usually above 90%), mostly in the mesopore range. This extensive and fine porosity guarantees a very high specific surface area (500–1200 $m^2\ g^{-1}$), low density (~0.03–0.3 $g\ cm^{-3}$), superinsulation performance (0.012–0.025 $W{\cdot}m^{-1}{\cdot}K^{-1}$), ultra-low dielectric constant ($k = 1.0$–2.0) and low index of refraction (~1.05) [31–35].

Due to their extraordinary properties, in particular their low thermal conductivity and optical transparency, silica aerogels can be applied in buildings, especially for energy-efficient retrofitting solutions [36], from covering building façades to insulating window panes [22–28]. But other purposes for their use are emerging, such as for solar collector covers [37–39]. Being one of the most promising high performance thermal insulation materials for buildings, the application of aerogels in this sector have already been the focus of a few reviews and book chapters in past years [27,36,40–48]. As most of these works were published before 2015, and there has been a significant increase in publications since that year, as can be observed in Fig. 1, the main goal in this review is to present the recent advances in the field, with a focus on the works developed with silica aerogel-containing materials between 2015 and 2020.

In this review, the most representative information on silica aerogel-based composites used for building applications is summarized. It is composed of four main parts: i) a brief description of the main stages of silica aerogel preparation and reinforcement; ii) a description of aerogels key-properties for building-related solutions; iii) the recent advances regarding the incorporation of silica aerogels in composites and structures developed for buildings insulation; and iv) main future trends and challenges for silica aerogels use in the buildings sector.

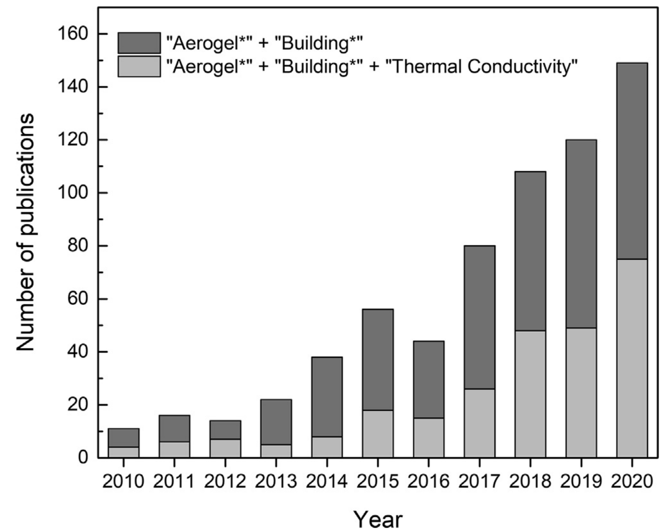

Fig. 1. Number of publications of last ten years containing "aerogel*" and "building*" words in the topic, and also adding the term "thermal conductivity" for a more restricted set (Web of Science; 24 January 2021).

2. Silica aerogels production process

The synthesis of silica aerogels has received significant attention and is extensively described [33–35,49–51]. Some investigators have studied the use of different precursors and many have focused on modification of synthesis parameters [52–57]. Thus, only a brief description is presented here. The synthesis of silica aerogels can be divided into the following general steps: i) gel preparation, ii) aging, iii) washing and iv) drying (Fig. 2).

2.1. Gel preparation

The most common methodology for synthesizing silica gels is the low-temperature sol–gel process. In this procedure, hydrolysis and condensation reactions take place near room temperature, leading to the formation of a nanostructured silica network. During these steps, siloxane bridges (Si–O–Si) are formed by the reaction of the chosen silica precursors. Some of the most common precursors for silica aerogels are silicon alkoxides, such as tetramethoxysilane ($Si(OCH_3)_4$, TMOS) and tetraethoxysilane ($Si(OC_2H_5)_4$, TEOS) [33].

The hydrolysis of silicon alkoxides is usually carried out with a catalyst [50] and involves the conversion of the alkoxide groups to silanol groups (Si-OH). While, during condensation reactions, two processes may occur [58]: i) silanols undergo condensation forming the siloxane linkage and one equivalent of water (water condensation); and ii) a silanol and an alkoxide group condense resulting in a siloxane bond and one equivalent of alcohol (alcohol condensation).

The solution pH has a significant impact on the hydrolysis and condensation reactions [59], leading to the formation of considerable different structures of the gels [60]. When acid catalysts are used (Scheme 1 [60,61]), the hydrolysis is faster than the condensation, resulting in a less branched silica network [34,62–65] that can be easily re-dissolved in aqueous solutions [50]. In base-catalysed reactions (Scheme 2 [60,61]), the opposite is verified, with the condensation step being favoured instead of the hydrolysis, which leads to highly condensed networks with fewer residual alkoxide and silanol groups, if compared with the ones catalysed with acid [34,62,63]. It is often assumed that the hydrolysis and condensation reactions are nearly complete when the sol reaches the gel point [33].

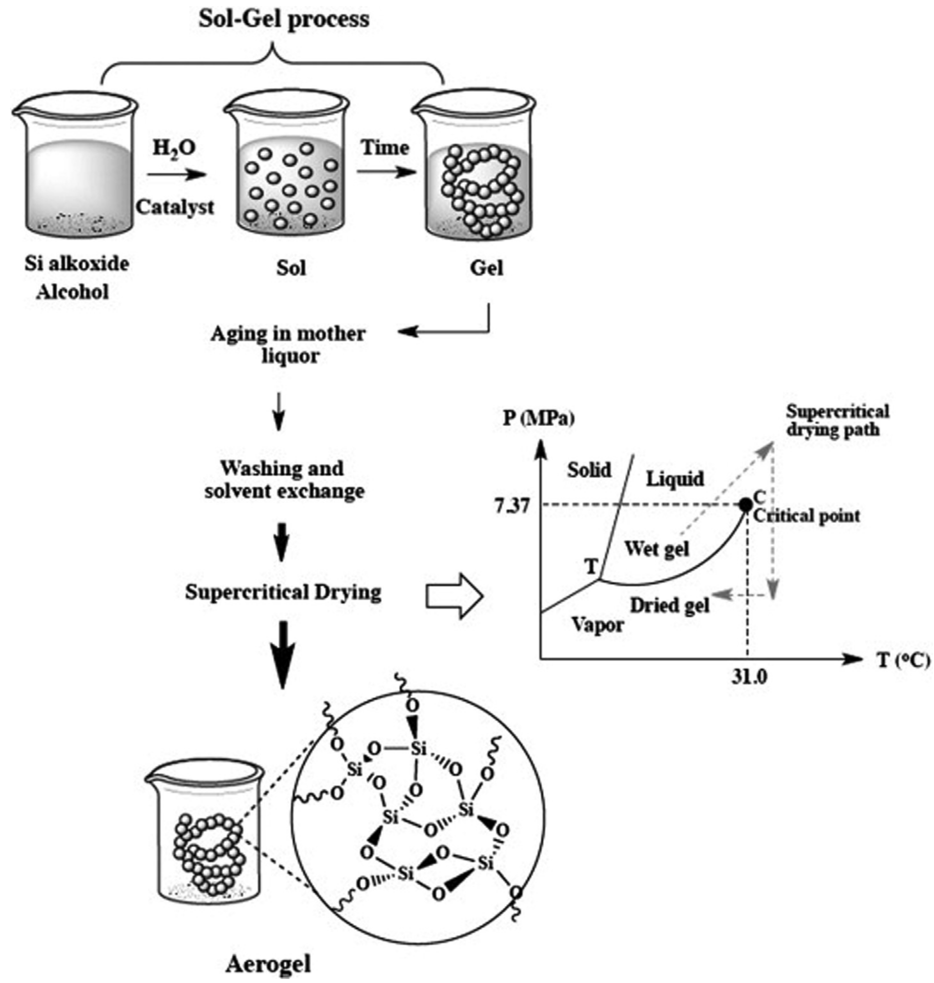

Fig. 2. Schematic representation of typical sol–gel synthesis procedure for aerogels preparation. Reprinted with permission from Ref. [33]. Copyright (2014) Elsevier.

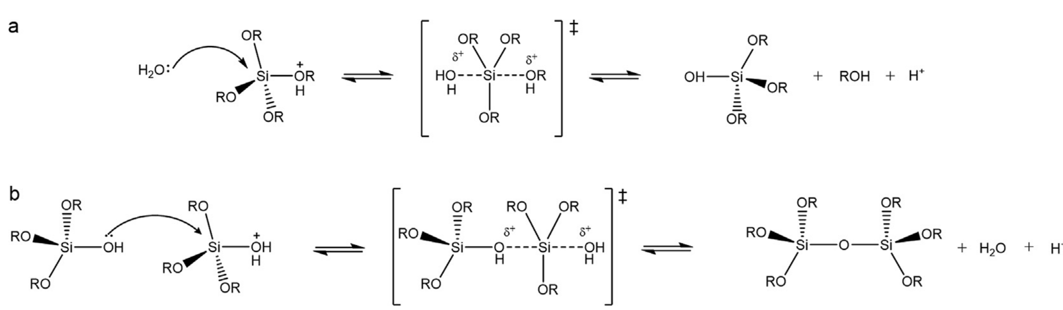

Scheme 1. Acid catalyzed a) hydrolysis and b) condensation of silicon alkoxides. Mechanisms based on Refs. [60,61].

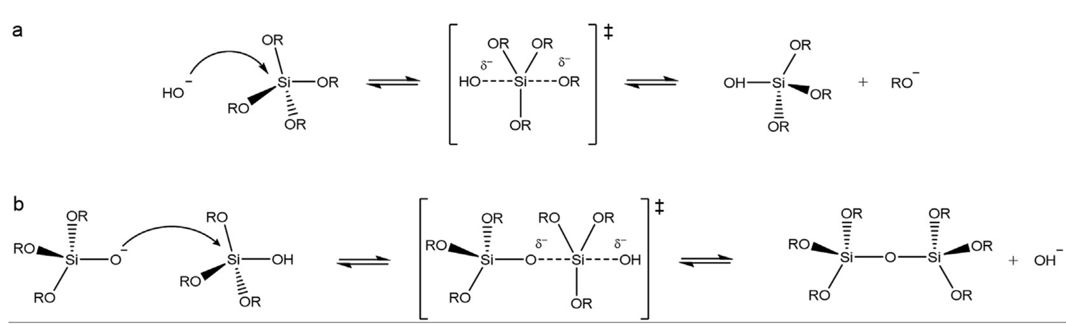

Scheme 2. Base catalyzed a) hydrolysis and b) condensation of silicon alkoxides. Mechanisms based on Refs. [60,61].

Besides silicon alkoxides, sodium silicate (Na_2SiO_3), otherwise known as waterglass, is also widely used for silica aerogel synthesis, as it is probably the cheapest source from which silica gels can be obtained [49,50]. The preparation of the sol is quite different than that referred above. In this case, the waterglass reacts with water, exchanging Na^+ ions with H^+ [49] to form silicic acid (H_2SiO_3), and then this acid will polymerize and form the silica gel [50]. However, a major drawback of this route is the time-consuming step for removing the sodium ions from the solution. For this, usually the sodium silicate sol is passed through an ion-exchange column filled with a strong acidic resin, which can take several hours for complete exchange [49,50,66]. During this procedure the silica sol pH changes from around 11.5 to approximately 2.5 at the end. After the sol preparation, a base is added as catalyst, usually ammonium hydroxide, for gelation [49,67].

2.2. Gel aging and washing

The hydrolysis and condensation reactions continue after the gel point is achieved, but at a much lower rate due to diffusional limitations and decrease of reactive species. This process is called aging, and those reactions cause the strengthening and stiffening of the silica network, leading to a significant impact in the aerogel microstructure [43,68,69]. The aging can be controlled/enhanced by altering different parameters, such as the solution pH, as well as the precursors concentration and the water content of the covering solution [43,70,71].

The strengthening of the gel's network occurs due to two main mechanisms: the first one is the neck growth, a result of the reprecipitation of dissolved silica from the secondary particles surface onto the neck region; the second is known as Ostwald ripening mechanism, in which the dissolution of smaller silica particles occurs and then the reprecipitation onto larger ones [33,34,72].

Often, the aging procedure involves the immersion of the silica gel into a solution with silane precursors, such as TMOS or TEOS, to increase the degree of cross-linking [43,69,73]. This process is similar to a surface modification, and helps preventing the fracture of the silica material during drying at ambient pressure or in supercritical conditions [69,74,75].

After aging, a washing step is usually performed to remove the catalyst, water, non-reacted precursors, as well as some additives when they are used, like surfactants. The presence of these impurities may lead to partial collapse of the porous network during drying, which can result in an increase of the gel's bulk density. This happens because some of these compounds, for instance water, can interact with silanol groups on the silica surface increasing the capillary forces during drying. The washing is usually done by immersing the gel in a pure alcohol (for instance, the same used for the synthesis), in several steps, and exchanging in this way the liquid in the pores through a diffusional process. Frequently, alkanes are also used, due to their low surface tension, in order to decrease the capillary forces [76].

2.3. Gel drying

The last and most critical step in the production of aerogels is the drying of the gel. The primary purpose is to maintain the gel's initial pore structure after drying, which can be achieved by minimizing the damage in the gel network caused by capillary forces during this step, in order to enhance the properties of the aerogel [77]. Three different drying methods are often used: (1) ambient pressure drying (APD), (2) supercritical drying (SCD) and (3) freeze drying (FD).

The minimization of the capillary tension and pressure gradients when using APD involves the implementation of solvent-exchange protocols, as already mentioned, and/or surface modification of the gels (silylation). In the latter, the silylated surfaces repel each other and condensation reactions do not occur during drying. Thus, the gel does not undergo irreversible shrinkage in this stage and recovers its original porous state after drying [33,77,78]. This phenomenon is called spring-back effect [51]. As APD is carried out at ambient pressure and mild temperatures, this method is more attractive in terms of cost and versatility of samples' size, if compared with SCD and FD.

SCD was the first methodology used to obtain aerogels [30], and still is the preferred method to fabricate aerogels, since the supercritical fluids avoid the surface tension effects during the drying step [79], therefore significantly reducing the shrinkage and collapse of the pore structure. There are two different methods of supercritical drying [77]: high temperature supercritical drying (HTSCD) and low temperature supercritical drying (LTSCD). In the first method, the synthesis solvent is converted in a supercritical fluid by increasing the pressure and temperature inside an autoclave, being subsequently slowly vented at constant temperature [40]. The second method (LTSCD) usually uses supercritical CO_2 ($scCO_2$) to extract the organic solvent of the synthesis, which must be soluble in $scCO_2$. This process can be carried out by two approaches: (1) liquid CO_2 is pumped into the sample while the organic solvent is flushed out and, then, the temperature is increased, at high pressure, followed by the removal of $scCO_2$; (2) $scCO_2$ passes continuously through the sample to extract the organic solvent [77].

In FD method, the solvent in the pores is frozen and then sublimated under vacuum. The nanostructured matrix might undergo cracking due to the formation of large crystals within the pores. This situation is even worse if water is the solvent, as it expands when freezing, which causes severe damage to the pore structure [80]. This methodology leads to powder-like silica materials with macropores [33].

2.4. Structural reinforcement of silica aerogels

The major drawback regarding native silica aerogels is their intrinsic fragility, which has significantly limited their practical applications. Therefore, different techniques and materials, from polymers to nanostructures, have been reported in literature to mechanically reinforce silica aerogels [33–35]. The main methodologies applied to improve the mechanical properties of silica aerogels, as well as a few examples for each procedure to give an overall view, are reported in Table 1.

Reinforcement strategies of silica aerogel such as the addition of organosilanes and polymers have already been described and discussed in an overview by Maleki et al. [33]. Thus, only a brief view will be given here.

The modification of the gels at silica skeletal level can be achieved via the co-precursor method, as reported in Table 1, using an organosilane in the initial mixture that features a non-hydrolysable group, as for example the methyl groups in MTMS [81] or the propyl methacrylate in TMSPM [82]. When adding tri-functional organosilane compounds of the type $RSiX_3$ (where, R = alkyl, aryl or vinyl groups, X = Cl or alkoxy groups) in the beginning of the synthesis, flexible aerogels with reduced overall bonding and good hydrophobicity are obtained [54]. The inclusion of flexible bis-silanes, such as 1,6-bis(trimethoxysilyl)hexane (BTMSH), into the silica backbone creates a more open structure that can also bear higher loads [83]. The modification can also be achieved through the surface derivatization method, by modifying the surface groups of the sol–gel-derived materials through post-gelation addition of the modifying agent [34,84]. Several organosilanes were already used for the silica network modification with co-precursor or surface derivatization methods [33,34,85], including methyltriethoxysilane (MTES) [86], MTMS [87],

Table 1
General view of reinforcing strategies and agents for silica-based aerogels.

Reinforcement strategy	Reinforcing agent		Thermal conductivity ($W \cdot m^{-1} \cdot K^{-1}$)	Mechanical Property	Advantages	Disadvantages
Co-precursor	Biopolymers	Bacterial cellulose [95]	0.0292 ± 0.003	Young's modulus = 485 kPa (strain at 60%)	- Simple synthesis methodology - Higher thermal stability and hydrophobicity if compared with derivatization method [96]	- Leads to non-uniform and irregular shaped particles [96] - Larger pores and particle sizes if compared with the derivatization method [96]
		Pectin [97]	<0.018	Young's moduli up to 10 MPa		
	Organically modified silanes	Methyltrimethoxysilane (MTMS) [81]	–	Compressive strength = 0.90 MPa		
		3-(trimethoxysilylpropyl) methacrylate (TMSPM) [82]	0.038	Young's modulus = 1.26 GPa		
In-situ polymerization	Polymers	Di-Isocyanate [98]	0.020	Young's Modulus = 6.48 MPa	- Significant improvement of the mechanical properties	- Complex procedures - Density increases - Lower resistance to high temperatures [99]
		Polystyrene (PSt) [100]	0.037 ± 0.001	Compressive strength = 124 kPa		
		Poly(butyl acrylate) (PBA) [100]	0.042 ± 0.002	Compressive strength = 98 kPa		
Surface derivatization	Silane	Solution of hexamethyldisiloxane and HCl [101]	0.0221	Young's modulus = 1.07 MPa	- Higher transparency than the ones obtained by the co-precursor method, for the same silane modifier [96] - Does not affect the growth and structure of SiO_2 particles [96]	- Does not improve the materials' thermal stability [96]
	Polymer	Toluene diisocyanate [102]	–	Young's modulus = 36.16 MPa		
		Methyl-methacrylate (MMA) monomer [103]	–	Young's modulus = 61.6 MPa		
Fibers	Organic	Recycled polyethylene tetraphalate (rPET) fibers [104]	0.037 ± 0.001	Young's modulus = 2.19 ± 0.34 kPa	- Simple synthesis methodology - Samples in a wide range of sizes/shapes - Fibers increase the elasticity of the composite [99]	- The materials tend to be dusty - Lower resistance to high temperatures if polymer fibers are used [99]
		Cellulose fibers [105]	0.0158 ± 0.0004	Young's modulus = 3.50 ± 0.30 MPa		
	Inorganic	Silica fibers [106]	0.0210 ± 0.0001	Young's modulus = 48 kPa		
		ZrO_2 fibers [107]	0.0236	Compressive strength = 0.65 MPa		
		Glass fibers [108]	0.0179 ± 0.0005	Young's modulus table = 1.53 MPa		
Nanomaterials	1D materials	Attapulgite nanofiber [109]	0.0228	Compressive strength = 2.5 MPa	- Unique properties	- Nanomaterials are usually expensive
		Carbon nanotubes [110]	0.0418 ± 0.001	Young's modulus = 201.5 ± 1.6 kPa		
	2D material	Graphene Oxide [111]	0.035	Compressive strength = 0.65 MPa		

vinyltrimethoxysilane (VTMS) [87,88], hexamethyldisilazane (HMDZ) [89,90], hexamethyldisiloxane (HMDSO) [91,92] and trimethylchlorosilane (TMCS) [93,94].

Mechanical reinforcement of silica aerogels can also be achieved by the grafting of polymers from the organically-modified silica surface (Table 1). Meador and co-authors [98] studied the effects of four processing parameters (initial silane, water, polymer concentration and number of washings) on the properties of polymer (di-isocyanate) cross-linked aerogels. The polymers' addition increased the silica aerogel mechanical resistance (6.48 MPa), while maintaining low values of density (0.184 g·cm^{-3}) and thermal conductivity (20 mW·m^{-1}·K^{-1}). Maleki et al. [112] also achieved a good mechanical reinforcement by including BTMSH or 1,4-bis(triethoxysilyl)-benzene (BTESB) into the TMOS-derived underlying structure of tri-methacrylate crosslinked silica aerogels. The authors optimized these APD aerogels' properties, developing materials with mechanical strength two times higher than their $scCO_2$ dried counterparts, and 400 times stronger than the plain silica framework.

Organic and inorganic fibers are another possibility to surpass the intrinsic fragility of silica aerogels. An extensive range of fibers can be used for the development of silica aerogel composites, including for example recycled PET [104], cellulose [105], silica [106], ZrO_2 [107] and glass fibers [108], and these fibers can introduce different properties to the final composite (Table 1). The fiber-silica aerogel composites allow the possibility of improving the mechanical strength without compromising the low densities and high specific surface areas [113–116]. Polymer fibers increase the elasticity of silica aerogels but undergo degradation at high temperatures [116]. On the other hand, ceramic and glass fibers improve the silica aerogel thermal resistance, but can cause a decrease in the specific surface area and an increase in the composites' density [99].

Another reinforcement methodology is the incorporation of nanostructures into the silica network (Table 1), which has been presented in reviews written by Lamy-Mendes et al. [34] and Slosarczyk [99]. Both 1D and 2D nanomaterials were already used in the silica aerogels composites. For example, carbon nanotubes-silica aerogels composites showed improved mechanical properties, doubling the Young's modulus when compared to their silica-based aerogel counterpart [110], without compromising the densities and porosities. By including 20 wt% of attapulgite nanofibers in the silica backbone of TEOS-based silica aerogels, Li et al. [109] were able to obtain a 3-fold increase in the compressive strength and elastic modulus. When adding graphene oxide (GO) to silica aerogels, Hong-Li and co-authors [111] also obtained an enhancement of the TEOS-based silica materials' compressive strength (from 0.04 MPa to 0.65 MPa), but the thermal conductivity also increased from 0.025 to 0.035 W·m^{-1}·K^{-1}.

3. Silica aerogel key properties for buildings' applications

In this section, the more relevant properties of silica aerogels for building-related applications are detailed, considering their correlation to the material's structure. The more widely accepted assessment methods for these properties are also indicated.

3.1. Pore structure and density

Silica aerogels are materials composed by ultrafine particles, linked in a pearl necklace 3D arrangement, and air-filled pores that usually contribute to 85–99.8% of the total aerogel volume [49]. Therefore, when incorporated in composites, they lead to a reduction of their overall density and, thus, the weight of the building envelope, as well as an increase in the thermal resistance due to their low thermal conductivity.

The interconnected pore network of silica aerogels is mostly composed by mesopores (pore sizes between 2 and 50 nm), with an average pore diameter between 20 and 40 nm [49,76]. However, they can also present pores in the micro- (pore diameters lower than 2 nm) and macropores (diameters higher than 50 nm) range [49,76]. The predominant range of pore sizes in the final material can be tailored by the sol–gel process, for example, micropores become significant when acid catalysis conditions are used, while the addition of organically modified silica precursors with basic moieties, such as amine groups, leads to generation of large macropores [76,110,117].

Due to the combination of high porosity and small pore sizes in aerogels, the most used conventional technique for characterization of pore structure and porosity, i.e. mercury intrusion porosimetry, is not appropriate for silica aerogels. This method is based on the application of pressure on the materials network, which, in the case of aerogels, leads to large volumetric compression and cracking, originating incorrect values for pore size and volume. The most applied technique for the pore size distribution (mesopores) characterization of aerogels is the nitrogen adsorption/desorption technique [49], which operates at relative pressures lower than 1 relatively to the N_2 saturation pressure at 77 K. However, this technique also has some limitations, in particular when evaluating samples with a relatively flexible structure [118,119]. Due to these constrains, it is common to rely on the density values to obtain the porosity and average pore size of aerogels [69,106,110,120].

Two different physical characteristics are used to define silica aerogels in terms of density: bulk density (ρ_b) and skeletal density (ρ_s). Bulk density is defined as the ratio of the aerogel's mass to its volume including pores. This property can be obtained by weighing and measuring the dimensions of cut or shaped regular pieces of aerogel. If this regularity cannot be achieved, liquid (non-wetting fluids) or granular solids (dry flow method) displacement can be used for the bulk density assessment, always ensuring that the filling medium will not enter in the pores and will not compress the sample in the case of flexible aerogels.

The skeletal density refers to the density of the silica particles that compose the aerogel structure, and is usually very close to that of amorphous silica (2.2 g·cm^{-3} [76,121]) when pristine silica aerogels are measured. However, lower values are expected for organically modified silica aerogels [122], confirming that the skeletal density largely depends on the aerogel synthesis precursors and conditions [123]. Submitting the aerogel to heat treatment can also affect this property [124], since dehydroxylation and removal of network defects occur. The skeletal density may be obtained by using helium pycnometry [121], with the sample previously milled to obtain a fine powder form, in order to minimize the number of closed pores.

The bulk and skeletal densities of the aerogel may provide the porosity and pore volume (V_P) values through the following expressions [106,110]:

$$\text{Porosity}\ (\%) = (1 - \rho_b/\rho_s) \times 100 \tag{1}$$

$$V_P(\text{cm}^3 \cdot \text{g}^{-1}) = 1/\rho_b - 1/\rho_s \tag{2}$$

To estimate the average pore size, Eq. (3) is used, with the total pore volume determined by Eq. (2) and specific surface area (S_{BET}) obtained by nitrogen gas adsorption [106,110].

$$\text{Average pore diameter} = 4(V_P)/S_{BET} \tag{3}$$

3.2. Thermal conductivity

The thermal energy is transferred through silica aerogels by three mechanisms: solid conduction (λ_s), gaseous conduction (λ_g), and radiative (infrared) transmission (λ_r) [49,76]. The effective thermal conductivity is a result of the three contributions, as follows (Eq. (4)):

$$\lambda = \lambda_s + \lambda_g + \lambda_r \tag{4}$$

The intrinsic solid thermal conductivity (λ_s) of aerogels depends on the network structure and connectivity, as well as their chemical composition [76]. This thermal conduction proceeds via phonon diffusion through the aerogel backbone, having a mean free path in the order of 1 nm, therefore, it is a local transport phenomenon [125,126]. According to Fricke et al. [127] the solid conductivity of monolithic silica aerogels, with bulk densities from 70 to 230 kg·m^{-3}, can be described as a function of their densities by Eq. (5).

$$\lambda_s \propto \rho_b^{\alpha} \tag{5}$$

where ρ_b is the bulk density of the aerogel, and α is a constant found to be ~1.5.

The gas phase can also transport thermal energy through the aerogel. The low gaseous thermal conductivity (λ_g) of aerogels, can be mainly explained by the Knudsen effect, and can be expressed by Eq. (6) [76,128–130]:

$$\lambda_g = \frac{\lambda_{g,0}\varphi}{(1 + 2\beta_n)} \tag{6}$$

where, $\lambda_{g,0}$ is the thermal conductivity of the non-convecting free gas, φ the porosity of the aerogel, β is a parameter that represents the energy transfer between the gas and the limiting aerogel nanostructure and K_n is the Knudsen number ($K_n = l_g/D$, where l_g is the mean free path of the gas molecules and D is the effective pore diameter).

The thermal conductivity referent to the gaseous component is highly dependent of the aerogels pore structure, as it will be higher in larger pores than in smaller ones. Aerogels are nano-porous materials with a random distribution of pore size, and, as the non-uniformity of the pore size distribution increases, also does the number of larger pores, which will leads to an enhancement of the heat transfer by gas molecules [131]. The pore volume also has an influence in the aerogels' thermal conductivity, with the combination of smaller pore sizes with high pore volumes leading to a decrease in the thermal conductivity [106,132]. It is important to mention that, usually, the aerogels' pore size is below the micron range, so the heat transfer due to the gaseous phase within the aerogels structure is already lower than the heat transfer within the free gas, which gives the possibility of these materials to achieve lower thermal conductivities than the free air (0.026 W·m^{-1}·K^{-1} at ambient temperature) [76].

The final mode of thermal transport through silica aerogels involves infrared radiation. The radiative heat transfer within an aerogel, diffuse or non-diffuse, will depend on the optical thickness of the specific type of the aerogel [76]. The radiative component of thermal conductivity is negligible at room temperature, and for optically thick materials [133], but becomes a significant term at higher temperatures [76]. It can be evaluated by the expression in Eq. (7) [76,126,129,134–136]:

$$\lambda_r = \frac{16n^2\sigma T^3}{3e\rho_b} \tag{7}$$

where n is the mean index of refraction of the insulation material (for low density insulations, it is close to 1), σ is the Stefan-Boltzmann constant (σ = 5.67 × 10^{-8} W·m^{-2}·K^{-4}), T is the medium's local temperature in Kelvin, ρb is the bulk density and e is the temperature-dependent effective specific extinction coefficient.

As already mentioned, aerogels' thermal conductivity has a strong correlation with the density, and different authors [76,133,137–142] have demonstrated that this dependence has usually a U-shape, as can be observed in Fig. 3 for monolithic silica aerogels made from polyethoxydisiloxane [137]. The solid thermal conductivity is enhanced with higher densities, while lower densities lead to an increase in the gaseous thermal conductivity due to the presence of larger pores which do not contribute to Knudsen effect [133].

Different approaches can be applied to improve the thermal insulation properties of silica aerogels. The solid thermal conductivity can be reduced with the control of the aerogel's bulk density. For the reduction of the gaseous contribution, there are two options: first, evacuation of the gas and, second, controlling the pore size into the mesopore region [118]. In order to decrease the influence of the radiation thermal conductivity of silica aerogels, the addition of infrared opacifiers such as carbon soot or TiO_2 is a possibility [127].

The thermal conductivity can be determined by different methodologies, which can be generally divided in two classes: (1) steady-state methods, that measure thermal properties by establishing a temperature difference which remains unaltered through time, and (2) transient-state methods, which usually measure the sample's time-dependent energy dissipation process [143]. For the thermal conductivity determination of aerogel samples, the most widely applied methods are the Guarded Hot Plate (GHP) [26,144–147], in the steady-state case, and the Transient Plane Source (TPS) method [110,138,148–150], for the transient methodologies.

The apparatus and testing procedure for the GHP method are described in different standards, ASTM C177 [151], European Standard EN 12667 [152] and International Standard ISO 8302 [153]. Even though this method has been extensively used, the technique presents some drawbacks, such as the necessity of relatively large testing samples and usually long waiting time [143]. The TPS method, especially the "Hot Disk ®" variants, has been adopted for fast characterization of thermal properties [143,154,155]. The ASTM D7984 [156] and the ISO 22007-2 [157] define the devices and procedures for this methodology. The TPS method is reportedly capable of measuring thermal conductivities from 0.005 to 500 mW·m^{-1}·K^{-1}, in a large temperature range (cryogenic temperatures to 500 K) [143]. However, the two sample pieces needed must be similar and feature one entirely planar side [158], which can be sometimes challenging for aerogel samples.

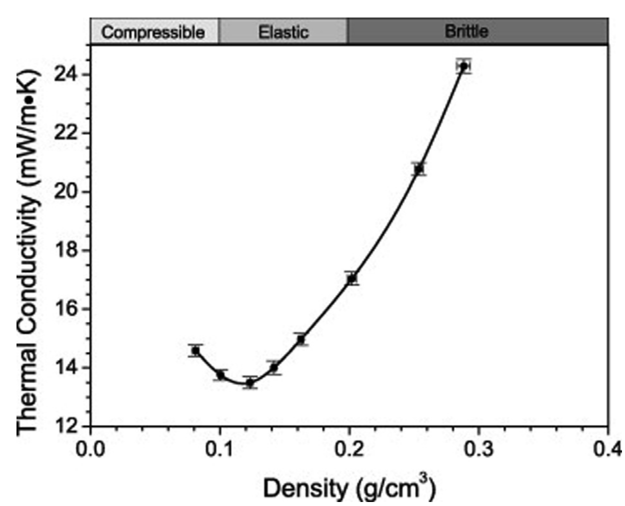

Fig. 3. Thermal conductivity of the aerogels as a function of density. A minimum thermal conductivity of 13.5 mW·m^{-1}·K^{-1} was found when the density of the silica aerogels was approximately 0.123 g·cm^{-3}, the same density range in which the aerogels exhibit elastic properties. Reprinted with permission from Ref. [137]. Copyright (2014) Elsevier.

3.3. Optical properties

Silica aerogels show optical properties between transparent and translucent, depending on their internal structure, as a result of the Rayleigh scattering, which happens due to two different sources: from the nanoporous aerogel network and the micrometer-size imperfections of the external aerogel surface [159–161]. It is possible to apply the Rayleigh-Gans approximation for most silica aerogels, since they present particle sizes or agglomerates smaller than 40 nm (<10% of the visible light wavelengths), and have a relative refractive index close to unity [162]. To achieve high optical transparency, the size of silica particles should be kept small. Thus, the aerogels' optical properties can be influenced by changing parameters of the sol–gel process, such as the precursors, the molar ratio between the precursors, the pH value of the starting solution, the addition of surfactants and the parameters of the aging [160–162].

The influence of the synthesis parameters in the optical properties of silica aerogels was studied by Xia and co-authors [55]. By changing the TMOS addition method, they were able to tailor the pore size of silica aerogels, and, as consequence, the aerogels' properties. When the mean pore size decreased from 20.7 to 16.6 nm, the aerogels showed an increase in the surface area, from 845 to 1060 $m^2 \cdot g^{-1}$, and in the transparency ratio at 550 nm wavelength, from 71% to 88%. Besides, a reduction in the thermal conductivity was verified, from 24.6 to 20.2 $mW \cdot m^{-1} \cdot K^{-1}$.

Tabata et al. [163] concluded that the drying methodology also has a significant impact in the optical properties of silica aerogels. These authors were able to control the refractive indices (n) of the aerogels by using the pinhole drying method. In this process they were able to control the shrinkage of the alcogel, by adjusting the containers design and the drying period. Highly transparent aerogels, with n from 1.06 to 1.26 were obtained, which can be used as a Cherenkov radiator.

Due to their unique optical properties, silica aerogels can be used in very distinct applications, such as Cherenkov radiators [164,165], in optical fiber devices [166], solar collectors [167], and windows [168]. And these optical properties, such as the transmittance and reflectance of the samples, can be assessed by using an Ultraviolet–Visible–NIR spectrophotometer [23,169–172]. The UV–Vis spectrometer allows measuring the samples' extinction, comprising the absorption, reflection and scattering [173].

3.4. Acoustic properties

Besides thermal insulation performance and the light transmission properties, the acoustic insulation in building envelope materials is very important, regarding both noise insulation and sound absorption [174–176]. Among the unique properties of aerogels, their high porosity leads to low sound velocity (100 $m \cdot s^{-1}$) [159,177], allowing them to be also applied as noise insulators and sound absorbing materials. The acoustic properties of silica aerogels are influenced by their porous structure, which depends on the synthesis conditions and selected chemicals [177,178]. For silica porous systems, Caponi et al. [179] were able to conclude that when the pore sizes are smaller than 8 nm the largest contribution in the absorption comes from the attenuation due to dynamic mechanism, such as relaxation processes and two-level systems. While, when the pores sizes are superior to 8 nm, a higher sound attenuation is detected, and it is assigned to the scattering of phonons by the sample's structural disorder, which is a static mechanism. As silica aerogels usually have a pore size distribution in the range of 2 and 50 nm, the presence of both mechanisms, static and dynamical attenuation, can coexist in these samples.

Moretti et al. [180] compared the influence of granules size of silica granular aerogels, supplied by Cabot Corporation, as well as their densities, on thermal and acoustic performance characteristics. The obtained results showed that small granules, with sizes between 0.01 and 1.2 mm, which are the ones with higher values of density (80–85 $kg \cdot m^{-3}$), achieved the best results regarding thermal and acoustic properties. At ambient temperatures, the thermal conductivity of these small granules was around 20 $mW \cdot m^{-1} \cdot K^{-1}$, and the transmission loss (TL) at normal incidence was of 19 dB at about 6400 Hz for 40 mm thickness.

The thermal and sound insulation properties were also studied by Li et al. [181]. The authors obtained MTES-based silica aerogels with thermal conductivities between 21.5 and 25.5 $mW \cdot m^{-1} \cdot K^{-1}$. When the silica aerogel presented a thickness of 11.8 mm and a density of 60 $kg \cdot m^{-3}$, it showed a sound absorption coefficient of 0.91 for sound waves at 2000 Hz frequency, and the sound TL was 13–21 dB between 500 and 1600 Hz.

To determine distinct acoustic properties of aerogels, different methodologies must be applied. The sound velocities in aerogels are obtained by using two piezoelectric transducers, one for signal transmitting and one for signal receiving. The velocity is evaluated from the time span between the consecutive echoes [182–184]. On the other hand, the four-microphone impedance tube setup [185] is frequently used to determine the absorption coefficient and the TL, which is an important factor for the quantification of the acoustic insulation properties [180,186,187].

3.5. Other properties

The crystalline form of silica is an hazardous material and, if inhaled, can cause silicosis, an irreversible and incurable serious lung disease and one of the most important occupational diseases [188]. Several other pulmonary conditions may also occur, such as tuberculosis and lung cancer [189]. However, commercial silica aerogels are usually composed by amorphous silica, and, there are no evidence that synthetic amorphous silica can cause damage to human lungs [189].

While the crystalline silica is classified as carcinogenic to humans (Group 1) by the International Agency for Research on Cancer (IARC) [190], synthetic amorphous silica is in Group 3, *i.e.*, this material is not classifiable regarding its carcinogenicity to humans [191].

Silica aerogels also show other advantageous properties, as nonflammability, non-toxicity and easy disposal when compared with other insulation products in the market [43,50]. The commercial products containing silica aerogels are also considered as having the same properties [40,43].

4. Thermal insulation enhanced materials with silica aerogels

Building envelopes are composed by different structural and functional components, for instance walls, roofs and windows. As all these parts have a significant role on the overall energy efficiency [192], different technologies are proposed to improve the building energy performance. New materials and solutions are being established with the goal of achieving the best thermal insulation possible without increasing the thickness in the building envelope, as this increase has a negative impact regarding the buildings' floor areas [193]. A special focus is given to the transparent elements [194], such as windows which are usually the weakest part of the thermal building envelope [195]. Usually transparent glass is used, but aerogel windows have been considered, since the 1980s [196], as a translucent option for building fenestration systems. In fact, besides the excellent thermal insulation feature (very low U-values), silica aerogels also show good optical properties enabling provision of daylight [197,198]. Therefore, many efforts are being made to develop aerogel-based products that can be used in fenestration to reduce energy losses.

Regarding the thermal insulation properties, it is possible to classify the works found in the literature in two main groups of building applications of silica aerogels: i) thermal insulation materials in which the transparency is not a requirement, and focused on the use of silica aerogels with high thermal insulation performance; and, ii) glazing systems, for which the transparency/translucence is a prerequisite, but the thermal insulation feature may be also important. Both perspectives are presented in this section.

For a better understanding of the developed composite materials reported in the works described in this overview, some of the basic terms used in construction are here defined: cement is a powder that, when mixed with water, forms a plastic paste that gradually gets harder and shows an increasing strength [199]; mortar is composed by a cementitious material binder, water and sand as fine aggregate; with the addition of a coarse aggregate to the previous mixture, concrete is obtained [200]. Mortars are often divided into two categories – rendering and plastering mortar and masonry mortar – each defined by their application [201]. It should be also referred that the binder can be a material different from cement, such as mineral-based binder systems [202] and geopolymers [203]. Due to these definitions, in this overview, the works in which plasters and renders were the focus of the study will be presented in the same category as mortars.

It should be noted that the terms used to classify the aerogel composite materials into the respective categories were the ones given by the original articles' authors, since it is often difficult to access specific information about the formulation to better frame its type.

In this section, the newest articles published on panels, blankets, cement, mortar, plaster, renders, concrete, glazing systems, solar collector covers and other materials containing silica aerogels for building applications will be presented.

4.1. Panels and blankets

The application of aerogel blankets in the building industry is relatively new, however they have already been applied, for example, in projects where space and weight constraints exist, and in technical services thermal insulation, such as pipes and ductworks [28,36,40,204,205]. As blankets and panels developed with silica aerogels have better mechanical performance than the native aerogel, without compromising their outstanding insulation properties, they captured an increased interest in the recent years. Some of the works developed with these materials are presented in Table 2.

Liang and co-authors developed two research works with the goal of improving the thermal conductivity of VIP with fiber felt/silica aerogel composite core [206,207]. In their first work [206], they studied the influence of the aerogel density and fiber content in the thermal performance and service life of these VIPs, while maintaining the gas pressure at 1.0 Pa. The authors tested different aerogels' densities, from 50 to 200 $kg \cdot m^{-3}$, and observed an increase in the effective thermal conductivity with the density increase, as well as the need to change the thickness from 3.6 to 9.9 mm to maintain an *U*-value of 0.6 $W \cdot m^{-2} \cdot K^{-1}$. The fiber content was also modified from 0 to 20 vol%, with the optimum value being 6.6 vol%, which corresponded to a thermal conductivity of 4.3 $mW \cdot m^{-1} \cdot K^{-1}$ and a thickness of 5.6 mm. The aerogel density and fiber content can be controlled, as shown in Fig. 4, to achieve the maximum service life of 63 years (densities lower than 90 $kg \cdot m^{-3}$ and fiber content between 6 and 16%) of these materials for building applications.

In the second work of Liang and co-authors [207], they studied the effect of aerogel density and fiber content variations, as in the previous research. However, while also altering the gas pressure of the VIP. The same behaviour verified in their earlier work was observed regarding the aerogels' densities at pressures of 1 and 10^3 Pa: when the density increases (50–150 $kg \cdot m^{-3}$), the thermal conductivity follows the same tendency (~2 to ~5.5 $mW \cdot m^{-1} \cdot K^{-1}$). But at 10^5 Pa, a minimum thermal conductivity of

Table 2
Published works using silica aerogel-based blankets and panels for thermal insulation of buildings.

Ref.	Composite material	Thermal conductivity ($W \cdot m^{-1} \cdot K^{-1}$)	Bulk density ($kg \cdot m^{-3}$)	Tensile strength (kPa)	Compressive stress (kPa)[a]
Liang et al. [206,207]	**Silica aerogel precursor**: TEOS modified with TMCS **Silica aerogel-containing composite**: VIP with fiber felt/silica aerogel composite core	0.0043 (1 Pa) 0.0039 (0.1 Pa)	110	–	–
Yang et al. [208]	**Silica aerogel precursor**: TEOS modified with TMCS **Silica aerogel-containing composite**: panels with glass felt	0.0208	266.2	–	–
Joly et al. [209]	**Silica aerogel precursor**: modified alkoxysilane **Silica aerogel-containing composite**: panels with needle glass fiber	0.0156	194.9	15.2	38.6
Nocentini et al. [24]	**Silica aerogel precursor**: TEOS modified with HMDSO **Silica aerogel-containing composite**: blanket with glass fiber mat	0.0147	110	0.8	58.5
Hoseini et al. [210,211]	Commercial aerogel blankets: Cryogel®Z (Aspen Aerogel)	0.014	130	–	–
	ThermalWrap™ (Cabot Corp.)	0.023	70	–	–
Guo et al. [212]	**Silica aerogel-containing composite**: blanket with fiberglass matrix	0.020	170	–	–
Lakatos [213]	**Silica aerogel-containing composite**: Glass fiber reinforced blanket	0.014	–	–	80.0
Nosrati and Berardi [204,214]	Aerogel blanket – Spaceloft ® (Aspen Aerogel)	0.0179	160	–	–
	Aerogel fiber board (Aspen Aerogel)	0.0195	160	–	–
	Aerogel gypsum boards – Type A (Aderma Locatelli Co)	0.0392	350	–	–
	Aerogel gypsum boards – Type B (Aderma Locatelli Co)	0.0416	250	–	–
Huang et al. [215]	**Silica aerogel precursor**: TEOS modified with TMCS **Silica aerogel-containing composite**: blanket with glass fiber	0.014	130	–	–
Ibrahim et al. [216]	**Silica aerogel precursor**: TEOS modified with HMDSO **Silica aerogel-containing composite**: blanket with needle glass fiber	0.0165	–	8.4	12.9
Berardi and Lakatos [217]	Aerogel blanket – Spaceloft ® (Aspen Aerogel)	0.014	–	–	80.0
Kosny et al. [218]	Aerogel-based radiant barrier	0.0145	–	–	–

[a] – Unless specified, the compressive stress is obtained at 10% strain.

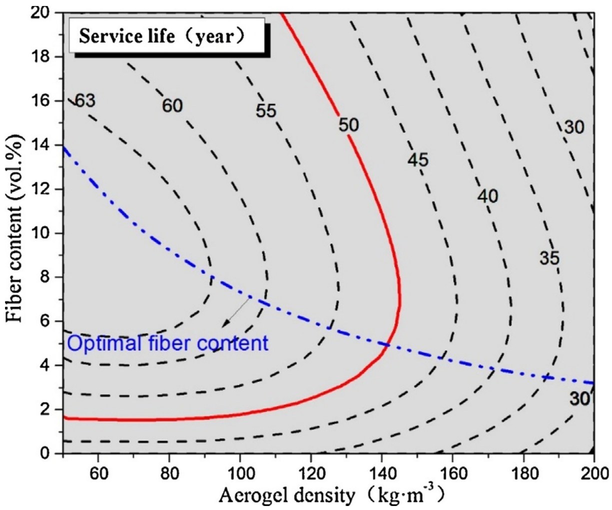

Fig. 4. Service life contour plot of VIPs for various aerogel densities and fiber contents. Reprinted with permission from Ref. [206]. Copyright (2017) Elsevier.

15.8 mW·m^{-1}·K^{-1} is achieved at the density of 75 kg·m^{-3}. For aerogels with a density of 110 kg·m^{-3}, at the pressure of 0.1 and 10^5 Pa, the optimum fiber content for maximum insulation performance was 6.6 and 2.3 vol%, with thermal conductivities of 3.9 and 16 mW·m^{-1}·K^{-1}, respectively.

Yang and co-authors [208] compared the thermal performance of aerogel insulating panels (AIP) with two traditional materials used in insulation: expanded polystyrene (EPS) and glass felt (GF). The authors were able to experimentally assess the critical time for the interior air temperature to reach its maximum, with AIP showing the longest time (more than 10 h). These results were used to validate a simplified thermal network model, able to predict the dynamic thermal performance of the panels. The AIP showed the best results, if compared with EPS and GF cells – a twice longer time lag and a reduction of 35% in the daily heat loss. The authors also predicted the thermal performances of typical exterior walls with different insulation positions, and once again the AIP exhibited better results, with a predicted 20% decrease in temperature fluctuation amplitude and 40% decrease in the heat flow amplitude, if compared with the other insulating materials.

A new aerogel-based composite was presented in the work of Joly et al. [209]. The authors were able to produce an insulation material, with a low-cost process, that can be competitive in the superinsulation European market. The developed composite was produced with a combination of silica aerogel and needle glass fiber, and presented low density, good insulating and mechanical

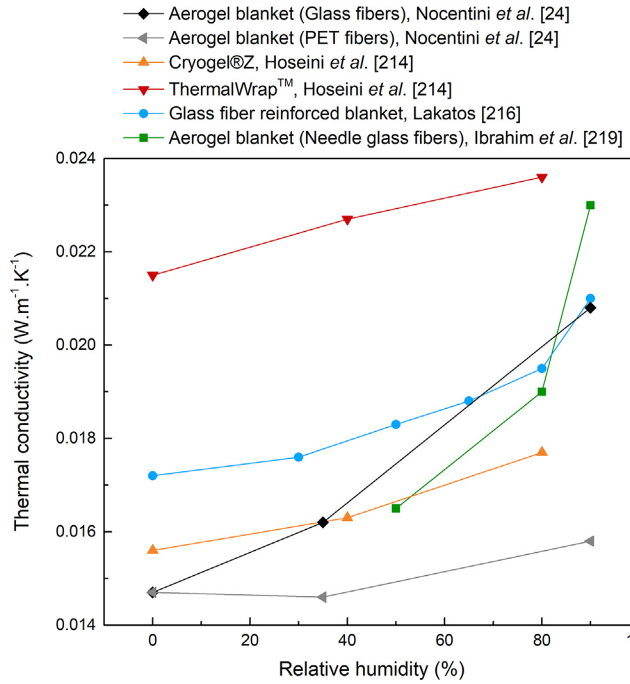

Fig. 6. Thermal conductivity of aerogel blankets for different moisture contents.

properties, as reported in Table 2. A 20 mm thick aerogel insulation panel was already applied in the FACT (FACade Tool) test facility in Chambery, France, as shown in Fig. 5, for assessing the impact of the retrofitting intervention with the composite. These ongoing measurements will be used to validate the data obtained by numerical simulations.

Relative humidity (RH) is a relevant environmental variable that was studied by several authors, since it has a significant impact in the thermal insulation performance of aerogel blankets, as demonstrated in Fig. 6.

Nocentini and co-authors [24] characterized new silica aerogel blankets, dried by microwave heating, for building thermal insulation. Two different fibrous networks, polyethylene terephthalate (PET) and glass fibers, were investigated. The studied blankets presented low bulk densities (110 kg·m^{-3}) and high porosities (90%), which are very similar to the values obtained for the silica aerogel itself. Both aerogel blankets have thermal conductivities in the superinsulation range, and have values lower than 0.021 W·m^{-1}·K^{-1} even in environments with high RH (Fig. 6). However, a significant reduction was observed in the specific

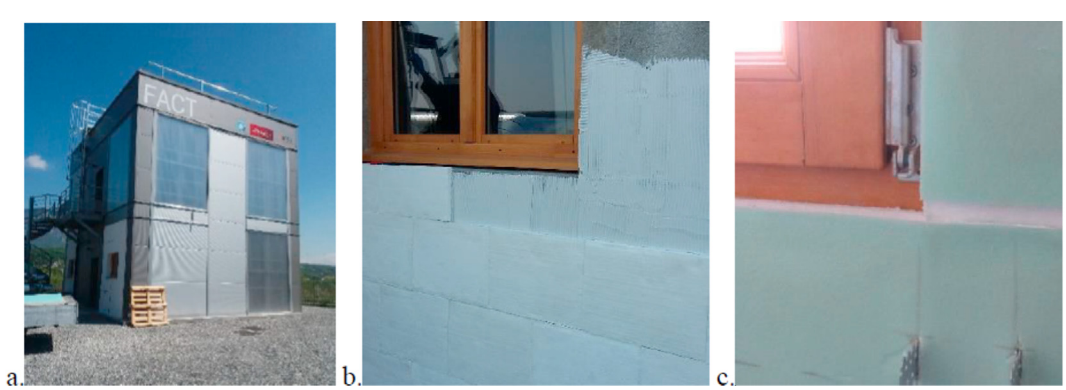

Fig. 5. Pictures of testing facilities. a) Entire FACT in the Institut National de l'Énergie Solaire (INES), France; b) the cell 1 with outdoor ETICS system, and c) the cell 2 with indoor insulation. Reprinted with permission from Ref. [209]. Copyright (2017) Elsevier.

surface areas: values of 210 $m^2 \cdot g^{-1}$ for the glass fiber composite and 310 $m^2 \cdot g^{-1}$ for the PET fiber composite, while silica aerogel featured 820 $m^2 \cdot g^{-1}$. These smaller surface area values are due to higher average pore sizes, which can justify the slight increase observed in the composites thermal conductivity (0.015 $W \cdot m^{-1} \cdot K^{-1}$), if compared with native silica aerogels, but these results regarding their thermal performance are still at least two times better than usual insulating materials. The mechanical properties were also assessed for the glass fiber composite, with the material having a compressive stress and a tensile strength perpendicular to faces (Table 2), better than for the pure silica aerogel. However, the tensile strength is still too low to satisfy the building standards [219].

Hoseini et al. [210,211] investigated the thermal performance of commercial aerogel blankets when submitted to compressive mechanical load cycles and several humidity environments. Four insulation materials were tested, 5 mm and 10 mm thick Cryogel®Z (CZ, Aspen Aerogel) and 5 mm and 8 mm thick ThermalWrap™ (TW, Cabot Corporation), under loads of up to 8 kPa [210] or, for the samples with 5 mm, in RH between 0 and 90% [211]. These tests showed that the blankets maintain their thermal efficiency even under compression. Also, after twenty compression-decompression loading cycles, the variation of the blankets thermal conductivities was inferior to 5%, confirming the excellent insulation properties of these materials [210]. Moreover, in the humidity tests [211], the obtained data showed that thermal conductivity increased over time, in cycles with constant RH, indicating that moisture is retained inside the pores. The thermal conductivity also increases, up to ~ 15%, as the RH changes from 0 to 90%, at 25 °C (Fig. 6). These results indicate that the thermal performance of these commercial aerogel-blankets is much more affected by the increase of humidity than by mechanical compression. Between the two 5 mm blankets, the CZ suffered higher changes under both tests; under high RH, a 15% increase in the thermal conductivity, and a thickness reduction of 2% after the cycles of mechanical deformation.

Besides the work developed by Hoseini et al. [211], other authors have also studied the influence of humidity levels on the aerogel blankets performance, such as Guo et al. [212], Lakatos [213] and Nosrati and Berardi [204,214]. The goal of the investigation of Guo et al. [212] was to provide a simultaneous test method and visual identification to study the heat and moisture transfer in thermal insulation materials, such as aerogel blankets. Two aerogel blankets were tested, both of which are composites of silica aerogel with a fiberglass matrix, having the same thickness and thermal conductivity (0.020 $W \cdot m^{-1} \cdot K^{-1}$) but distinct densities, one with 170 $kg \cdot m^{-3}$ named A1 and the other with 212 $kg \cdot m^{-3}$, called A2. Phenolic (PF) and polyisocyanurate (PIR) foams were selected as conventional types of insulation. In dry conditions, the thermal conductivity of the tested materials increased almost linearly by 24%, 13% and 14%, for A2, PF and PIR, respectively, as the temperature varied from 280 K to 300 K. This variation can be justified by the enhancement of gas conduction heat transfer during the temperature increase. In wet conditions, the aerogel samples thermal conductivities show around 3 and 3.3-fold the initial value with a maximum moisture content of 29% and 32% after 23 and 16 days, for A1 and A2, respectively. The increase of the thermal conductivity with the increase of moisture content is roughly linear in the initial stages. However, as the moisture content increases in a slower pace, the thermal conductivity is still rising, indicating that other factors can be causing the deterioration of their thermal conductivity. Moisture affects the connections between aerogel and fibers, causing a detach of the aerogel (Fig. 7), and the formation of powdery particles aggregates, which easily separate from the fibers.

Lakatos [213] also observed a significant change in the thermal conductivity of a glass fiber reinforced silica aerogel blanket with the variation of relative humidity, having the same trend than other aerogel blankets (Fig. 6). After the samples were submitted to an environment with 65% RH at 23 °C for 24 h, a 10% increase was observed in the thermal conductivity, while, when 90% RH was applied, the change was about 20% (Fig. 6). The thermal performance of the aerogel blankets was also evaluated after being heat treated in an oven at 70 °C for 42 days. The samples maintained their insulation capacity, thus further thermal treatment tests were conducted at temperatures up to 210 °C for 1 day. Changes in the thermal conductivity start to be observed above 180 °C, and the samples treated at 210 °C show an increase of 17% of this property.

Nosrati and Berardi [204] studied the hygrothermal characteristics of different aerogel-enhanced materials, such as synthesized

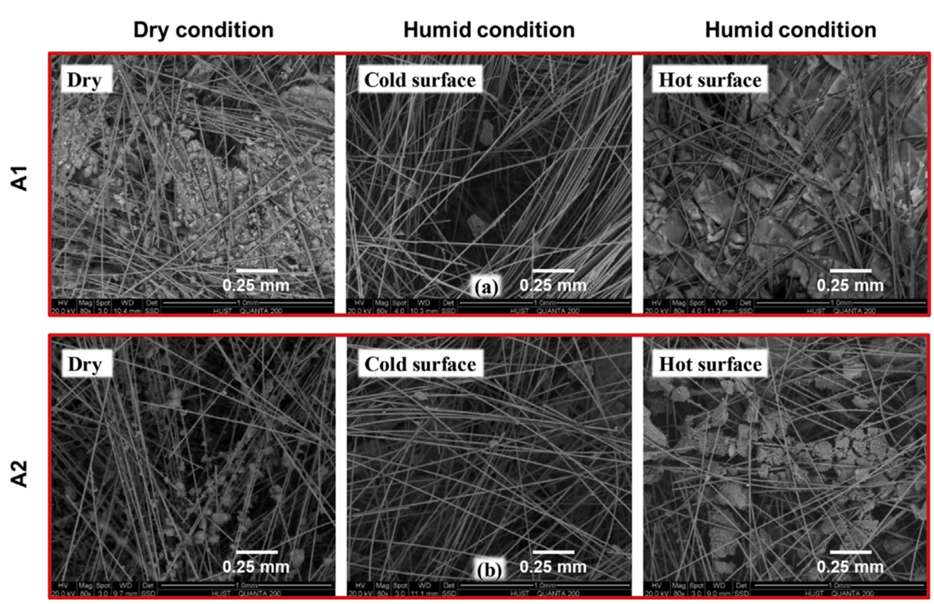

Fig. 7. SEM images of the samples under dry conditions and after being submitted to moisture tests (a) A1 (RH of 80%); (b) A2 (RH of 90%). Reprinted with permission from Ref. [212]. Copyright (2020) Elsevier.

plasters with 0–90 vol% aerogel (see Section 4.3), and commercially manufactured blankets and boards. Among the studied materials, under standard conditions, aerogel-based blankets and fiber boards presented superior thermal performance (Table 2), with the values being 2 to 3-fold lower than conventional materials used for thermal insulation. The authors found a linear relationship between thermal conductivity and temperature, as expected [76]. The conductivity shows a slight change (±7%) with the temperature, from −10 °C to 50 °C, when compared to the standard conditions (23 °C; 50% RH). Moreover, significant increase in the thermal conductivity was observed when the samples were submitted to extreme humidity. For example, for the aerogel gypsum boards an increase of 100% was observed, compared to standard conditions, when the level of RH was 95%. So, to prevent the decrease of the materials' thermal resistance under high humidity conditions, a protection layer must be considered to avoid the accumulation of moisture. These authors also studied the long-term thermal performance of the various aerogel-enhanced materials was assessed when submitted to different laboratory aging conditions [214]. The accelerated aging tests conditions included freeze–thaw cycles, elevated temperature, high humidity levels, and the exposure to cycles of high ultraviolet (UV) levels alternated to high temperature and moisture levels. The change of thermal conductivity (in %) for the aerogel-enhanced materials, under different aging factors, is reported in Fig. 8a. The most significant aging process for the deterioration of thermal performance was the high humidity. Among the studied products, the aerogel fiber board presented the best results, as it was only slightly affected by all the aging factors. Also, even after being submitted to 20 years of aging, the aerogel blanket and aerogel fiber board materials showed superior thermal performance (50% lower thermal conductivity) than non-aged conventional insulation materials – Fig. 8b.

All the works that studied the influence of humidity in the aerogel blankets attained the same conclusion, which was that the insulation performance of these materials was negatively affected by the humidity increase. Moreover, this trend is also easily confirmed in Fig. 6. These findings indicate that significant attention must be given to the environment conditions where these blankets are applied to make the most of their insulating properties. A sylilation step is a good strategy to mitigate this effect.

Although most of the work with aerogel blankets has been carried out on a laboratory scale, some studies have already started the scale-up process of these composites, as reported by Huang et al. [215], Ibrahim et al. [216], Berardi and Lakatos [217] and Kosny et al. [218].

The application of a new aerogel blanket superinsulation material for building-energy-conservation was investigated by Huang et al. [215]. The authors used a typical office building in a humid subtropical climate as a model, and analysed the effects of this new material, as well as four common insulation materials (EPS, extruded polystyrene (XPS), foamed polyurethane (PU), and GF). The experimental results show that the aerogel had the minimum optimum insulation thickness, 3.7 mm, if compared with PU (38 mm), XPS (44 mm), GF (45 mm) or EPS (70 mm) in an aerated concrete wall. When the aerogel blanket was applied with the optimum thickness in a simulation based on the typical building office, the annual cooling and heating loads were reduced by 7.5% and 18.2%, respectively. Moreover, reducing the thermal losses via building envelope leads to a decrease in the fuel consumption, and, consequently, a reduction in greenhouse gas emissions. Huang et al. [215] were able to determine the effect of the insulation materials thickness in the emissions of CO_2 and SO_2. As shown in Fig. 9, the use of aerogel blankets leads to a significant reduction in the emissions of both gases, independently of the fuel type. The aerogel materials have the best results and present the faster reduction in the emissions, with the increase of thickness, among the tested insulating materials. When using aerogel blankets, the minimum CO_2 emissions (8.169 $kg{\cdot}m^{-2}{\cdot}yr^{-1}$) were calculated with LPG fuel. Based on these results, it is possible to conclude that the use of aerogel-based materials is preferable for environmental protection and is in line with the United Nations Sustainable Development Goals (2030 agenda of UN) – Goal 13 "Climate Action", which aims the reduction of the greenhouse gas emissions as one of the priorities.

The use of aerogel blankets into two thermal insulation systems, one as external thermal insulation composite system (ETICS)

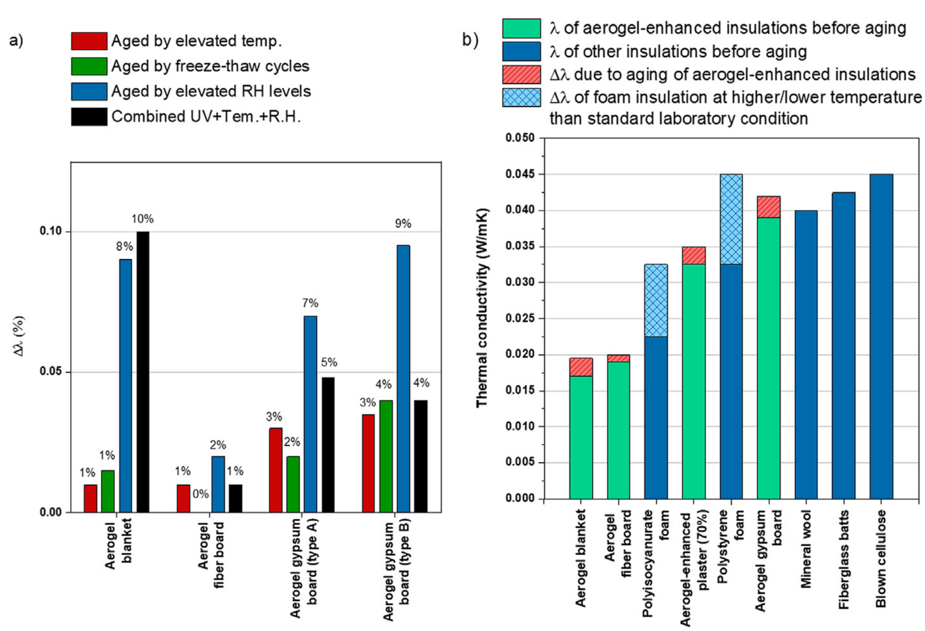

Fig. 8. a) Aging effect for an equivalent time of 20 years under various conditions on the thermal conductivity (λ) of aerogels blankets and boards. b) Comparison between the thermal conductivity of aerogel-enhanced insulations (before and after aging) and non-aged traditional insulation materials. Adapted with permission of Ref. [214]. Copyright (2018) Elsevier.

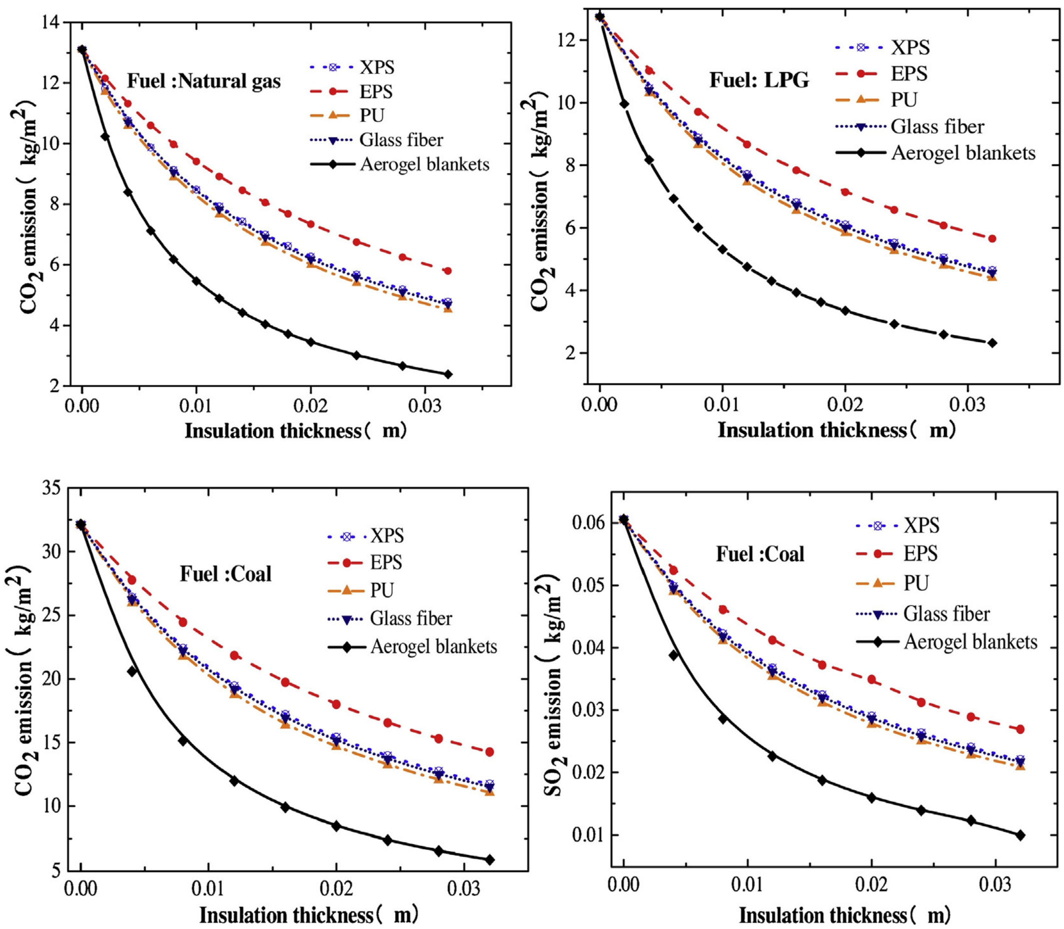

Fig. 9. Effect on CO_2 and SO_2 emissions versus the thickness of five insulation materials. Reprinted with permission from Ref. [215]. Copyright (2020) Elsevier.

and another one as internal thermal insulation multi-layer system (ITI) (Fig. 10), were studied by Ibrahim et al. [216]. The aerogel blanket by itself presented good thermal performance, even with high values of RH (Fig. 6). However, this material does not have good mechanical properties (Table 2). To be applied in buildings, due to the low tensile strength, these blankets need to be glued and anchored into a wall. When the aerogel blanket, which has 2–2.5 cm of thickness, was applied in an interior insulating system, the *U*-value decreased from 0.63 $W{\cdot}m^{-2}{\cdot}K^{-1}$ to 0.33 $W{\cdot}m^{-2}{\cdot}K^{-1}$, which is acceptable to retrofit existing buildings in France, but not for the case of new buildings (*U*-value must be lower than 0.25 $W{\cdot}m^{-2}{\cdot}K^{-1}$). The use of these materials also improved the acoustic insulation, providing a noise reduction to one quarter compared to the wall without insulation. Hygrothermal tests were also performed, and while for the interior wall long-term monitoring data is necessary to provide more conclusive results, as moisture transfer is a slow physical phenomenon, for the external insulation system, the use of aerogel blankets protected the wall against moisture risks. Concerning fire safety, for the external system, there was no ignition, and a low smoke emission was observed during a fire case. However, in the case of the internal wall, the composite ignited and released more energy, due to the higher organic content in the components.

The effect of steel anchors over the aerogel-enhanced blankets' effective thermal conductivity was studied by Berardi and Lakatos [217]. To replicate in-situ applications, the blankets were firstly glued onto the wall, and then fixed with different numbers of steel fasteners. The measurements show a deterioration of the thermal resistance of the wall, with a reduction of 15% and 45% when 3 and 6 anchors per m^2 were applied, respectively. The effective thermal conductivity was significantly affected, increasing from 0.021 $W{\cdot}m^{-1}{\cdot}K^{-1}$ without any fastener, to 0.044 $W{\cdot}m^{-1}{\cdot}K^{-1}$ when 6 fasteners per m^2 were used. To further assess the effect of the anchors, infrared thermography measurements were carried out, and revel that the temperatures through the fasteners and the wall surface are much higher for the wall with 6 fasteners per m^2. This shows that the thermal performance of aerogel-enhanced blankets has a strong dependency on the number and the materials of the used anchors, which allows a better understanding of the system and the possibility of controlling the thermal bridges effects during the installation of the blankets.

The main goal of Kosny and co-authors [218] was to characterize the thermal performance of an aerogel-based radiant barrier for residential attics. The barriers were composed by the following layers: 1.1 cm thick oriented strand board (OSB) layer, 9.0 cm air cavity, 1.0 cm laminated aerogel, again, 9.0 cm air cavity, and 1.1 cm OSB. For some tests, a reflective foil was added into the barrier. Comparative thermal performance field testing of the aerogel-based radiant barrier, as shown in Fig. 11, was performed during the summer of 2014 in climatic conditions of Albuquerque, NM, USA. This composite was able to reduce, on average, the ceiling heat flow in 36% and the attic temperature in 10–12 °C. In the simulated data, for different climates, the aerogel-based barrier allowed a temperature reduction of at least 10 °C, with the highest difference being observed in Riyadh, Saudi Arabia (15 °C). The heat flux also showed a substantial reduction, with the composite easily exceeding 35–40%, when compared to conventional insulation materials.

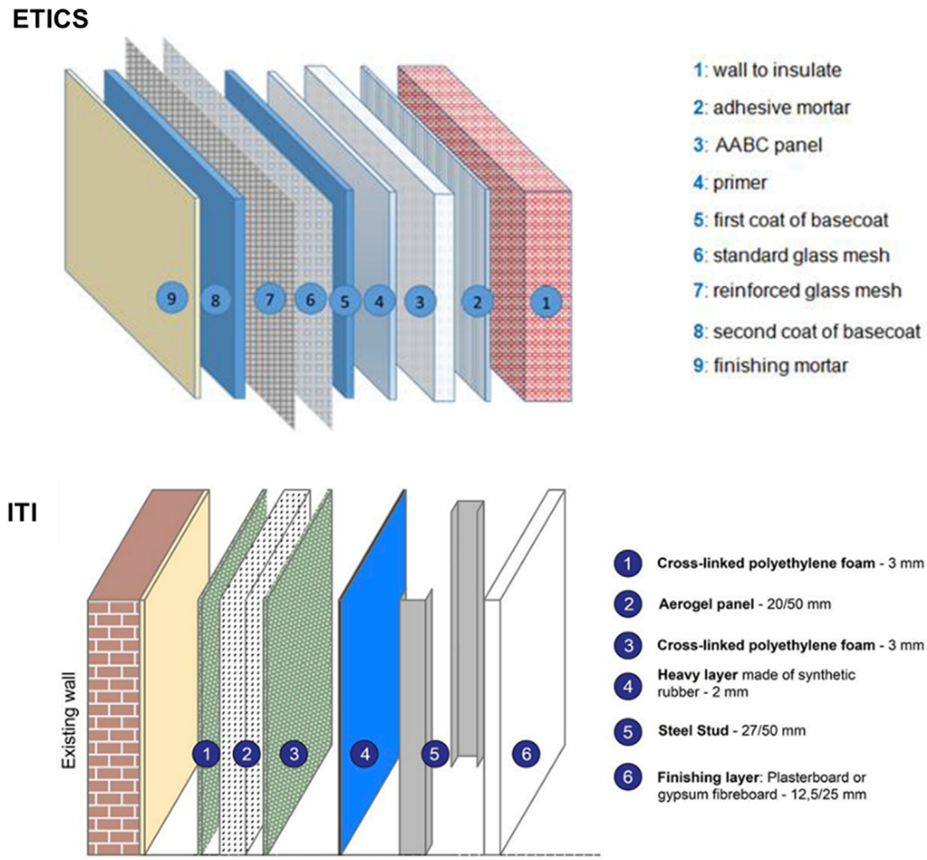

Fig. 10. Representation of the external thermal insulation composite system (ETICS) and of the internal thermal insulation multi-layer system (ITI). Adapted with permission from Ref. [216] Copyright (2019) Elsevier.

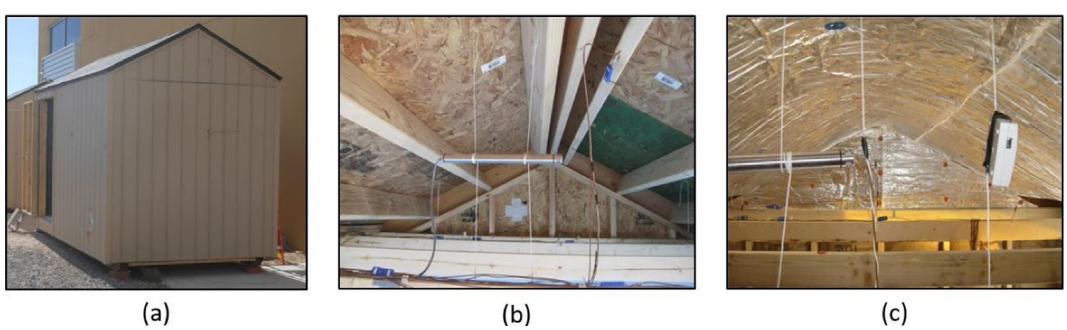

Fig. 11. (a) Test hut on the left side. (b) Views of the instrumented conventional attic, and (c) attic deck area insulated with the aerogel-based radiant barrier. Reprinted with permission from Ref. [218]. Copyright (2018) Elsevier.

Even though the thermal conductivity of aerogel blankets is affected by the installation process, as showed by Berardi and Lakatos [217], the use of these materials still reduces significantly the heat flow and temperature inside the buildings, even when tested in large-scale, as demonstrated by Huang et al. [215], Ibrahim et al. [216] and Kosny et al. [218]. The possibility of maintaining their unique properties with a low-cost production opens a larger range of possibilities for aerogel blankets and panels applications.

4.2. Cement

Another possible application of silica aerogel in buildings is their use in the preparation of composites with cement. Some of the works developed regarding these composites, as well as some properties of these materials are presented in Table 3.

The main focus of the research developed by Hanif et al. [220] was to develop an ultra-lightweight cementitious composite, with good thermal and mechanical properties, by adding fly ash cenospheres (FAC – 70 wt%) and silica aerogel (1–5 wt%) as filler materials. The addition of these materials leads to a reduction on the mechanical properties, probably due to the density decrease. However, even with 5 wt% of aerogel, the composites showed good mechanical behaviour, with a compressive strength of 18.63 MPa and a flexural strength of 3.66 MPa. Regarding the thermal properties, the composites showed a reduction in the thermal conductivities, achieving the lowest value of 0.3197 $W{\cdot}m^{-1}{\cdot}K^{-1}$ for the highest amount of aerogel. The specimens were also submitted to steady thermal tests, with this same material presenting the best results, with a 12 °C of difference between exterior and interior surfaces (7 °C higher than the material without aerogel), as shown in Fig. 12. These results can be justified by the enhancement

Table 3
Published works using composites with silica aerogel and cement for thermal insulation of buildings.

Ref.	Composite material	Amount of silica aerogel	Thermal conductivity ($W{\cdot}m^{-1}{\cdot}K^{-1}$)	Bulk density ($kg{\cdot}m^{-3}$)	Flexural strength (MPa)	Compressive strength (MPa)
Hanif et al. [220]	**Silica aerogel**: From Guangdong Alison Hi-Tech Co. **Silica aerogel-containing composite**: Ultra-lightweight cementitious composite	5 wt% (aerogel as filler)	0.32	1003	3.66	18.6
Zeng et al. [221]	**Silica aerogel**: Commercial nano-silica aerogel (Jinna Co.Ltda) **Silica aerogel-containing composite**: Nano-silica aerogel cement-based composite	10 vol% (aerogel as filler)	~0.17	~800	1.5	5.0
Lu et al. [222]	**Silica aerogel**: Commercial silica aerogel (Aerogel Technology Co. Ltd.) modified with KH-550 silane coupling agent **Silica aerogel-containing composite**: Hybrid aerogel/cement composite	25 vol% 66 vol% (aerogel substitutes part of cement paste)	0.337 0.067	1,280 390	– -	34.1 1.2

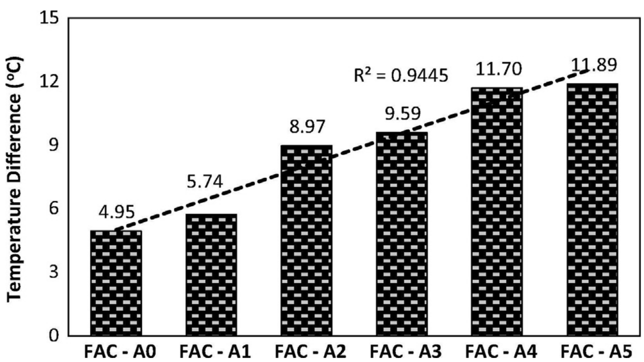

Fig. 12. Peak temperature difference between inner and outer surfaces during steady thermal test, as function of the aerogel content in a cementitious composite (from 0 – A0 – to 5 wt% – A5). Reprinted with permission from Ref. [220]. Copyright (2016) Elsevier.

of the composites pore volume with the increasing content of aerogel and also by the hollow structure of the FAC particles. With these improvements, the new developed composites are appropriate for energy conservation in buildings and constructions.

Glass bead (GB) and nano-silica aerogel (NSA) were incorporated as coarse and fine fillers, respectively, into cement-based composites by Zeng et al. [221]. As expected, the increase of NSA content (0–25 vol%) decreases the composites densities, while increasing the porosity and specific surface area (around 70% and 131.5 $m^2{\cdot}g^{-1}$, for 25 vol% of NSA). The amount of silica aerogel also reduced the thermal conductivity, from 0.36 $W{\cdot}m^{-1}{\cdot}K^{-1}$, without the addition of NSA, to 0.08 $W{\cdot}m^{-1}{\cdot}K^{-1}$, for the higher amount of NSA. The mechanical properties were also significantly affected by the addition of the aerogel, with a sharp decrease being verified after the addition of 10 vol% of NSA, with the values of compressive and flexural strengths changing from 26 and 5.8 MPa, respectively, when only GB was added to the composite, to 5 and 1.3 MPa. When the NSA amount increases further, only small variations are obtained in these properties. However, a good mechanical performance is essential to the materials application in the fields of construction, so, the use of NSA as the only filler may not be the best way to achieve improvements in both thermal and mechanical properties. The combination of silica aerogels and other fillers may lead to the desired thermal conductivity reduction while maintaining the strength of cement-based composites.

Lu and co-authors [222] studied the influence of the aerogel slurry modification with a silane coupling agent (KH-550, Qufu Yishun Chemical Co., Ltd.) in the properties of lightweight aerogel/cement composites. The surface modification contributed to a better compatibility between the aerogel slurry and the cement matrix, as this silane acted as bridging agent in the inter-phase region, between the inorganic and organic substrates. These materials show lower water absorption, if compared with the samples with commercial aerogel, and the composite with the 25 vol% of modified-aerogel content, for example, has a water absorption rate of 20.5 vol%. As expected, with the increase of volume replacement of cement paste by aerogel slurry, a decrease in the composites densities was observed (Table 3), having the reference sample a density of 1805 $kg{\cdot}m^{-3}$. Higher aerogel content also yields to lower thermal conductivity, with the values dropping from 0.618 $W{\cdot}m^{-1}{\cdot}K^{-1}$ to 0.067 $W{\cdot}m^{-1}{\cdot}K^{-1}$, for 0 vol% and 66 vol% of modified aerogel content, respectively. However, the higher content of aerogel causes a substantial reduction in the composites' compressive strength (Table 3), if compared with the reference sample (94.1 MPa). This decrease can be explained by the fact that the hydrophobic aerogel repels the surrounding aqueous solution, preventing the reaction between the cement and the aerogel, and, consequently, affecting the samples strength [20]. The composites obtained with the modified aerogel always presented better mechanical properties than the ones synthesized with the commercial ones, at the same density. For example, when the slurry content is 25 vol%, the composite with the commercial aerogel shows a compressive strength of 26.7 MPa, a result 22% lower than for the sample with modified aerogel. These results indicate that the samples obtained with the modified silica aerogel slurry have great potential to be used in the thermal insulation systems of building.

From the reported works, it is observed that the improvement in the thermal insulation features of cement-based pastes can be achieved compounding them with aerogel. However, with this addition, in general, the mechanical resistance of the composites deteriorates. Still, there are some intermediate amounts that allow a good compromise between these two important characteristics.

4.3. Mortars, plasters and renders

To improve the thermal conductivity of building materials, silica aerogels can also be incorporated into mortars, plasters and renders. It is also worth mentioning that the words plaster and render have different meanings in UK and US English, and are often used interchangeably, so the material used in rendering is often called plaster [223]. The studies published with the focus in these materials are described in Tables 4 and 6.

The main goal of Ng et al. [193] was to reduce the thermal conductivity of ultra-high performance concrete (UHPC) composites without compromising their mechanical strength. The authors prepared aerogel-incorporated mortars with up to 80 vol% of aerogels to develop the UHPC samples. With the increase of aerogel content, a decrease in the compressive strength and the thermal conductivity was detected, with this same trend also being noticed for other aerogel-incorporated mortars, as observed in Fig. 13. With the

Table 4
Published works about mortars developed with silica aerogel for thermal insulation of buildings.

Ref.	Composite material	Amount of silica aerogel	Thermal conductivity ($W·m^{-1}·K^{-1}$)	Bulk density ($kg·m^{-3}$)	Flexural strength (MPa)	Compressive strength (MPa)
Ng et al. [193 224 225]	**Silica aerogel**: P100, from Cabot Corporation **Silica aerogel-containing composite:** Aerogel-incorporated mortars	50 vol% 60 vol% 70 vol% (aerogel as aggregate)	0.55 ~0.4 0.25	~1350 ~1150 –	~5.0 3.0 –	20.0 18.1 1.7
Gomes et al. [226]	**Silica aerogel precursor**: TEOS modified with HMDZ **Silica aerogel-containing composite**: Aerogel-based mortars	19.7 wt% (aerogel as aggregate)	0.0571	411.8	–	–
Gomes et al. [227]	**Silica aerogel-containing composite**: Mortar with expanded polystyrene and silica aerogel	50 wt%	0.035	138	–	–
Zhu et al. [228]	**Silica aerogel**: P300, from Cabot **Silica aerogel-containing composite**: Aerogel mortar	50 vol% (aerogel as aggregate)	~0.2	1140	1.5	6.0
Al Zaidi et al. [229]	**Silica aerogel**: From Rem-Tech. **Silica aerogel-containing composite**: Mortar containing aerogel	60 vol% (aerogel as aggregate)	0.833	–	5.96	31.05
Bostanci [230]	**Silica aerogel**: From ENSATE Insulation Technologies **Silica aerogel-containing composite**: Alkali-activated slag mortars	0.3 wt% (aerogel as aggregate)	0.89	–	–	29.24
Abbas et al. [231]	**Silica aerogel precursor**: Sodium silicate (from Rice rusk) modified with TMCS **Silica aerogel-containing composite**: Aerogel-incorporated cement-based composites	62 vol% (aerogel as aggregate)	0.327	1133	–	8.85
Pedroso et al. [232]	**Silica aerogel**: Kwark® aerogel from Enersens **Silica aerogel-containing composite**: Cement-based mortar (nanoSIR)	~37 wt% (aerogel as aggregate)	0.029 (at 10 °C)	160	0.099	0.227

Table 5
Results for hardened state at 28 days of curing of mortars with EPS and EPS + silica aerogel. Reprinted with permission from Ref. [227] Copyright (2018) Elsevier.

Tests	Samples	ρ ($kg·m^{-3}$)	CV_ρ	Ψ ($m^3·m^{-3}$)	λ ($W·m^{-1}·K^{-1}$)	CV_λ	$\lambda_{23\ °C,28\ d}$ ($W·m^{-1}·K^{-1}$)
MTPS	A^{EPS}	216	0.030	0.0063	0.054	0.009	0.054
	A^{EPS+A}	140	0.020	0.0051	0.041*	0.001	0.041
TLS	A^{EPS}	229	0.039	0.0081	0.058	0.032	0.058
	A^{EPS+A}	138	0.053	0.0051	0.035	0.059	0.035
HFM1	A^{EPS}	222	0.076	0.0073	0.067	0.047	0.064
	A^{EPS+A}	119	–	0.0050	0.031	–	0.029
HFM2	A^{EPS}	228	~0	–	0.053	0.169	0.050
	A^{EPS+A}	135	–	–	0.029	0.012	0.027
Lee's disk	A^{EPS}	225	–	–	0.056	–	0.055
	A^{EPS+A}	138	–	–	0.037	–	0.036

ρ_b = bulk density; CV – coefficient of variation (ratio between standard deviation to the mean); Ψ – moisture content; λ – thermal conductivity; $\lambda_{23\ °C,28\ d}$ – thermal conductivity for 23 °C at 28 days of curing (approximately the IIb condition of ISO 10456 [236]); A^{EPS} – industrial thermal insulating mortar with EPS; A^{EPS+A} – formulation with the incorporation of silica aerogel in the A^{EPS}; – not available. * Inaccurate value near the threshold low limit measurement range of MTPS.

Table 6
Published works related to the development of plasters and renders with silica aerogel for thermal insulation of buildings.

Ref.	Composite material	Amount of silica aerogel	Thermal conductivity ($W·m^{-1}·K^{-1}$)	Bulk density ($kg·m^{-3}$)
Nosrati and Berardi [204]	**Silica aerogel**: P300, from Cabot Corporation **Silica aerogel-containing composite:** Aerogel-enhanced plaster	25–90 vol%	0.1136–0.0268	735–199
Buratti et al. [241]	**Silica aerogel**: From Cabot Corporation **Silica aerogel-containing composite**: Aerogel-based plaster	80 vol%	0.05	300
Westgate et al. [242]	**Silica aerogel**: From Aerogel UK **Silica aerogel-containing composite**: Lime-based plaster	49.5 vol% (aerogel as aggregate)	0.1	682
Ibrahim et al. [243]	**Silica aerogel**: Hydrophobic silica aerogel **Silica aerogel-containing composite**: Aerogel-based rendering	–	0.026 (at 10 °C)	120
De Fátima Júlio et al. [244]	**Silica aerogel precursor**: TEOS modified with HMDZ **Silica aerogel-containing composite**: Aerogel-based renders	100 vol% (aerogel as aggregate)	0.085	412
Wakili et al. [245]	**Silica aerogel-containing composite**: Aerogel based rendering	–	0.028	–

higher amount of aerogel content, materials with a thermal conductivity of 0.30 $W·m^{-1}·K^{-1}$ were obtained. However, this composite completely lost its strength, possibly due to the insufficient amount of binder. With an aerogel content of 50 vol%, the authors were able to obtain a composite with a better compressive strength (Table 4), but even with the reduction in the aerogel amount the developed system was unsuitable to be used as a standalone system for insulating purposes. To overcome the

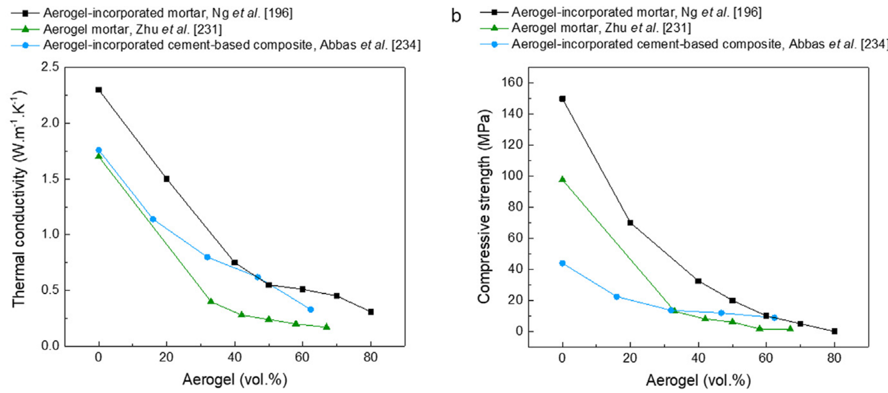

Fig. 13. Variation in a) thermal conductivity and b) compressive strength of mortars as a function of aerogel amount (vol%).

applicability limitation, but maintaining a significant thermal conductivity reduction (pure UHPC has a thermal conductivity of 2.3 $W{\cdot}m^{-1}{\cdot}K^{-1}$), the authors suggested the incorporation of other binder materials with low thermal conductivities, as well as improving the binding force between the aerogel and the cement matrix by incorporating amphiphilic materials for example.

The influence of the storing and curing conditions on the thermal insulation and mechanical strength of aerogel-incorporated mortars was also investigated by Ng et al. [224]. The authors tested two different conditions after casting (24 h) and three conditions during the curing process (28 days), with and without the addition of aerogel. A significant influence of the storage/curing conditions was detected in mechanical and thermal properties. When 70 vol% of aerogel was added into the sample, a substantial reduction in the compressive strength, for all the conditions, was observed, which can be attributed to the higher aerogel/binder ratio. Although that the samples with 70 vol% of aerogel have lower thermal conductivities, their poor mechanical strength determined their exclusion. An effective content of 60 vol% of aerogel with the conditions of storing at 80 °C (dry) and cured at 80 °C submerged in water produced the samples with the best properties.

As a continuation of their work, Ng and co-authors [225] decided to test calcined clays as binders in the aerogel-incorporated formulations, in order to further improve the insulating properties of the composites, as the cement binder usually contributes to a large part of the bulk volume, and thus determines the materials' thermal properties. The replacement of cement by calcined clay caused an enhancement in the thermal insulation properties of the composites, with an improvement of the thermal conductivity values up to 20% when the amount of aerogel was between 40 vol% and 70 vol%, and up to 40% when more than 70 vol% of aerogel was used. However, when more than 40% by weight of binder (cement) was substituted by clay, worse mechanical behaviour was observed, especially for the clay rich in kaolin. While, when only 35% of cement was replaced, the compressive strengths remained similar to the ones without the substitution. This article showed a new perspective for synthesizing insulating concretes, which can lead to the development of more sustainable materials, since the cement production has a high carbon dioxide footprint [233,234].

A study to evaluate the influence of moisture in the thermal conductivity of mortars was conducted by Gomes et al. [226]. A total of 17 mortars having different lightweight and insulating aggregates (silica aerogel, expanded cork granules, and expanded clay) were tested. Two silica aerogels were used for this work, one with a bulk density of ~70 $kg{\cdot}m^{-3}$, and the other with ~306 $kg{\cdot}m^{-3}$. All these mortars have low bulk densities and can be classified as T1 or T2 (λ of <0.1 and 0.2 $W{\cdot}m^{-1}{\cdot}K^{-1}$, respectively) by the European standard EN 998-1 [235]. The behaviour of the thermal conductivities for the different mortars in the presence of moisture is presented in Fig. 14. The samples containing expanded clay mortar (N5 and N6) are more sensitive to moisture content than the mortars with expanded cork and/or aerogels. This difference can be explained by the hydrophilic character of the

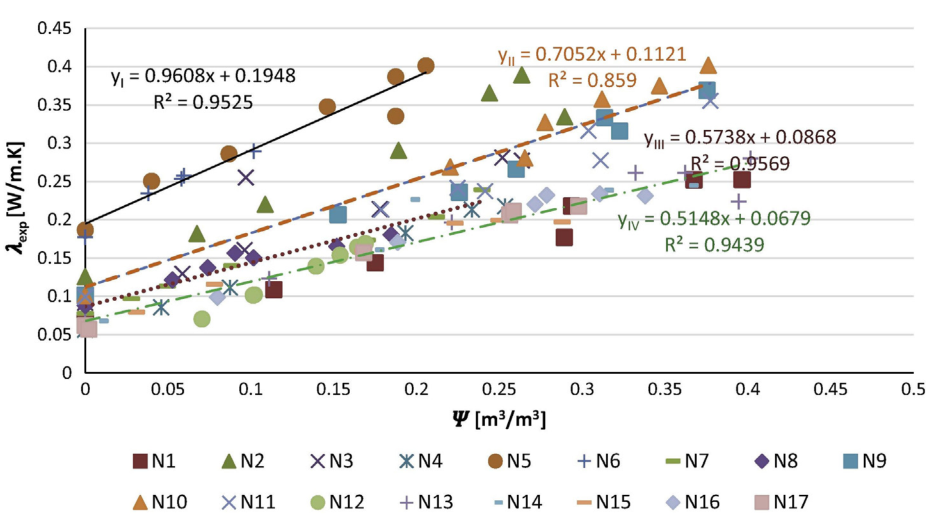

Fig. 14. Thermal conductivity (λ_{exp}) as a function of moisture content (ψ) for mortars composed with different aggregates. Reprinted with permission from Ref. [226]. Copyright (2017) Elsevier.

expanded clay, while the cork and the used aerogels have a hydrophobic nature. This study shows that the thermal conductivity of all samples is significantly dependent on the moisture content, as already shown for the case of cement, panels and blankets (Sections 4.1 and 4.2).

The aim of a second work presented by Gomes et al. [227] was to compare the impact of different measuring conditions and methods on the thermal conductivity of thermal insulating mortars, one with only EPS granules and the other with both EPS and silica aerogel. The thermal conductivity was evaluated by two steady-state methods (heat flow meter (HFM) and Lee's disk) and two transient methods (modified transient plane source (MTPS) and transient line source (TLS)). The first factor assessed by the authors was the influence of the addition of silica aerogel into the mortar, being observed a reduction of up to 55% on the thermal conductivity, and the density followed the same trend (Table 5). As verified in other works here reported, Gomes and co-authors [227] concluded that the moisture content has a significant impact in the thermal insulation properties of these materials. Taking into account all the methods applied to measure the thermal conductivity, and the different operating temperatures for each one, the obtained results were converted to 23 °C (conditions IIa for dry state and IIb for 28 days of curing from ISO 10456 [236]) to allow a direct comparison. A considerable variation between the results was observed, with differences up to 14% for the EPS based mortar and 21% for EPS + aerogel mortar – Table 5. Usually the steady state methods give lower values of thermal conductivity than the transient methods. By analysing the data, the authors were able to conclude that the transient methods (MTPS and TLS) are more appropriate for small samples, and that they also demand less time and operator dependency and have more simple procedures than the steady-state methodologies. These results highlight the importance of specifying the conditions and methods used to measure the thermal conductivity of highly insulating materials.

With the aim of improving the fire safety of high-performance concrete in tunnels, Zhu et al. [228] developed a composite with a highly insulating aerogel-cement mortar layer. The aerogel granules were evenly distributed in the cementitious matrix, however their pore structure was altered at the cement/aerogel interface, as a result of a chemical reaction between the silica and the alkaline pore solution. While the composites' thermal conductivity, for the different amounts of aerogel in the mortars (Fig. 13a), was close to the expected range of cellular concrete with comparable density, the composites' mechanical strength was lower than the ones reported for this concrete. With 31 days of cure, the reference sample, without the aerogel layer, presents a compressive strength of 97.7 MPa, while the addition of aerogel leads to a significant reduction (~98.6%) of the materials' mechanical strength (Fig. 13b). However, even with such significant decrease, the mechanical properties of these mortars were adequate for brushing or spraying applications of thermal insulation layers. A series of preliminary tests of high-temperature spalling were performed, and layers of 40–50 mm of aerogel mortars were able to prevent fire spalling of the studied concrete cubes.

The influence of different storage conditions in the thermal and mechanical properties of mortars prepared with the replacement of 60 vol% of the cement with aerogel, 50% of the sand with fly ash, and by the addition of nano-silica, has been investigated by Al Zaidi et al. [229]. Three storage methods were used, with the samples being submitted to: (1) air drying for 24 h, then stored in air for 7 days at 25 °C and 50% RH, and then kept open until test day; (2) air drying for 24 h, then kept immersed in water for 7 days, and then dried in air at room temperature for 21 days; (3) a waiting period of 24 h and then dipped in water for 28 days, and finally dried in air for 24 h at room temperature. The second curing methodology showed the best results regarding compressive strength, with the values being in the range of 29.3 and 31 MPa. As the worse results in the compressive strength were obtained for the first method, it can be concluded that the water has an important role in improving the mechanical properties of these composites. As for the thermal conductivity, the samples submitted to the first curing method showed values changing between 0.762 and 0.865 $W{\cdot}m^{-1}{\cdot}K^{-1}$. The second method presented relatively similar results (from 0.75 to 0.973 $W{\cdot}m^{-1}{\cdot}K^{-1}$), indicating that the presence of water, during the curing process, does not affect much the samples thermal performance. However, the obtained thermal conductivities were high when compared to other systems with the same content of aerogel (Table 4), and considering the properties of the aerogel given by the supplier REM-Tech [237]. This may be possibly a result of the pre-treatment of the aerogel powder with hot methanol, but it is most likely the effect of moisture retained in the samples (the thermal conductivity values for the samples with curing method 3 were not significantly different from those for the samples from curing methods 1 and 2) [229]. It should also be referred that the authors did not perform the measurement on samples without the aerogel, which makes difficult to conclude about its effect on the thermal conductivity. Moreover, the used thermal conductivity analyser performs better in homogenous samples, which is not the case.

The effect of incorporating small amounts of silica aerogel and scrap rubber into alkali-activated slag mortars was studied by Bostanci [230]. When 0.3 wt% of silica aerogel was added to the system, a decrease to 1.0 $W{\cdot}m^{-1}{\cdot}K^{-1}$ was observed in the thermal conductivity (reference sample: 1.32 $W{\cdot}m^{-1}{\cdot}K^{-1}$). However, when the amount of aerogel was of 0.6 wt%, a remarkable increase in the thermal conductivity was verified (1.29 $W{\cdot}m^{-1}{\cdot}K^{-1}$), if compared to the system with lower aerogel content. For both amounts of aerogel, the addition of scrap rubber enhanced the thermal insulation properties of the composites. A decrease to 0.89 $W{\cdot}m^{-1}{\cdot}K^{-1}$ was observed in the thermal conductivity of the mortars when 0.3 wt% of aerogel and 3 wt% of scrap rubber were added to the system, indicating a synergistic effect of these materials when the optimum content was used. Although the addition of either silica aerogel or scrap rubber led to lower strengths of the composites, when both components were added, the composite showed a 48.35% and 77.55% increase in the compressive toughness and post–peak compressive toughness, respectively. As mentioned before, a small amount of silica aerogel or rubber particles led to a decrease in the thermal conductivity of the calcium silicate structure, while higher contents of aerogel caused an increase in this property. The authors explain that the rubber particles were coated with a thicker and well-conductive layer of cement in a porous network caused by the higher aerogel amount (0.6 wt%), indicating a cumulative effect in the heat transfer, which was caused by the interaction between cement, rubber and aerogel. However, an increase in the thermal conductivity was also observed in the sample without rubber. Thus, it is likely that other factors were also affecting the thermal properties of these samples. One possible explanation is a higher water retention during the curing process, as the aerogel used here is hydrophilic.

Abbas et al. [231] synthesized an aerogel using rice husk, an agronomical waste. The mortar samples were prepared with different percentages of sand replacement by aerogel (0–100 vol%). A decrease trend was observed in the composite density with the increase of aerogel amount, as values changed from 2102 to 1133 $kg{\cdot}m^{-3}$. Two samples (75 and 100 vol% of aerogel) presented densities inferior to 1300 $kg.m^{-3}$, so these mortar-based composites can be labelled as "ultra-lightweight". The authors were able to reduce around 80% of the samples' thermal conductivity, from 1.76 to 0.33 $W{\cdot}m^{-1}{\cdot}K^{-1}$, when the aggregate (sand) was totally replaced by silica aerogel (Fig. 13a). However, such exchange contributed to a significant decrease in the compressive strength. This variation was not linear, having a drastic variation for lower ratios of aerogel, as observed in Fig. 13b. Even though the reduction in the mechanical properties was substantial, the decrease was inferior if compared with other works, and a 5-fold decrease was obtained in the thermal conductivity, indicating that green sources, such as rice rusk, can be used for the development of new building materials.

A superinsulating thermal render to be applied in the Mediterranean climate zone was developed by Pedroso et al. [232] by incorporating silica aerogel. The authors obtained a lightweight cement-based composite (nanoSIR) with high thermal insulation performance, featuring a thermal conductivity of 0.029 $W{\cdot}m^{-1}{\cdot}K^{-1}$ and a density of 160 $kg{\cdot}m^{-3}$. The render formulation shows low values of mechanical properties, however this is a positive result for the flexural strength (0.099 MPa) and the dynamic modulus of elasticity (50.01 MPa), as these indicate the ability of the material to move with the support. But as the compressive strength is also low (Table 4) additional mechanical reinforcement is needed. The samples also present a high water-vapour permeability, but a low resistance to liquid water which can limit their external applications. Due to the presented properties, the developed composite can be used in both new construction and rehabilitation. Such properties were improved by designing a multilayer system, with a protective finishing layer (nanoSIR.SYS) [238].

The authors show that this multilayer system can be applied for energy saving in buildings, with a significant improvement in the mechanical and water absorption behaviours if compared with the nanoSIR by itself. A reduction in the results of the impact resistance test (hard-body impact 3 J [239]) was observed, with the nanoSIR having values of 30.25 mm and the nanoSIR.SYS of 20.20 mm, and significant performance improvements in hardness (pendulum hammer PT [240]), with the results increasing from 59.4 for the nanoSIR to 73.10 for the nanoSIR.SYS. A substantial reduction in the permeability to liquid water was obtained, achieving values as low as 0.022 $kg{\cdot}m^{-2}{\cdot}min^{-0.5}$ for the nanoSIR.SYS. Thus, when applied in buildings, this multilayer system can provide both resistance to mechanical impacts and high thermal insulation, while avoiding liquid water penetration. This solution has competitive results, which encourage its test in real conditions.

As already mentioned, the incorporation of silica aerogels in plasters and renders is also possible. Different studies are being developed with these materials, and some of these works are reported in Table 6.

For the plasters studied by Nosrati and Berardi [204], the thermal conductivity decreases as the amount of aerogel increases (0–90 vol%), as expected. However, for the higher volumes of aerogel the mechanical properties are substantially affected, preventing their use [204].

The influence of the aerogel granules size on thermal and acoustic properties was investigated by Buratti et al. [241]. First, the authors studied the silica aerogel granules by themselves. The lowest value of thermal conductivity, 19.6 $mW{\cdot}m^{-1}{\cdot}K^{-1}$, was obtained for the smaller granules (0.01–1.2 mm diameter), a reduction of 17% if compared with the larger granules (0.7–4.0 mm). This difference can be justified by the fact that, as the granule size decreases, the voids also become smaller, reducing the heat transfer by convection and radiation. The best sound insulation was also obtained for the smaller granules, with a transmission loss (TL) of 17 dB at 1700 Hz for 40 mm thickness. Due to the remarkable properties of silica aerogels, composite plasters and translucent polycarbonate panels were developed by the authors. The aerogel-based plaster showed better acoustic performance, absorption coefficient equal to 0.29 at 1050 Hz, than conventional plasters, which have an absorption coefficient of 0.1. Also, the thermal conductivity was reduced from 0.7 $W{\cdot}m^{-1}{\cdot}K^{-1}$ to 0.05 $W{\cdot}m^{-1}{\cdot}K^{-1}$. When the silica granules were added into the interspace of a multi-sheet polycarbonate panel, the TL increased around 3–5 dB in the 280–1200 Hz frequency range, if compared with the sample with air in the interspace.

Lime-based plasters, with lime putty as the binder and a mixture of sand and aerogel granules, in different proportions, as aggregate, were synthesized by Westgate and co-authors [242]. The addition of aerogel has a substantial impact in the thermal efficiency of the composite, reducing their thermal conductivity from 0.5 $W{\cdot}m^{-1}{\cdot}K^{-1}$, without aerogel, to values below 0.1 $W{\cdot}m^{-1}{\cdot}K^{-1}$, with almost 50 vol% of aerogel in the system. The aerogel also has a positive influence in the moisture vapour permeability. The mechanical performance was significantly affected by the silica materials' incorporation, with a reduction in the strength. However, the presence of other components in the composite, such as polypropylene fibers, gave the material a high level of flexibility and toughness, which can be an advantage, as the plaster can accommodate building "movement".

Experimental and numerical studies were performed by Ibrahim et al. [243] with the goal of determining the optimum aerogel-based insulating rendering thickness for different climates. The composition of the insulating coating based on the (super)insulating silica aerogels is described in a patent [246]. The first step in their study was to compare the necessary thickness of different insulating materials for retrofitting the exterior envelope of an old house, as showed in Fig. 15a. A significant difference was observed in the materials thickness, with the aerogel-based render having the smallest thickness required to achieve the insulation target. In the sequence, the aerogel-based material was applied in a full-scale test facility developed in 2008 by the French National Solar Energy Institute (INES), as exhibited in Fig. 15b. The authors established a numerical model for the heat transfer process that was validated by the on-site measurements of the test facility. Besides, the authors were able to also optimize the rendering thickness for different climates, with results showing that the optimum thickness for the cities of Nice and Moscow is of approximately 1.7 and 4.4 cm, respectively. The payback period when the best thickness is applied is in the range of 1.4–2.7 years depending on the climate.

The influence of three types of aerogel, used as a substituent of the silica sand, in aerogel-based renders was studied by De Fátima Júlio et al. [244]. The first one was an inorganic aerogel based on TEOS, the second was TEOS-based modified with HMDZ and the last was a commercial aerogel, with the two first being dried under subcritical conditions, while the last in supercritical conditions. When the inorganic aerogel was used to replace the sand in the material, a significant decrease of the thermal conductivity was observed, with a reduction of 56% when 24 vol% of sand was replaced by aerogel, and a decrease of 92% when only aerogel was applied in the material. However, these materials required a water/cement weight ratio of 2 (instead of 1 as used in the reference) to reach an appropriate workability, which led to mortars with an inadequate cohesion. The use of hybrid aerogels can surpass this problem, thus modified and commercial aerogels were incorporated in the render mixtures. The aerogel modified with HMDZ showed higher specific surface areas and total pore volume than the commercial one, probably due to the lower average of pore size. But, when 100% of sand was replaced by hybrid aerogels in the mixture, all samples, for both modified and commercial aerogels, were classified as T1 thermal mortar ($\lambda < 0.1$ $W{\cdot}m^{-1}{\cdot}K^{-1}$). As both hybrid aerogels achieved good thermal insulation properties, the use of a material dried by a subcritical methodology is advantageous, as it reduces the safety risks for manufacturers and appliers, and leads to a more sustainable render.

The first application of a commercially available aerogel-based render, for energy efficient retrofit on the external façades of a 30 m high building, was reported by Wakili et al. [245]. The investigated buildings are part of one of the last prefabricated concrete

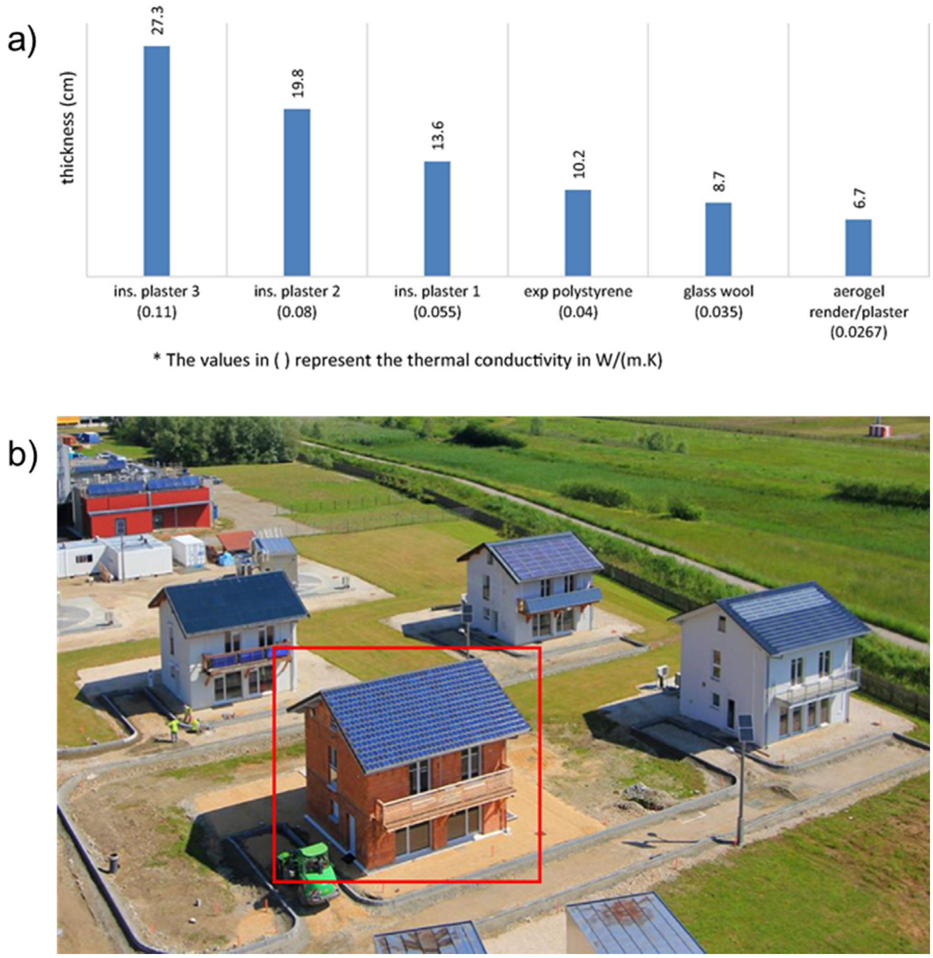

Fig. 15. a) Comparison of the thickness required to retrofit an old exterior envelope from an initial *U*-value of 6.4 W/(m^2·K) to a target *U*-value of 0.4 W/(m^2·K). b) INES experimental platform and the experimental test house in red (note: this figure was taken before applying the rendering). Reprinted with permission from Ref. [243]. Copyright (2015) Elsevier. (For interpretation of the references to colour in this figure legend, the reader is referred to the web version of this article.)

building series (Plattenbau) built in 1989–1990 in the former German Democratic Republic. An aerogel-based rendering with 6 cm of thickness was applied into a whole façade of the building, approximately 11,100 m^2, but to ensure their stability, a wavy metallic grid was fixed prior the application of this rendering. For comparison, similar neighbouring buildings were also investigated, one building remaining without insulation and another receiving a conventional perlite-based insulating. Based on hygrothermal simulations, the authors concluded that the best finish needs to be water repellent but vapour open, to avoid damages caused by moisture accumulation. In terms of thermal properties, the infrared pictures presented in Fig. 16 show the improvement caused by the aerogel-based rendering, as a reduced façade surface temperature is observed, as well as the disappearance of the thermal bridges caused by the gap between the concrete plates. Besides, a reduction of the *U*-value from its original value (1.0 W·m^{-2}·K^{-1}) to around 0.3 W·m^{-2}·K^{-1} was achieved when the aerogel solution was applied.

4.4. Concrete

Composites with silica aerogel can also be prepared to be used as structural materials such as concrete. The studies including these composites are reported in Table 7.

Fickler and co-authors [247] were able to develop a high performance aerogel concrete by controlling the amount of silica aerogel in the composite and the conditions of the final material storage. The authors concluded that the influence of the heat treatment during storage is negligible on the composite compressive strength. They were able to obtain materials with compressive strengths as high as 23.6 MPa. However, a significant increase in the density and thermal conductivity (1170 kg·m^{-3} and 0.37 W·m^{-1}·K^{-1}, respectively) were observed in these composites. The most appropriate mixture, with 60 vol% of aerogel in the cement matrix, showed a density of 860 kg·m^{-3} and achieved a compressive strength of 10 MPa, while having a thermal conductivity of 0.17 W·m^{-1}·K^{-1} (Table 7).

A novel foam concrete (FC) reinforced with silica aerogel (FC-SA) was produced by Liu et al. [248]. The authors synthesized the material using three different technologies, the sol–gel technique, vacuum impregnation method and rapid supercritical drying process. The silica aerogel can fill up to 74 vol% of the FC matrix, being evenly distributed through the porous structure. The composite FC-SA has a thermal conductivity 48.4% lower than the FC, while maintaining good mechanical properties, with a flexural and compression strength of 0.62 MPa and 1.12 MPa, respectively. Besides the materials' characterization, the authors performed simulations regarding the energy conservation effect when applying the materials in building envelopes. In Chicago, that has a cold winter, the use of FC-SA leads to 98.3 MW·h (6.64%) of energy saving in a whole winter. While in hot areas, such as Miami, applying FC-SA, to replace traditional concrete materials, reduces not only space cooling energy consumption (80.7 MW·h – 6.07%) but also the cooling water usage (1122.4 m^3 – 6.62%). With these results, and

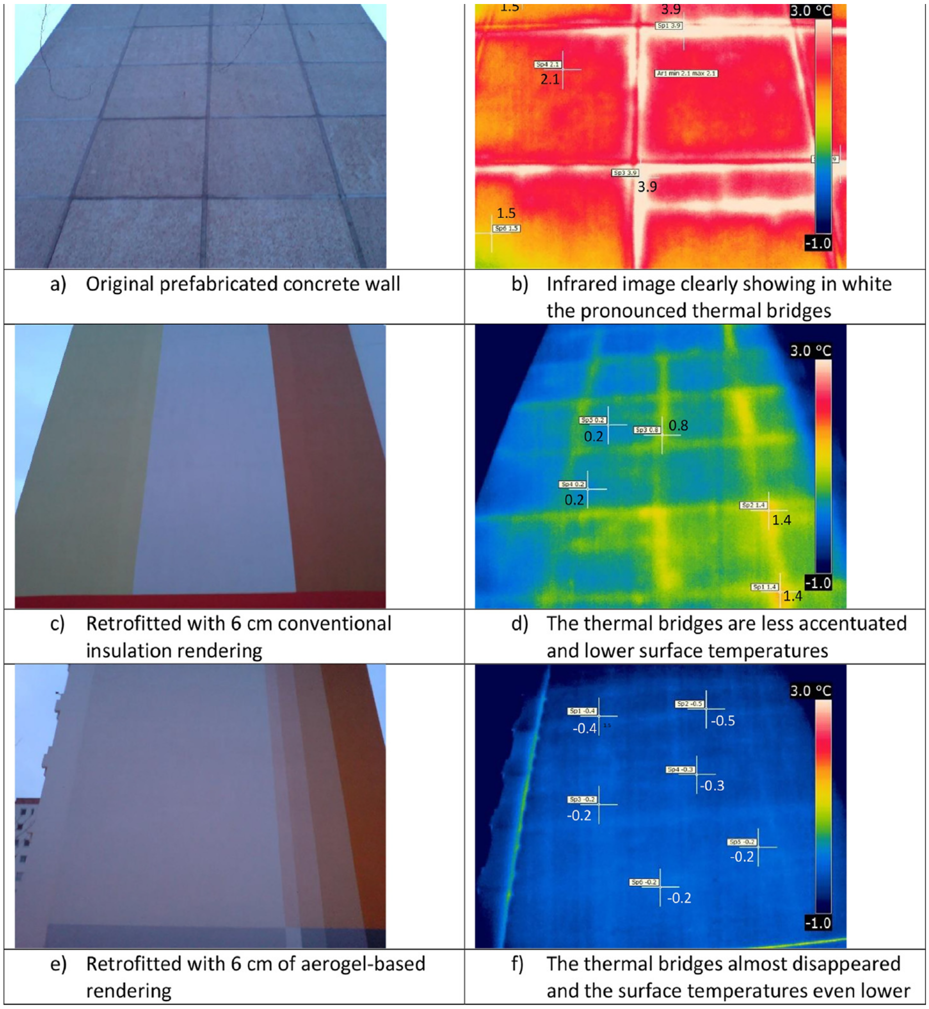

Fig. 16. Visual and corresponding infrared pictures of an untreated wall and the two cases of conventional insulating rendering and aerogel-based rendering applied to it. Reprinted with permission from Ref. [245] Copyright (2018) Elsevier.

Table 7
Published works using composites with silica aerogel and concrete for thermal insulation of buildings.

Ref.	Composite material	Amount of silica aerogel	Thermal conductivity ($W{\cdot}m^{-1}{\cdot}K^{-1}$)	Bulk density ($kg{\cdot}m^{-3}$)	Flexural strength (MPa)	Compressive strength (MPa)
Fickler et al. [247]	**Silica aerogel**: Silica aerogel granules **Silica aerogel-containing composite**: High performance aerogel concrete	60 vol% of the cement matrix	0.17	860	–	10.0
Liu et al. [248]	**Silica aerogel precursor**: TEOS **Silica aerogel-containing composite**: Foam concrete reinforced with silica aerogel	74 vol% of the foam	0.049	392	0.62	1.12
Li et al. [249]	**Silica aerogel precursor**: TEOS modified with TMCS **Silica aerogel-containing composite**: Aerogel foam concrete	30.8 vol% of the slurry	0.049	198	–	–
Wang et al. [250]	**Silica aerogel**: P100 from Cabot Co. **Silica aerogel-containing composite**: Aerogel-incorporated concrete	60 vol% (aerogel as aggregate)	0.18	1183	–	–
Yoon et al. [251]	**Silica aerogel precursor**: MTMS and TEOS **Silica aerogel-containing composite**: Nano-aerogel-embedded foam concrete	–	0.086	310		0.78

the good mechanical and thermal performances showed by this new material, the FC-SA can be used in building exterior wall applications.

The optimization of an aerogel foam concrete thermal conductivity was performed by Li et al. [249]. Based on a model, the authors studied the influence of aerogel content, cement amount and porosity on the composites thermal performance and were able to obtain a ternary variable graph (Fig. 17), which allowed a clearer view of the effect of each factor. By analysing Fig. 17, one can see that, for example, when the composites porosity is 0.5, and a volume ratio of aerogel 0.45 is added to the system, the thermal conductivity decreases by 90.4%, if compared to the concrete

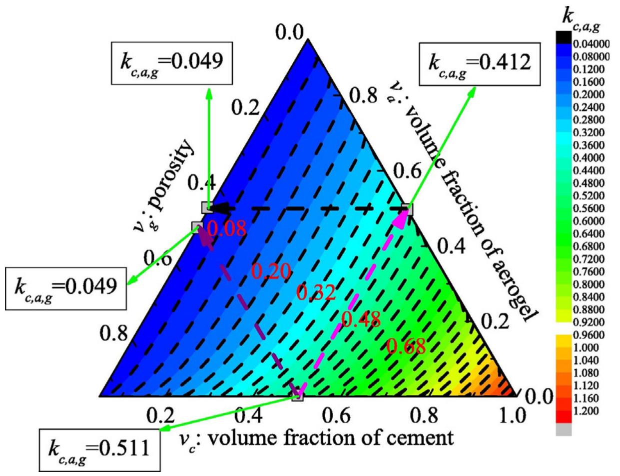

Fig. 17. Thermal conductivity contour distribution of the ternary aerogel foam concrete system. Reprinted with permission from Ref. [249]. Copyright (2019) Elsevier.

without aerogel. To obtain a minimum thermal conductivity, the aerogel foam concrete was synthesized with concrete, aerogel and foam volume ratios of 0.05, 0.308 and 0.642, respectively. The high-performance aerogel foamed concrete presented a thermal conductivity of 0.049 W·m^{-1}·K^{-1} and a density of 198 kg·m^{-3}.

Another study that focused on the influence of temperature and relative humidity in the thermal conductivity of buildings' materials was developed by Wang et al. [250]. As observed in other works, the increase in aerogel's content caused a decrease in the composites' thermal conductivity, with a reduction of 79.3% when the aerogel amount changed from 0 to 60 vol% (0.18 W·m^{-1}·K^{-1}, RH = 0%), following a quadratic function. As expected, the thermal conductivity of the aerogel-incorporated concrete (AIC) increased with the temperature increase, between 0.23 and 0.26 W·m^{-1}·K^{-1} for a temperature amplitude of 70 °C (composite with 60% of aerogel). The variation of thermal conductivity with the relative humidity can be fitted to a cubic polynomial function. As the aerogel content changes from 0 to 60 vol%, the thermal conductivity decrease is the largest in a dry state (79.3%) and the smallest for a RH of 85% (65.25%).

Yoon et al. [251] added aerogels to preformed foam concrete in order to enhance their thermal properties and moisture resistance. Two types of aerogels were tested in the composites; one synthesized with only MTMS and another obtained with a mixture of MTMS and TEOS as silica precursors. Embedding these silica materials into the foam concrete did not affect significantly the mechanical properties, as the reference sample has a compressive strength of 0.81 MPa, and the composites presented values of 0.82 and 0.78 MPa, for the ones obtained with MTMS-aerogel and MTMS + TEOS aerogel, respectively. As expected, the thermal conductivities showed an improvement with the addition of the aerogels. The MTMS and MTMS + TEOS-based aerogel foam concretes presented reductions of 13% and 18%, respectively, when compared to the conventional foam concrete. The hydrophobicity of the materials increased by the addition of aerogels. The results obtained by the authors suggest that aerogel-embedded foam concrete has great potential as a material for thermal insulation in building structures.

4.5. Glazing systems

Glazing units or windows are classified as highly insulating when their heat transfer coefficient (*U*-value) is lower than 0.7 W·m^{-2}·K^{-1}. These systems have been developed over the last years in order to achieve energy efficient buildings and reached the market as multi-layered windows and aerogel glazing [252,253]. Aerogel glazing systems are structurally similar to double glazing, but with silica aerogels instead of air in between the two glass panels. Table 8 summarizes the main properties of some aerogel glazing materials studied in the open literature.

The silica aerogels used are monolithic or granular (with low thermal conductivities and enhanced light scattering) (Table 8). Aerogel granules where the first choice for this application, due to the weak mechanical strength of monolithic aerogel [19,198,252], however, even though both materials have similar light transmittance (Table 8), monolithic aerogels have better transparency, which make them more suitable for applications requiring direct view through the windows [258,261]. Besides that, there is no settling effect, as observed in aerogel granules, which is an important improvement for glazing applications [198]. Fig. 18 shows the difference in the optical properties between a granular and a monolithic aerogel glazing unit.

However, there are only granular aerogels glazing commercially available, since this type of aerogels are easier to fill the cavity of the glazing system and because the large-scale manufacturing of monolithic aerogel glazing often leads to cracks in the aerogel plates due to their brittleness. Nonetheless, some efforts have been made in order to scale up the production of monolithic aerogels. Bhuiya et al. [256] scaled up the procedure to obtain a monolithic aerogel and found that the heat treatment removes residual solvents and improved the transparency properties of the obtained aerogel by 10%. Later, in 2019 Zinzi and co-workers [258] published a research work where they produced monolithic silica aerogels by rapid supercritical extraction technique, which they claimed to be easily scaled up and affordable, but the monoliths obtained are still small (14 × 14 cm) to be applied in windows.

Due to all these production problems, granular aerogels are still the best option for aerogel glazing, but it is important to highlight the effect of the particle size of the granular aerogels used in the glazing systems: lower particle sized aerogel (size < 0.5 mm) usually produce lower *U*-value, but leads to lower visible light transmittance, than larger aerogel granules (3–5 mm) [19]. Fig. 19 shows an example of silica aerogel granules (a) and the effect of their incorporation in between two clear glass panels (b).

From Fig. 20 it is obvious that the visible light will be minimized and a diffuse daylight will be obtained inside the area [252], however this kind of diffuse light might be an option to be applied in certain areas. For example, according to a study of Ihara and co-workers [254] the use of aerogel granulates glazing systems allows a reduction in the energy demand, when compared to a double glazing façade, in warm (Tokyo) and hot (Singapore) regions, by decreasing cooling demand. Yang and co-workers [255] obtained a reduction of 31% in the envelope heat gain, while maintaining the indoor illumination requirements, just by replacing the single glazing by aerogel glazing.

Hence, several authors have been working on improving buildings performance by improving the glazing systems with aerogels and even substituting the glass panels. Moreti and co-workers [257] obtained a polycarbonate glazing system filled with granular silica aerogel, which turned out to present low density, low thermal conductivity at room temperature (0.018–0.020 W·m^{-1}·K^{-1}) and *U*-values from 0.6 to 1.4 W·m^{-2}·K^{-1}. Moreover, when compared to the void polycarbonate glazing system, the aerogel filling reduced the thermal transmittance by about 45 and 70%, depending on the thickness of the panels (16 and 40 mm, respectively). This effect of the aerogel has already been reported by Garnier and co-workers [197] who studied the influence in daylight, thermal loss and solar gain of an aerogel window when compared to the traditional Argon-filled, coated double-glazing. They found that the aerogel glazing presented a lower *U*-value and decreased solar

Table 8
Published works using aerogel in glazing units of buildings.

Ref.	Glazing unit	Bulk density ($kg{\cdot}m^{-3}$)	Thermal conductivity ($W{\cdot}m^{-1}{\cdot}K^{-1}$)	*U*-value ($W{\cdot}m^{-2}{\cdot}K^{-1}$)	Light transmittance
Garnier et al. [197]	Hydrophobic silica aerogel glazing	–	–	0.3	–
Gao et al. [252]	Aerogel granules into the cavity of double-glazing units	–	0.023	0.6–1.19	0.17–0.50
Ihara et al. [254]	Aerogel granulate glazing systems	–	0.018–0.021	0.25–1.38	0.18–0.59
Yang et al. [255]	Silica aerogel glazing	1000[a]	0.020–0.026	–	0.14–0.33
Buratti et al. [241]	Granular silica aerogel	65–70	0.019–0.022	–	–
Bhuiya et al. [256]	Monolithic silica aerogel between two polycarbonate sheets	100	0.020–0.025	0.65[b]–1.16[c]	–
Moretti et al. [257]	Polycarbonate glazing system filled with granular silica aerogel	–	0.018–0.020	0.6–1.4	0.42–0.61
Buratti et al. [194]	Monolithic aerogel between two glass panes	–	0.020	1.1	0.69
Zinzi et al. [258]	Aerogel monoliths between two pieces of float glass	–	–	0.99	0.69
Li et al. [259]	Glass, silica aerogel and phase change material (PCM)	40–100	0.014–0.022	0.6	–
Büttner et al. [260]	Vacuum and silica aerogels in between glass panels	–	–	0.5	–
Zheng et al. [261]	Aerogel glazed skylight	100	0.024	–	–
Valachova et al. [253]	Aerogel into the chambers of the window frame	–	–	0.81	–

[a] – Filling density.
[b] – with the prototype under vacuum.
[c] – with ambient pressure air in the prototype.

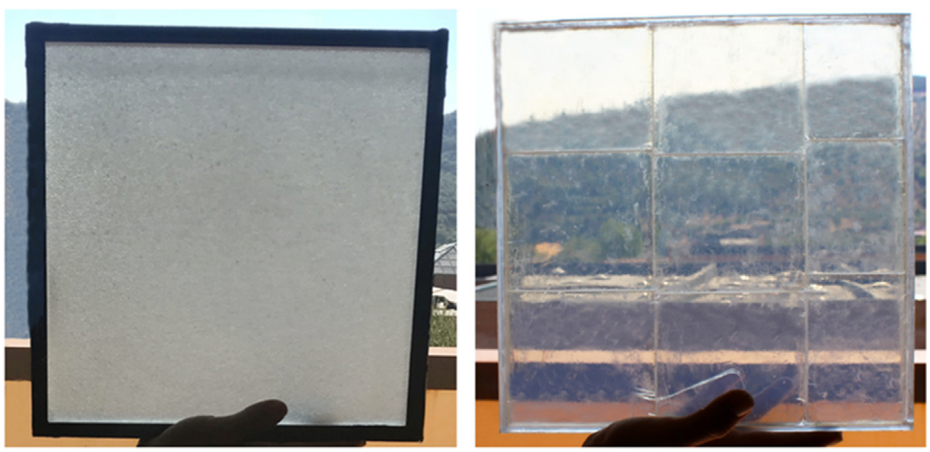

Fig. 18. Examples of (left) a granular aerogel glazing unit and (right) a monolithic aerogel glazing unit (30 × 30 cm glazing sample constructed from nine 15-mm-thick aerogel monoliths sandwiched between two pieces of 4.7-mm-thick float glass). Reprinted with permission from Ref. [258]. Copyright (2019) Elsevier.

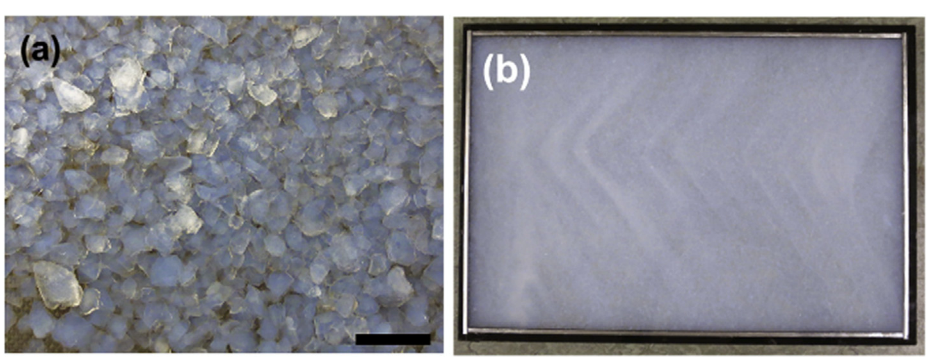

Fig. 19. Example of (a) silica aerogel granules and (b) the corresponding aerogel glazing unit. Reprinted with permission from Ref. [252]. Copyright (2016) Elsevier.

radiant heat transmission, which contribute to an improved interior thermal stability.

Recently, phase change materials (PCM) have been incorporated in the glazing system along with glass and silica aerogel [259,262–265], due to their ability of storing high amounts of energy, during melting, and then, releasing it during solidification, at constant temperature [259].

Büttner and co-workers [260] presented a work where they combined vacuum and silica aerogels in between glass panels in order to enhance both convection and thermal conductivity properties in the final gazing unit. They used silica aerogel pillars in the gap of the glass panels with excellent *U*-values (*ca.* 0.5 $W{\cdot}m^{-2}{\cdot}K^{-1}$), high transmittance and high solar gains.

Zheng and co-workers [261] studied the performance of aerogel glazed skylight when compared with double glazed skylight. These authors carried out this study under real climate conditions in China and found that the aerogel influenced the solar radiation through the glazing system. A significant reduction (~40%) in solar radiation and illuminance rates for aerogel glazed skylight was recorded.

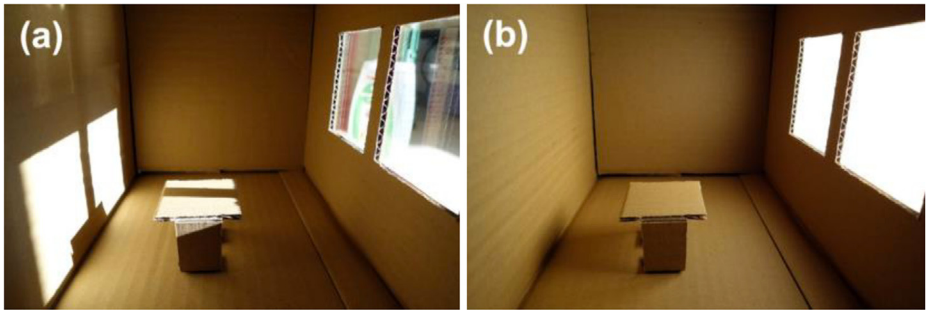

Fig. 20. Example of (a) double glazing unit and (b) aerogel glazing unit. Reprinted with permission from Ref. [252]. Copyright (2016) Elsevier.

Thermal insulating properties of windows are very important, and it was found that not only the thickness of the glazing, but also the window frame, are the main responsible factors for it. In some cases, a thin window is needed and, for this reason, Valachova and co-workers [253] suggested to insert aerogel not just in between the glazing units, but also into the chambers of the window frame. Due to the very low thermal conductivity of aerogels these authors proved that for low thickness, the composite frames were beneficial.

Despite there are already some aerogel glazing solutions in the market with improved thermal and optical properties, there are still some work to be done and some great improvements to be reached in a near future in the field of buildings energy efficiency.

4.6. Solar collector covers

Aerogels have also been used in solar collector covers [167]. Aerogel glazing shows outstanding insulation performance with a U-value below 0.5 W $\cdot m^{-2}\cdot K^{-1}$, a thickness of only 50 mm, and superior daylighting properties [266]. Thus, the silica aerogel glazing is effective in reducing heat losses from the upper surface of the solar tank [38]. Also, it is known that the density of the aerogel influences the solar transmission and radiative loss; by decreasing the density of an aerogel, it is possible to increase solar transmission and the radiative heat loss, which indicates the need of optimization [135,267].

The ability to introduce surface-treated aerogel-based translucent panels provides superior thermal performance over current technology with no contaminant loss in optical properties [37] – these are the so called Optically Transparent and Thermally Insulating (OTTI) aerogel. Table 9 summarizes the main parameters presented in some works with OTTI aerogels used for solar covers.

The effect of aerogel annealing time and temperature on the optical and thermal properties were studied by Strobach and coworkers [267]. They developed high solar transparency, thermally insulating monolithic aerogel able to operate in solar thermal receivers. Depending on the annealing time, this aerogel presented a receiver efficiency of 89.5–91.5% and a solar transmission of 95.5–97.5%. Although the annealing time appears to have little influence, the small 1% increase in the receiver efficiency, may have a significant impact on both system efficiency and cost of electricity production.

Günay and co-workers [39] prepared tetramethyl orthosilicate-based silica aerogels, both hydrophilic and hydrophobic, for solar thermal collectors on black coatings. The hydrophobic OTTI aerogels showed to have improved performance when compared to the hydrophilic OTTI aerogels due to the solar absorption induced by the hydroxyl groups, which decreased the thermal efficiency of the aerogel from 52% to 36%, respectively. These authors also showed that the efficiency depended on the thickness of the aerogel coating, therefore, it is possible to tune the efficiency by changing the aerogel thickness according to the intended application.

Zhao and co-workers [268] developed a solar collector prototype using a layer of a monolithic aerogel on top of a absorber and thermal insulation surface (BlueTec eta plus). They demonstrated that the OTTI aerogel simultaneously suppresses the conduction, convection and radiation losses, and consequently reduces the absorbed heat loss. This behaviour was also observed by Zhao and co-workers [269], who developed an aerogel-based solar thermal receiver from an optimized silica aerogel monolith coated on a blackbody absorber to transmit sunlight with an efficiency higher than 50%, depending on the thickness of the aerogel.

Li and co-workers [270] investigated the optical and thermal performance of a modified evacuated receiver (used to concentrate the solar energy and then transform it into thermal energy). These authors added a layer of a solar transparent aerogel directly in the illumination region and reported no significant optical variations but significant efficiency improvement in the overall system, from 0.01 to 3%.

4.7. Other materials

Due to the versatility of silica aerogels, new composite materials are being developed by incorporating them in diverse matrices

Table 9
Published works using solar panels with aerogel for improved energy outputs.

Ref.	Panels material	Panels cover	Bulk density ($kg\cdot m^{-3}$)	Aerogel thermal conductivity ($W\cdot m^{-1}\cdot K^{-1}$)	Thermal efficiency (%)
Strobach et al. [267]	–	TMOS-based aerogel	160–180	0.05–0.08[a]	89.5–91.5[b]
Günay et al. [39]	Black surface	TMOS-based silica aerogels(hydrophilic)	30	0.16	36
	Black surface	TMOS-based silica aerogels(hydrophobic)	147	0.13	52
Zhao et al. [268]	Absorber surface (BlueTec eta plus)	Monolithic transparent silica aerogel	–	0.02–0.1	–
Zhao et al. [269]	Black body absorber	Low scattering aerogel monolith	180–200	0.01–0.35	50[c]
Li et al. [270]	Glass support	Monolithic transparent silica aerogel	180	0.02–0.07	–

a – The thermal conductivity of the aerogel was modelled using the measured IR transmittance as well as the density and thickness. b – Receiver efficiency. c – Absorber efficiency.

(non-cementitious) for the replacement of the more conventional materials in building application. Some of these composites are reported in Table 10.

An innovative solution to improve the thermal insulation of buildings was developed by Masera et al. [271]. These authors designed an aerogel-based textile wallpaper for indoor energy retrofit. The system was composed by an aerogel-impregnated textile layer, which forms the insulating core, and a fabric finishing that can be easily installed. The composite showed low water absorption after being immersed into water up to 28 days, with a maximum value of only 11.12 $kg \cdot m^{-3}$ (around 7% of the samples' weight), and good thermal performance, presenting values of 25 $mW \cdot m^{-1} \cdot K^{-1}$, for 0% of RH, and 35.4 $mW \cdot m^{-1} \cdot K^{-1}$, with high moisture. The material was submitted to real scale tests, as showed in Fig. 21, and promising results were achieved for indoor thermal retrofitting.

Jia and co-authors [272] developed a new thermal insulation composite by filling the expanded perlite (EP) with silica aerogel. The addition of aerogel, with different particle sizes, caused an improvement in the EP pore structure, with mesoporous volume and Brunauer–Emmett–Teller (BET) specific surface area 100–280 times and 50–150 times higher than those obtained for pure EP, respectively. These changes in the materials' microstructure led to a decrease of 14.7–31.8% in the thermal conductivity, which was also influenced by the drying methodology used during processing (ambient or vacuum pressure). As these aerogel/expanded perlite composites have good thermal properties, a reasonable cost and are easily produced, they can be used to replace traditional thermal insulation materials in buildings.

A new composite with silica aerogel onto the surface of a polyurethane foam (PUF) was synthesized by Li et al. [273] for building insulation, in an effort to reduce the flammability and smoke release of the PUF while maintaining its low thermal conductivity and density. The addition of silica aerogel leads to an enhancement in the compressive strength, achieving values of 486 kPa, and provided an even further improvement regarding the materials' thermal performance, reducing the thermal conductivity from 30.9 $mW \cdot m^{-1} \cdot K^{-1}$, for neat PUF, to 28.2 $mW \cdot m^{-1} \cdot K^{-1}$. The SiO_2/PUF composite showed self-extinguishing in vertical burning tests and a high limiting oxygen index of 32.5%. Besides, the presence of silica contributed to a reduction in the peak heat release rate, from 260 $kW \cdot m^{-2}$ for PUF to 155 $kW \cdot m^{-2}$ for the composite with the highest amount of silica aerogel, and in the peak smoke production release, from 0.090 $m^2 \cdot s^{-1}$ (neat PUF) to 0.049 $m^2 \cdot s^{-1}$ (SiO_2/PUF). Notably, a 55.7% decrease of the specific optical density in the smoke density chamber test was obtained for the composite, indicating an excellent smoke-suppression.

Stazi et al. [274] developed a study focused on sprayed foams with enhanced mechanical properties for External Thermal Insulation Composite System (ETICS) or engineered infills within cavity walls, as exemplified in Fig. 22. The authors studied the influence of adding different particles, clay nanoparticles and spherical silicon dioxide microparticles (aerogel) into polyurethane foams with two densities (15 and 30 $kg \cdot m^{-3}$). Both fillers enhanced the hygroscopic resistance and had negligible influence on thermal stability of the foams. Overall, the composites obtained with 4 wt% of nanoclay presented improvements in thermal and mechanical resis-

Table 10
Published works using composites of different matrices with silica aerogel for thermal insulation of buildings.

Ref.	Composite material	Thermal conductivity ($W \cdot m^{-1} \cdot K^{-1}$)	Bulk density ($kg \cdot m^{-3}$)	Flexural strength (MPa)	Compressive strength (MPa)
Masera et al. [271]	**Silica aerogel precursor**: Polyethoxydisiloxane modified with hexamethyldisiloxane **Silica aerogel-containing composite**: Aerogel-based textile wallpaper	0.025	135.8	–	–
Jia et al. [272]	**Silica aerogel precursor**: Sodium silicate modified with TMCS **Silica aerogel-containing composite**: Composite aerogel/expanded perlite	0.030	~85	–	–
Li et al. [273]	**Silica aerogel precursor**: TEOS **Silica aerogel-containing composite**: SiO_2/polyurethane foam composites	0.0282	37.9	–	0.486
Stazi et al. [274]	**Silica aerogel precursor**: Silicon dioxide microparticles (Tec-Star srl.) **Silica aerogel-containing composite**: Low density nanofoams	0.0382	25.7	0.076	0.0165
Chen et al. [275]	**Silica aerogel precursor**: TEOS modified with TMCS **Silica aerogel-containing composite**: Fly ash based lightweight wall material incorporating EP/SiO_2 aerogel composite	0.050	335	–	0.88

Fig. 21. The assembly of the first prototype of an insulating wallpaper with aerogel; July 2014. Reprinted with permission from Ref. [271]. Copyright (2017) Elsevier.

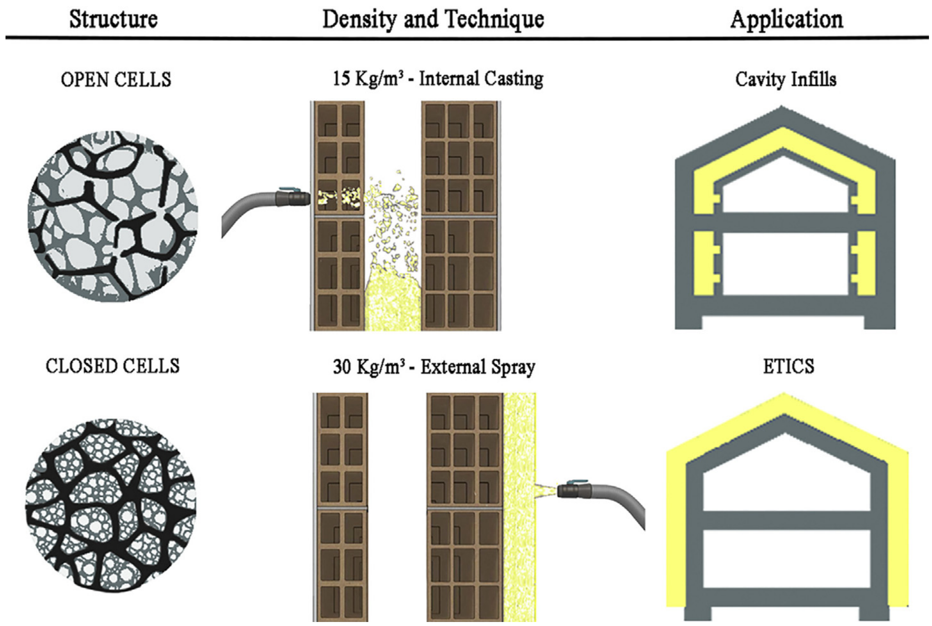

Fig. 22. Structure, density and application technique of the foams. Reprinted with permission from Ref. [274]. Copyright (2019) Elsevier.

tance aspects, for both low and high-density foams, but the samples with the aerogel microparticles were not so promising.

Chen and co-authors [275] developed fly ash-based lightweight wall materials (LWM) with low thermal conductivity, by incorporating air expanded perlite/SiO_2 aerogel composite. The use of SiO_2 aerogel as padding aims the enhancement of the thermal insulation performance of the final composite. The effect of the hydrolysis conditions on the aerogels' properties was studied, with the authors being able to produce a low-density (119 kg·m^{-3}) and low thermal conductivity (27.7 mW·m^{-1}·K^{-1}) SiO_2 aerogel by using the following optimal conditions: H_2SO_4/TEOS molar ratio of 0.8 × 10^{-3}:1, hydrolysis time of 24 h, hydrolysis temperature of 25 °C, and NH_4OH/TEOS molar ratio of 6.0 × 10^{-3}:1. To prepare the fly ash based LWM, different mass ratios (0% to 30%) of a lightweight aggregate, composed by expanded perlite and silica aerogel (EP/SiO_2), were blended with the fly ash slurry. As the amount of EP/SiO_2 increases, a reduction in compressive strength, from 1.16 to 0.76 MPa, and thermal conductivity, from 0.064 to 0.046 W·m^{-1}·K^{-1}, is observed in the composites. As a balance between these properties is necessary, the sample with 20% of EP/SiO_2 was the best to be applied as a thermal insulating material, resulting in a compressive strength of 0.88 MPa, a bulk density of 335 kg·m^{-3} and a thermal conductivity around 0.050 W·m^{-1}·K^{-1}.

5. Conclusions and future trends

Aerogels are one of the most promising thermal insulation materials of the last decades. One growing application of aerogels is their incorporation in diverse matrices for the replacement of more conventional materials. The recent advances regarding the incorporation of silica aerogels in composites and structures developed for buildings were described in this survey. As shown, aerogel-containing materials are already being widely developed and tested for building applications, namely as panels and blankets, incorporation in cement, mortars, plasters, renders and concrete, and for glazing systems and solar collector covers, in order to create a more efficient alternative to current traditional building thermal insulation materials. This can be achieved, as reported here, by combining the benefit of most traditional building materials with silica aerogels, and not by substituting the first. This, in fact, allows to fade the main negative issue regarding the application of aerogel in this sector – its high production cost. By incorporating the aerogel materials in already existing solutions, not only dilutes the cost of the aerogel but also facilitates the acceptance of the new systems in this conservative sector.

The newly developed materials show excellent insulation properties when incorporating silica aerogels. The thermal conductivities vary between 14 and 26 mW·m^{-1}·K^{-1} when the aerogel is applied in the form of VIPs, panels, blankets or glazing systems, and reaches values up to one order of magnitude higher when the aerogel is incorporated in cement, mortars or concrete, being this increase obviously dependent on the amount of aerogel in the mixtures. Still, in general, the addition of aerogel into these building materials leads to great reductions in the composites densities and thermal conductivities, when compared to the systems without aerogel. However, the mechanical properties are usually negatively affected by this incorporation. As both thermal and mechanical properties are essential for the application of insulating materials in the construction industry, a compromise needs to be made between these properties, with the addition of an optimum amount of aerogel that allows a good thermal performance while maintaining the mechanical properties normally observed in building materials. The search for the optimum amount of aerogel can be supported by design of experiments tools, in order to reduce the number of experimental tests.

Besides that, as the use of aerogels have a positive impact in the energy conservation of the building's envelope, it leads to a significant reduction in the emission of greenhouse gases (up to ~65%), if compared with traditional building insulation materials, such as XPS, EPS and PU. The reduction of carbon emissions is in agreement with the goals determined by United Nations Member States, in particular with the Sustainable Development Goal 13 (Climate action).

Funding

This research was co-funded by European Regional Development Funds (ERDF), through the Operational Programme for Competitiveness and Internationalisation —COMPETE2020, and by national funds through FCT—Foundation for Science and Technology, under the scope of the project POCI-01-0145-FEDER-032061 – TYRE4BUILDINS: Recycled Tyre Rubber Resin-Bonded for Building Insulation Systems Towards Energy Efficiency, developed by University of Coimbra. Alyne Lamy-Mendes acknowledges CNPq (Brazil) for the funding of the PhD fellowship project 234184/2014-0/GDE, under the programme "Ciência sem Fronteiras".

Declaration of Competing Interest

The authors declare that they have no known competing financial interests or personal relationships that could have appeared to influence the work reported in this paper.

References

[1] P. Santos, Energy efficiency of light-weight steel-framed buildings, in: E.H. Yap (Ed.), Energy Efficient Buildings, IntechOpen, London, UK, 2017, pp. 35–60.
[2] T. Abergel, B. Dean, J. Dulac, "Towards a zero-emission, efficient, and resilient buildings and construction sector: Global Status Report 2017," UN Environ. Int. Energy Agency Paris, Fr., 2017.
[3] E. Roque, P. Santos, A.C. Pereira, Thermal and sound insulation of lightweight steel-framed façade walls, Sci. Technol. Built Environ. 25 (2) (2019) 156–176, https://doi.org/10.1080/23744731.2018.1506677.
[4] E. Roque, P. Santos, The effectiveness of thermal insulation in lightweight steel-framed walls with respect to its position, Buildings 7 (1) (2017) 13, https://doi.org/10.3390/buildings7010013.
[5] N. Soares, P. Santos, H. Gervásio, J.J. Costa, L. Simões da Silva, L.S. Da Silva, Energy efficiency and thermal performance of lightweight steel-framed (LSF) construction: A review, Renew. Sustain. Energy Rev. 78 (2017) 194–209, https://doi.org/10.1016/j.rser.2017.04.066.
[6] A.J. Marszal, P. Heiselberg, J.S. Bourrelle, E. Musall, K. Voss, I. Sartori, A. Napolitano, Zero Energy Building – A review of definitions and calculation methodologies, Energy Build. 43 (4) (2011) 971–979, https://doi.org/10.1016/j.enbuild.2010.12.022.
[7] U. Berardi C. Sprengard, An overview of and introduction to current researches on super insulating materials for high-performance buildings, Energy Build., 214. 2020, 10.1016/j.enbuild.2020.109890.
[8] J. Adamczyk, R. Dylewski, The impact of thermal insulation investments on sustainability in the construction sector, Renew. Sustain. Energy Rev. 80 (2017) 421–429, https://doi.org/10.1016/j.rser.2017.05.173.
[9] I. Pinto, J.D. Silvestre, J. de Brito, M.F. Júlio, Environmental impact of the subcritical production of silica aerogels, J. Clean. Prod. 252 (2020), https://doi.org/10.1016/j.jclepro.2019.119696 119696.
[10] R. Garrido, J.D. Silvestre, I. Flores-Colen, M. de F. Júlio, M. Pedroso, Economic assessment of the production of subcritically dried silica-based aerogels, J. Non. Cryst. Solids 516 (April) (2019) 26–34, https://doi.org/10.1016/j.jnoncrysol.2019.04.016.
[11] S. Fantucci, S. Garbaccio, A. Lorenzati, M. Perino, Thermo-economic analysis of building energy retrofits using VIP – Vacuum Insulation Panels, Energy Build. 196 (2019) 269–279, https://doi.org/10.1016/j.enbuild.2019.05.019.
[12] J. Zach, J. Peterková, Z. Dufek, T. Sekavčnik, Development of vacuum insulating panels (VIP) with non-traditional core materials, Energy Build. 199 (2019) 12–19, https://doi.org/10.1016/j.enbuild.2019.06.026.
[13] R. Kou, Y. Zhong, J. Kim, Q. Wang, M. Wang, R. Chen, Y. Qiao, Elevating low-emissivity film for lower thermal transmittance, Energy Build. 193 (2019) 69–77, https://doi.org/10.1016/j.enbuild.2019.03.033.
[14] H. Gao, H. Liu, L. Liao, L. Mei, G. Lv, L. Liang, G. Zhu, Z. Wang, D. Huang, Improvement of performance of foam perlite thermal insulation material by the design of a triple-hierarchical porous structure, Energy Build. 200 (2019) 21–30, https://doi.org/10.1016/j.enbuild.2019.07.010.
[15] U. Berardi, S. (Mark) Zaidi, Characterization of commercial aerogel-enhanced blankets obtained with supercritical drying and of a new ambient pressure drying blanket, Energy Build. 198 (2019) 542–552, https://doi.org/10.1016/j.enbuild.2019.06.027.
[16] D.M. Smith, A. Maskara, U. Boes, Aerogel-based thermal insulation, J. Non. Cryst. Solids 225 (1998) 254–259, https://doi.org/10.1016/S0022-3093(98)00125-2.
[17] J.M. Schultz, K.I. Jensen, F.H. Kristiansen, Super insulating aerogel glazing, Sol. Energy Mater. Sol. Cells 89 (2–3) (2005) 275–285, https://doi.org/10.1016/j.solmat.2005.01.016.
[18] T. Gao, B.P. Jelle, A. Gustavsen, J. He, Lightweight and thermally insulating aerogel glass materials, Appl. Phys. A 117 (2) (2014) 799–808, https://doi.org/10.1007/s00339-014-8609-7.
[19] T. Gao, B.P. Jelle, T. Ihara, A. Gustavsen, Insulating glazing units with silica aerogel granules: The impact of particle size, Appl. Energy 128 (2014) 27–34, https://doi.org/10.1016/j.apenergy.2014.04.037.
[20] T. Gao, B.P. Jelle, A. Gustavsen, S. Jacobsen, Aerogel-incorporated concrete: An experimental study, Constr. Build. Mater. 52 (2014) 130–136, https://doi.org/10.1016/j.conbuildmat.2013.10.100.
[21] M. Schmidt, F. Schwertfeger, Applications for silica-based aerogel products on an industrial scale, MRS Online Proc. Libr. Arch., 521, 1998.
[22] N. Lolli, I. Andresen, Aerogel vs. argon insulation in windows: A greenhouse gas emissions analysis, Build. Environ. 101 (2016) 64–76, https://doi.org/10.1016/j.buildenv.2016.03.001.
[23] C.K.K. Leung, L. Lu, Y. Liu, H.S.S. Cheng, J.H. Tse, Optical and thermal performance analysis of aerogel glazing technology in a commercial building of Hong Kong, Energy Built Environ. 1 (2) (2020) 215–223, https://doi.org/10.1016/j.enbenv.2020.02.001.
[24] K. Nocentini, P. Achard, P. Biwole, M. Stipetic, Hygro-thermal properties of silica aerogel blankets dried using microwave heating for building thermal insulation, Energy Build. 158 (2018) 14–22, https://doi.org/10.1016/j.enbuild.2017.10.024.
[25] Z. Talebi, P. Soltani, N. Habibi, F. Latifi, Silica aerogel/polyester blankets for efficient sound absorption in buildings, Constr. Build. Mater. 220 (2019) 76–89, https://doi.org/10.1016/j.conbuildmat.2019.06.031.
[26] J. Wernery, A. Ben-Ishai, B. Binder, S. Brunner, Aerobrick — An aerogel-filled insulating brick, Energy Procedia 134 (2017) 490–498, https://doi.org/10.1016/j.egypro.2017.09.607.
[27] U. Berardi, The benefits of using aerogel-enhanced systems in building retrofits, Energy Procedia (2017), https://doi.org/10.1016/j.egypro.2017.09.576.
[28] U. Berardi, Aerogel-enhanced systems for building energy retrofits: Insights from a case study, Energy Build. (2018), https://doi.org/10.1016/j.enbuild.2017.10.092.
[29] P.C. Thapliyal, K. Singh, Aerogels as promising thermal insulating materials: An overview, J. Mater. 2014 (2014).
[30] S.S. Kistler, Coherent expanded aerogels and jellies, Nature 127 (3211) (1931) 741.
[31] Q. Feng, K. Chen, D. Ma, H. Lin, Z. Liu, S. Qin, Y. Luo, Synthesis of high specific surface area silica aerogel from rice husk ash via ambient pressure drying, Colloids Surfaces A Physicochem. Eng. Asp. 539 (2018) 399–406, https://doi.org/10.1016/j.colsurfa.2017.12.025.
[32] M. Li, H. Jiang, D. Xu, O. Hai, W. Zheng, Low density and hydrophobic silica aerogels dried under ambient pressure using a new co-precursor method, J. Non. Cryst. Solids 452 (2016) 187–193, https://doi.org/10.1016/j.jnoncrysol.2016.09.001.
[33] H. Maleki, L. Durães, A. Portugal, An overview on silica aerogels synthesis and different mechanical reinforcing strategies, J. Non. Cryst. Solids 385 (2014) 55–74, https://doi.org/10.1016/j.jnoncrysol.2013.10.017.
[34] A. Lamy-Mendes, R.F. Silva, L. Durães, Advances in carbon nanostructure–silica aerogel composites: a review, J. Mater. Chem. A, 6(4) 1340–1369, 2018, [Online]. Available: https://pubs.rsc.org/en/content/articlelanding/2018/ta/c7ta08959g#!divAbstract.
[35] S. Karamikamkar, H.E. Naguib, C.B. Park, Advances in precursor system for silica-based aerogel production toward improved mechanical properties, customized morphology, and multifunctionality: A review, Adv. Colloid Interface Sci., p. 102101, 2020, 10.1016/j.cis.2020.102101.
[36] E. Cuce, P.M. Cuce, C.J. Wood, S.B. Riffat, Toward aerogel based thermal superinsulation in buildings: a comprehensive review, Renew. Sustain. Energy Rev. 34 (2014) 273–299.
[37] W.C. Ackerman, M. Vlachos, S. Rouanet, J. Fruendt, Use of surface treated aerogels derived from various silica precursors in translucent insulation panels, J. Non. Cryst. Solids 285 (1–3) (2001) 264–271.
[38] K. Kamiuto, T. Miyamoto, S. Saitoh, Thermal characteristics of a solar tank with aerogel surface insulation, Appl. Energy 62 (3) (1999) 113–123.
[39] A.A. Günay, H. Kim, N. Nagarajan, et al., Optically transparent thermally insulating silica aerogels for solar thermal insulation, ACS Appl. Mater. Interfaces 10 (15) (2018) 12603–12611, https://doi.org/10.1021/acsami.7b18856.
[40] R. Baetens, B.P. Jelle, A. Gustavsen, Aerogel insulation for building applications: a state-of-the-art review, Energy Build. 43 (4) (2011) 761–769.
[41] M. Koebel, A. Rigacci, P. Achard, Aerogel-based thermal superinsulation: An overview, J. Sol-Gel Sci. Technol. 63 (3) (2012) 315–339, https://doi.org/10.1007/s10971-012-2792-9.
[42] M. Ibrahim, P.H. Biwole, P. Achard, E. Wurtz, Aerogel-based materials for improving the building envelope's thermal behavior: a brief review with a focus on a new aerogel-based rendering, in: Energy Sustainability through Green Energy, Springer, 2015, pp. 163–188.
[43] D. Levy, M. Zayat, The Sol-Gel Handbook, 3 Volume Set: Synthesis, Characterization, and Applications, vol. 2. John Wiley & Sons, 2015.
[44] S.B. Riffat, G. Qiu, A review of state-of-the-art aerogel applications in buildings, Int. J. Low-Carbon Technol. 8 (1) (2013) 1–6.
[45] Z.G. Yan, A review of aerogels and their application as a multi-functional building material, Appl. Mech. Mater. 253 (2013) 564–567.
[46] C. Buratti, E. Moretti, E. Belloni, Aerogel Plasters for Building Energy Efficiency BT – Nano and Biotech Based Materials for Energy Building Efficiency, F. Pacheco Torgal, C. Buratti, S. Kalaiselvam, C.-G. Granqvist, and V. Ivanov, Eds. Cham: Springer International Publishing, 2016, pp. 17–40.
[47] N. Shukla, A. Fallahi, J. Kosny, Aerogel thermal insulation–technology review and cost study for building enclosure applications, ASHRAE Trans. 120 (1) (2014) 294–308.
[48] L. Aditya, T.M.I. Mahlia, B. Rismanchi, H.M. Ng, M.H. Hasan, H.S.C. Metselaar, O. Muraza, H.B. Aditiya, A review on insulation materials for energy conservation in buildings, Renew. Sustain. Energy Rev. 73 (January) (2017) 1352–1365, https://doi.org/10.1016/j.rser.2017.02.034.

[49] A. Soleimani Dorcheh, M.H. Abbasi, Silica aerogel; synthesis, properties and characterization, J. Mater. Process. Technol. 199 (1) (2008) 10–26, https://doi.org/10.1016/j.jmatprotec.2007.10.060.
[50] J.L. Gurav, I.-K. Jung, H.-H. Park, E.S. Kang, D.Y. Nadargi, Silica aerogel: synthesis and applications, J. Nanomater. 2010 (2010).
[51] H. Maleki, Recent advances in aerogels for environmental remediation applications: A review, Chem. Eng. J. 300 (2016) 98–118, https://doi.org/10.1016/j.cej.2016.04.098.
[52] A.V. Rao, G.M. Pajonk, S.D. Bhagat, P. Barboux, Comparative studies on the surface chemical modification of silica aerogels based on various organosilane compounds of the type RnSiX4− n, J. Non. Cryst. Solids 350 (2004) 216–223, https://doi.org/10.1016/j.jnoncrysol.2004.06.034.
[53] S.D. Bhagat, A.V. Rao, Surface chemical modification of TEOS based silica aerogels synthesized by two step (acid–base) sol–gel process, Appl. Surf. Sci. 252 (12) (2006) 4289–4297, https://doi.org/10.1016/j.apsusc.2005.07.006.
[54] M. Ochoa, L. Durães, A.M. Beja, A. Portugal, Study of the suitability of silica based xerogels synthesized using ethyltrimethoxysilane and/or methyltrimethoxysilane precursors for aerospace applications, J. Sol-gel Sci. Technol. 61 (1) (2012) 151–160.
[55] T. Xia, H. Yang, J. Li, C. Sun, C. Lei, Z. Hu, Y. Zhang, Tailoring structure and properties of silica aerogels by varying the content of the Tetramethoxysilane added in batches, Microporous Mesoporous Mater. 280 (2019) 20–25, https://doi.org/10.1016/j.micromeso.2019.01.038.
[56] M. de F. Júlio, L.M. Ilharco, Hydrophobic granular silica-based aerogels obtained from ambient pressure monoliths, Materialia 9 (2020), https://doi.org/10.1016/j.mtla.2019.100527 100527.
[57] Afşin Kariper, İ. Afşin Kariper, Effect of acids on thermal insulation of solid powder silica aerogels, Ceram. Int., 46, no. December 2019, 8669–8674, 2019, 10.1016/j.ceramint.2019.12.100.
[58] L.L. Hench, J.K. West, The sol-gel process, Chem. Rev. 90 (1) (1990) 33–72.
[59] M. Stolarski, J. Walendziewski, M. Steininger, B. Pniak, Synthesis and characteristic of silica aerogels, Appl. Catal. A Gen. 177 (2) (1999) 139–148, https://doi.org/10.1016/S0926-860X(98)00296-8.
[60] A.E. Danks, S.R. Hall, Z. Schnepp, The evolution of 'sol–gel' chemistry as a technique for materials synthesis, Mater. Horizons 3 (2) (2016) 91–112, https://doi.org/10.1039/C5MH00260E.
[61] C. J. Brinker, G.W. Scherer, "CHAPTER 3 – Hydrolysis and Condensation II: Silicates," C. J. Brinker and G. W. B. T.-S.-G. S. Scherer, Eds. San Diego: Academic Press, 1990, pp. 96–233.
[62] K.J. Shea, D.A. Loy, Bridged polysilsesquioxanes. Molecular-engineered hybrid organic− inorganic materials, Chem. Mater. 13 (10) (2001) 3306–3319.
[63] C. Chiang, C.M. Ma, D. Wu, H. Kuan, Preparation, characterization, and properties of novolac-type phenolic/SiO2 hybrid organic–inorganic nanocomposite materials by sol–gel method, J. Polym. Sci. Part A Polym. Chem. 41 (7) (2003) 905–913.
[64] R. K. Iler, R. Iler, The chemistry of silica: solubility, polymerization, colloid and surface properties, and biochemistry, 1979.
[65] W.A.A. Twej, A.M. Alattar, M. Drexler, F.M. Alamgir, Tuned optical transmittance in single-step-derived silica aerogels through pH-controlled microstructure, Int. Nano Lett. 7 (4) (2017) 257–265, https://doi.org/10.1007/s40089-017-0216-0.
[66] J.L. Gurav, A.P.V. Rao, A.P.V. Rao, D.Y. Nadargi, S.D. Bhagat, Physical properties of sodium silicate based silica aerogels prepared by single step sol–gel process dried at ambient pressure, J. Alloys Compd. 476 (1–2) (2009) 397–402, https://doi.org/10.1016/j.jallcom.2008.09.029.
[67] C.J. Lee, G.S. Kim, S.H. Hyun, Synthesis of silica aerogels from waterglass via new modified ambient drying, J. Mater. Sci. 37 (11) (2002) 2237–2241, https://doi.org/10.1023/A:1015309014546.
[68] D.Y. Nadargi, S.S. Latthe, A. Venkateswara Rao, Effect of post-treatment (gel aging) on the properties of methyltrimethoxysilane based silica aerogels prepared by two-step sol–gel process, J. Sol-gel Sci. Technol. 49 (1) (2009) 53–59, https://doi.org/10.1007/s10971-008-1830-0.
[69] S. Iswar, W.J. Malfait, S. Balog, F. Winnefeld, M. Lattuada, M.M. Koebel, Effect of aging on silica aerogel properties, Microporous Mesoporous Mater. 241 (2017) 293–302, https://doi.org/10.1016/j.micromeso.2016.11.037.
[70] S. Smitha, P. Shajesh, P.R. Aravind, S.R. Kumar, P.K. Pillai, K.G.K.K. Warrier, Effect of aging time and concentration of aging solution on the porosity characteristics of subcritically dried silica aerogels, Microporous Mesoporous Mater. 91 (1–3) (2006) 286–292, https://doi.org/10.1016/j.micromeso.2005.11.051.
[71] S. Haereid, M. Dahle, S. Lima, M.-A.A. Einarsrud, S. Hæreid, M. Dahle, S. Lima, M.-A.A. Einarsrud, S. Haereid, M. Dahle, S. Lima, M.-A.A. Einarsrud, Preparation and properties of monolithic silica xerogels from TEOS-based alcogels aged in silane solutions, J. Non. Cryst. Solids 186 (1995) 96–103, https://doi.org/10.1016/0022-3093(95)00039-9.
[72] R.-A. Strøm, Y. Masmoudi, A. Rigacci, G. Petermann, L. Gullberg, B. Chevalier, M.-A. Einarsrud, Strengthening and aging of wet silica gels for up-scaling of aerogel preparation, J. Sol-gel Sci. Technol. 41 (3) (2007) 291–298.
[73] S. Hæreid, E. Nilsen, M.-A.A. Einarsrud, Properties of silica gels aged in TEOS, J. Non. Cryst. Solids 204 (3) (1996) 228–234, https://doi.org/10.1016/S0022-3093(96)00418-8.
[74] A. Rigacci, M.-A.A. Einarsrud, E. Nilsen, R. Pirard, F. Ehrburger-Dolle, B. Chevalier, Improvement of the silica aerogel strengthening process for scaling-up monolithic tile production, J. Non. Cryst. Solids 350 (2004) 196–201, https://doi.org/10.1016/j.jnoncrysol.2004.06.042.
[75] S. Smitha, P. Shajesh, S. Rajesh Kumar, P. Krishna Pillai, K.G.K. Warrier, Effect of aging temperature on the porosity characteristics of subcritically dried silica aerogels, J. Porous Mater. 14 (1) (2007) 1–6, https://doi.org/10.1007/s10934-006-9000-7.
[76] M.A. Aegerter, N. Leventis, M.M. Koebel, Aerogels Handbook, Springer Science & Business Media, 2011.
[77] J.P. Vareda, A. Lamy-Mendes, L. Durães, A reconsideration on the definition of the term aerogel based on current drying trends, Microporous Mesoporous Mater. 258 (Mar. 2018) 211–216, https://doi.org/10.1016/J.MICROMESO.2017.09.016.
[78] C.-Y.Y. Kim, J.-K.K. Lee, B.-I.I. Kim, Synthesis and pore analysis of aerogel–glass fiber composites by ambient drying method, Colloids Surfaces A Physicochem. Eng. Asp. 313 (2008) 179–182, https://doi.org/10.1016/j.colsurfa.2007.04.090.
[79] T. Błaszczyński, A. Ślosarczyk, M. Morawski, Synthesis of silica aerogel by supercritical drying method, Procedia Eng. 57 (2013) 200–206.
[80] İ. Şahin, Y. Özbakır, Z. İnönü, Z. Ulker, C. Erkey, Kinetics of Supercritical Drying of Gels, Gels 4 (1) (2017) 3, https://doi.org/10.3390/gels4010003.
[81] C. Lei, J. Li, C. Sun, H. Yang, T. Xia, Z. Hu, Y. Zhang, A co-precursor approach coupled with a supercritical modification method for constructing highly transparent and superhydrophobic polymethylsilsesquioxane aerogels, Molecules 23 (4) (2018) 797, https://doi.org/10.3390/molecules23040797.
[82] V.G. Parale, K.-Y. Lee, H.-Y. Nah, H. Choi, T.-H. Kim, V.D. Phadtare, H.-H. Park, Facile synthesis of hydrophobic, thermally stable, and insulative organically modified silica aerogels using co-precursor method, Ceram. Int. 44 (4) (2018) 3966–3972.
[83] H. Maleki, L. Durães, A. Portugal, Synthesis of lightweight polymer-reinforced silica aerogels with improved mechanical and thermal insulation properties for space applications, Microporous Mesoporous Mater. 197 (2014) 116–129, https://doi.org/10.1016/J.MICROMESO.2014.06.003.
[84] Z. Li, X. Cheng, S. He, X. Shi, H. Yang, Characteristics of ambient-pressure-dried aerogels synthesized via different surface modification methods, J. Sol-Gel Sci. Technol. 76 (1) (2015) 138–149, https://doi.org/10.1007/s10971-015-3760-y.
[85] W.J. Malfait, S. Zhao, R. Verel, S. Iswar, D. Rentsch, R. Fener, Y. Zhang, B. Milow, M.M. Koebel, Surface chemistry of hydrophobic silica aerogels, Chem. Mater. 27 (19) (2015) 6737–6745, https://doi.org/10.1021/acs.chemmater.5b02801.
[86] H. Yu, X. Liang, J. Wang, M. Wang, S. Yang, Preparation and characterization of hydrophobic silica aerogel sphere products by co-precursor method, Solid State Sci. 48 (2015) 155–162, https://doi.org/10.1016/j.solidstatesciences.2015.08.005.
[87] T. Matias, C. Varino, H.C. de Sousa, M.E.M. Braga, A. Portugal, J.F.J. Coelho, L. Durães, Novel flexible, hybrid aerogels with vinyl- and methyltrimethoxysilane in the underlying silica structure, J. Mater. Sci. 51 (14) (2016) 6781–6792, https://doi.org/10.1007/s10853-016-9965-9.
[88] J.P. Vareda, T. Matias, L. Durães, Facile preparation of ambient pressure dried aerogel-like monoliths with reduced shrinkage based on vinyl-modified silica networks, Ceram. Int. 44 (14) (2018) 17453–17458, https://doi.org/10.1016/J.CERAMINT.2018.06.213.
[89] D.B. Mahadik, A.V. Rao, A.P. Rao, P.B. Wagh, S.V. Ingale, S.C. Gupta, Effect of concentration of trimethylchlorosilane (TMCS) and hexamethyldisilazane (HMDZ) silylating agents on surface free energy of silica aerogels, J. Colloid Interface Sci. (2011), https://doi.org/10.1016/j.jcis.2010.12.088.
[90] M. de F. Júlio, L.M. Ilharco, "Ambient Pressure Hybrid Silica Monoliths with Hexamethyldisilazane: From Vitreous Hydrophilic Xerogels to Superhydrophobic Aerogels," ACS omega, vol. 2, no. 8, pp. 5060–5070, Aug. 2017, 10.1021/acsomega.7b00893.
[91] A. Parvathy Rao, A. Venkateswara Rao, Modifying the surface energy and hydrophobicity of the low-density silica aerogels through the use of combinations of surface-modification agents, J. Mater. Sci. 45 (1) (2010) 51–63, https://doi.org/10.1007/s10853-009-3888-7.
[92] X. Guo, J. Shan, Z. Lai, W. Lei, R. Ding, Y. Zhang, H. Yang, Facile synthesis of flexible methylsilsesquioxane aerogels with surface modifications for sound-absorbance, fast dye adsorption and oil/water separation, Molecules 23 (4) (2018) 945, https://doi.org/10.3390/molecules23040945.
[93] F. Shi, L. Wang, J. Liu, Synthesis and characterization of silica aerogels by a novel fast ambient pressure drying process, Mater. Lett. 60 (29–30) (2006) 3718–3722, https://doi.org/10.1016/J.MATLET.2006.03.095.
[94] P.B. Sarawade, J.-K. Kim, A. Hilonga, H.T. Kim, Production of low-density sodium silicate-based hydrophobic silica aerogel beads by a novel fast gelation process and ambient pressure drying process, Solid State Sci. 12 (5) (2010) 911–918, https://doi.org/10.1016/J.SOLIDSTATESCIENCES.2010.01.032.
[95] M. Cai, S. Shafi, Y. Zhao, Preparation of compressible silica aerogel reinforced by bacterial cellulose using tetraethylorthosilicate and methyltrimethoxylsilane co-precursor, J. Non. Cryst. Solids 481 (2018) 622–626, https://doi.org/10.1016/j.jnoncrysol.2017.12.015.
[96] A.V. Rao, R.R. Kalesh, Organic surface modification of TEOS based silica aerogels synthesized by co-precursor and derivatization methods, J. Sol-Gel Sci. Technol. 30 (3) (2004) 141–147, https://doi.org/10.1023/B:JSST.0000039498.61813.9e.
[97] S. Zhao, W.J. Malfait, A. Demilecamps, Y. Zhang, S. Brunner, L. Huber, P. Tingaut, A. Rigacci, T. Budtova, M.M. Koebel, Strong, thermally superinsulating biopolymer–silica aerogel hybrids by cogelation of silicic acid with pectin, Angew. Chemie Int. Ed. 54 (48) (2015) 14282–14286.

[98] M.A.B. Meador, L.A. Capadona, L. McCorkle, D.S. Papadopoulos, N. Leventis, Structure–property relationships in porous 3D nanostructures as a function of preparation conditions: isocyanate cross-linked silica aerogels, Chem. Mater. 19 (9) (2007) 2247–2260, https://doi.org/10.1021/cm070102p.
[99] A. Ślosarczyk, Recent advances in research on the synthetic fiber based silica aerogel nanocomposites, Nanomaterials 7 (2) (2017) 44, https://doi.org/10.3390/nano7020044.
[100] H. Maleki, L. Durães, A. Portugal, Synthesis of mechanically reinforced silica aerogels via surface-initiated reversible addition-fragmentation chain transfer (RAFT) polymerization, J. Mater. Chem. A 3 (4) (2015) 1594–1600, https://doi.org/10.1039/C4TA05618C.
[101] T. Li, A. Du, T. Zhang, W. Ding, M. Liu, J. Shen, Z. Zhang, B. Zhou, Efficient preparation of crack-free, low-density and transparent polymethylsilsesquioxane aerogels via ambient pressure drying and surface modification, RSC Adv. 8 (32) (2018) 17967–17975, https://doi.org/10.1039/C8RÃ1H.
[102] H. Yang, X. Kong, Y. Zhang, C. Wu, E. Cao, Mechanical properties of polymer-modified silica aerogels dried under ambient pressure, J. Non. Cryst. Solids 357 (19) (2011) 3447–3453, https://doi.org/10.1016/j.jnoncrysol.2011.06.017.
[103] H. Ma, B. Wang, L. Zhao, D. Yuna, Preparation and properties of PMMA modified silica aerogels from diatomite, J. Wuhan Univ. Technol. Sci. Ed. 29 (5) (2014) 877–884, https://doi.org/10.1007/s11595-014-1013-5.
[104] S. Salomo, T.X. Nguyen, D.K. Le, X. Zhang, N. Phan-Thien, H.M. Duong, Advanced fabrication and properties of hybrid polyethylene tetraphalate fiber–silica aerogels from plastic bottle waste, Colloids Surfaces A Physicochem. Eng. Asp. (2018), https://doi.org/10.1016/j.colsurfa.2018.08.015.
[105] J. Jaxel, G. Markevicius, A. Rigacci, T. Budtova, Thermal superinsulating silica aerogels reinforced with short man-made cellulose fibers, Compos. Part A Appl. Sci. Manuf. 103 (2017) 113–121, https://doi.org/10.1016/j.compositesa.2017.09.018.
[106] R.B. Torres, J.P. Vareda, A. Lamy-Mendes, L. Durães, Effect of different silylation agents on the properties of ambient pressure dried and supercritically dried vinyl-modified silica aerogels, J. Supercrit. Fluids 147 (2019) 81–89, https://doi.org/10.1016/j.supflu.2019.02.010.
[107] X. Hou, R. Zhang, D. Fang, An ultralight silica-modified ZrO2–SiO2 aerogel composite with ultra-low thermal conductivity and enhanced mechanical strength, Scr. Mater. 143 (2018) 113–116, https://doi.org/10.1016/j.scriptamat.2017.09.028.
[108] S. Shafi, R. Navik, X. Ding, Y. Zhao, Improved heat insulation and mechanical properties of silica aerogel/glass fiber composite by impregnating silica gel, J. Non. Cryst. Solids 503–504 (2019) 78–83, https://doi.org/10.1016/j.jnoncrysol.2018.09.029.
[109] J. Li, Y. Lei, D. Xu, F. Liu, J. Li, A. Sun, J. Guo, G. Xu, Improved mechanical and thermal insulation properties of monolithic attapulgite nanofiber/silica aerogel composites dried at ambient pressure, J. Sol-Gel Sci. Technol. 82 (3) (2017) 702–711, https://doi.org/10.1007/s10971-017-4359-2.
[110] A. Lamy-Mendes, A.V.V. Girão, R.F.F. Silva, L. Durães, Polysilsesquioxane-based silica aerogel monoliths with embedded CNTs, Microporous Mesoporous Mater. 288 (2019), https://doi.org/10.1016/j.micromeso.2019.109575.
[111] L. Hong-li, H. Xiang, L. Hong-yan, L. Jing, L. Ya-jing, Novel GO/silica composite aerogels with enhanced mechanical and thermal insulation properties prepared at ambient pressure, Ferroelectrics 528 (1) (2018) 15–21, https://doi.org/10.1080/00150193.2018.1448192.
[112] H. Maleki, L. Durães, A. Portugal, Development of mechanically strong ambient pressure dried silica aerogels with optimized properties, J. Phys. Chem. C 119 (14) (2015) 7689–7703.
[113] Z. Zhang, J. Shen, X. Ni, G. Wu, B. Zhou, M. Yang, X. Gu, M. Qian, Y. Wu, Hydrophobic silica aerogels strengthened with nonwoven fibers, J. Macromol. Sci. Part A Pure Appl. Chem. 43 (11) (2006) 1663–1670.
[114] L. Li, B. Yalcin, B.N. Nguyen, M.A.B. Meador, M. Cakmak, Flexible nanofiber-reinforced aerogel (xerogel) synthesis, manufacture, and characterization, ACS Appl. Mater. Interfaces 1 (11) (2009) 2491–2501.
[115] D.J. Boday, B. Muriithi, R.J. Stover, D.A. Loy, Polyaniline nanofiber–silica composite aerogels, J. Non. Cryst. Solids 358 (12) (2012) 1575–1580, https://doi.org/10.1016/j.jnoncrysol.2012.04.020.
[116] T. Linhares, M.T.P. de Amorim, L. Durães, Silica aerogel composites with embedded fibres: a review on their preparation, properties and applications, J. Mater. Chem. A 7 (40) (2019) 22768–22802.
[117] C. Alié, R. Pirard, J.-P. Pirard, The role of the main silica precursor and the additive in the preparation of low-density xerogels, J. Non. Cryst. Solids 311 (3) (2002) 304–313.
[118] G. Reichenauer, G.W. Scherer, Effects upon nitrogen sorption analysis in aerogels, J. Colloid Interface Sci. 236 (2) (2001) 385–386.
[119] G. Reichenauer, G.W. Scherer, Nitrogen sorption in aerogels, J. Non. Cryst. Solids 285 (1–3) (2001) 167–174.
[120] S. Iswar, G.M.B.F. Snellings, S. Zhao, R. Erni, Y.K. Bahk, J. Wang, M. Lattuada, M. M. Koebel, W.J. Malfait, Reinforced and superinsulating silica aerogel through in situ cross-linking with silane terminated prepolymers, Acta Mater. 147 (2018) 322–328.
[121] A. Ayral, J. Phalippou, T. Woignier, Skeletal density of silica aerogels determined by helium pycnometry, J. Mater. Sci. 27 (5) (1992) 1166–1170.
[122] N. Hüsing, U. Schubert, R. Mezei, P. Fratzl, B. Riegel, W. Kiefer, D. Kohler, W. Mader, Formation and Structure of Gel Networks from Si(OEt)4/(MeO)3Si(CH2)3NR'2 Mixtures (NR'2= NH2 or NHCH2CH2NH2), Chem. Mater. 11 (2) (1999) 451–457.
[123] T. Woignier, J. Phalippou, Skeletal density of silica aerogels, JNCS 93 (1) (1987) 17–21.
[124] K. Tajiri, K. Igarashi, T. Nishio, Effects of supercritical drying media on structure and properties of silica aerogel, J. Non. Cryst. Solids 186 (1995) 83–87.
[125] J. Fricke, R. Caps, D. Büttner, U. Heinemann, E. Hümmer, Silica aerogel — a light-transmitting thermal superinsulator, J. Non. Cryst. Solids 95–96 (1987) 1167–1174, https://doi.org/10.1016/S0022-3093(87)80730-5.
[126] J. Fricke, E. Hümmer, H.-J. Morper, P. Scheuerpflug, Thermal properties of silica aerogels, Le J. Phys. Colloq. 50 (C4) (1989) C4–87.
[127] J. Fricke, X. Lu, P. Wang, D. Büttner, U. Heinemann, Optimization of monolithic silica aerogel insulants, Int. J. Heat Mass Transf. 35 (9) (1992) 2305–2309.
[128] M.G. Kaganer, Thermal insulation in cryogenic engineering, 1969.
[129] X. Lu, M.C. Arduini-Schuster, J. Kuhn, O. Nilsson, J. Fricke, R.W. Pekala, "Thermal conductivity of monolithic organic aerogels," Science (80-.), 255 (5047) 971–972, 1992.
[130] G. Reichenauer, U. Heinemann, H.P. Ebert, Relationship between pore size and the gas pressure dependence of the gaseous thermal conductivity, Colloids Surfaces A Physicochem. Eng. Asp. (2007), https://doi.org/10.1016/j.colsurfa.2007.01.020.
[131] G.H. Tang, C. Bi, Y. Zhao, W.Q. Tao, Thermal transport in nano-porous insulation of aerogel: Factors, models and outlook, Energy (2015), https://doi.org/10.1016/j.energy.2015.07.109.
[132] Z. Shao, X. He, Z. Niu, T. Huang, X. Cheng, Y. Zhang, Ambient pressure dried shape-controllable sodium silicate based composite silica aerogel monoliths, Mater. Chem. Phys. 162 (2015) 346–353, https://doi.org/10.1016/j.matchemphys.2015.05.077.
[133] S. Groult, T. Budtova, Thermal conductivity/structure correlations in thermal super-insulating pectin aerogels, Carbohydr. Polym. (2018), https://doi.org/10.1016/j.carbpol.2018.05.026.
[134] R. Caps, J. Fricke, Radiative Heat Transfer in Silica Aerogel BT, Aerogels (1986) 110–115.
[135] L.W. Hrubesh, R.W. Pekala, Thermal properties of organic and inorganic aerogels, J. Mater. Res. 9 (3) (1994) 731–738, https://doi.org/10.1557/JMR.1994.0731.
[136] G. Wei, Y. Liu, X. Zhang, X. Du, Radiative heat transfer study on silica aerogel and its composite insulation materials, J. Non Cryst. Solids (2013), https://doi.org/10.1016/j.jnoncrysol.2012.11.041.
[137] J.C.H. Wong, H. Kaymak, S. Brunner, M.M. Koebel, Mechanical properties of monolithic silica aerogels made from polyethoxydisiloxanes, Microporous Mesoporous Mater. (2014), https://doi.org/10.1016/j.micromeso.2013.08.029.
[138] P. Gupta, B. Singh, A.K. Agrawal, P.K. Maji, Low density and high strength nanofibrillated cellulose aerogel for thermal insulation application, Mater. Des. 158 (2018) 224–236, https://doi.org/10.1016/j.matdes.2018.08.031.
[139] X. Lu, R. Caps, J. Fricke, C.T. Alviso, R.W. Pekala, Correlation between structure and thermal conductivity of organic aerogels, J. Non. Cryst. Solids 188 (1995) 226–234, https://doi.org/10.1016/0022-3093(95)00191-3.
[140] C. Jiménez-Saelices, B. Seantier, B. Cathala, Y. Grohens, Spray freeze-dried nanofibrillated cellulose aerogels with thermal superinsulating properties, Carbohydr. Polym. 157 (2017) 105–113, https://doi.org/10.1016/j.carbpol.2016.09.068.
[141] Y. Kobayashi, T. Saito, A. Isogai, Aerogels with 3D ordered nanofiber skeletons of liquid-crystalline nanocellulose derivatives as tough and transparent insulators, Angew. Chemie Int. Ed. 53 (39) (2014) 10394–10397, https://doi.org/10.1002/anie.201405123.
[142] N. Hüsing, U. Schubert, Aerogels—airy materials: chemistry, structure, and properties, Angew. Chemie Int. Ed. 37 (1–2) (1998) 22–45, https://doi.org/10.1002/(SICI)1521-3773(19980202)37:1/2<22::AID-ANIE22>3.0.CO;2-I.
[143] D. Zhao, X. Qian, X. Gu, S.A. Jajja, R. Yang, Measurement techniques for thermal conductivity and interfacial thermal conductance of bulk and thin film materials, J. Electron. Packag., vol. 138, no. 4, 2016.
[144] W. Yang, J. Liu, Y. Wang, S. Gao, Experimental study on the thermal conductivity of aerogel-enhanced insulating materials under various hygrothermal environments, Energy Build. 206 (2020), https://doi.org/10.1016/j.enbuild.2019.109583 109583.
[145] G. Hayase, K. Kugimiya, M. Ogawa, Y. Kodera, K. Kanamori, K. Nakanishi, The thermal conductivity of polymethylsilsesquioxane aerogels and xerogels with varied pore sizes for practical application as thermal superinsulators, J. Mater. Chem. A 2 (18) (2014) 6525–6531, https://doi.org/10.1039/C3TA15094A.
[146] L.-J. Wang, S.-Y. Zhao, M. Yang, Structural characteristics and thermal conductivity of ambient pressure dried silica aerogels with one-step solvent exchange/surface modification, Mater. Chem. Phys. 113 (1) (2009) 485–490, https://doi.org/10.1016/j.matchemphys.2008.07.124.
[147] A. Miros, B. Psiuk, B. Szpikowska-Sroka, Aerogel insulation materials for industrial installation: properties and structure of new factory-made products, J. Sol-Gel Sci. Technol. 84 (3) (2017) 496–506, https://doi.org/10.1007/s10971-017-4539-0.
[148] H. Rocha, U. Lafont, C. Semprimoschnig, Environmental testing and characterization of fibre reinforced silica aerogel materials for Mars exploration, Acta Astronaut. 165 (2019) 9–16, https://doi.org/10.1016/j.actaastro.2019.07.030.

[149] Y. Chen, D. Li, X.-Q. Xie, Y. Gao, Y.-L. He, Theoretical modeling and experimental validation for the effective thermal conductivity of moist silica aerogel, Int. J. Heat Mass Transf. 147 (2020), https://doi.org/10.1016/j.ijheatmasstransfer.2019.118842 118842.
[150] X. Wu, K. Zhong, J. Ding, X. Shen, S. Cui, Y. Zhong, J. Ma, X. Chen, Facile synthesis of flexible and hydrophobic polymethylsilsesquioxane based silica aerogel via the co-precursor method and ambient pressure drying technique, J. Non. Cryst. Solids 530 (2020), https://doi.org/10.1016/j.jnoncrysol.2019.119826 119826.
[151] ASTM C177-19, Standard Test Method for Steady-State Heat Flux Measurements and Thermal Transmission Properties by Means of the Guarded-Hot-Plate Apparatus. West Conshohocken, PA: ASTM International, 2019.
[152] EN 12667, Thermal performance of building materials and products-Determination of thermal resistance by means of guarded hot plate and heat flow meter methods-Products of high and medium thermal resistance, Prod. High Mediu. Therm. Resist. (2007).
[153] ISO 8302:1991, *Thermal insulation-determination of steady-state thermal resistance and related properties-guarded hot plate apparatus*, ISO (1991).
[154] Q. Zheng, S. Kaur, C. Dames, R.S. Prasher, Analysis and improvement of the hot disk transient plane source method for low thermal conductivity materials, Int. J. Heat Mass Transf. 151 (2020) 119331.
[155] S.E. Gustafsson, Transient plane source techniques for thermal conductivity and thermal diffusivity measurements of solid materials, Rev. Sci. Instrum. 62 (3) (1991) 797–804.
[156] ASTM D7984-16, "Standard Test Method for Measurement of Thermal Effusivity of Fabrics Using a Modified Transient Plane Source (MTPS) Instrument," Stand. Test Method Meas. Therm. Effusivity Fabr. Using a Modif. Transient Pl. Source Instrument, ASTM Int. West Conshohocken, PA, 2016.
[157] ISO 22007-2:2015, "22007-2: 2015 Plastics Determination of thermal conductivity and diffusivity Part 2: Transient plane source (hot disk) method," International Organization for Standardization (ISO),. Geneva, Switzerland, 2015.
[158] E.T. Afriyie, P. Karami, P. Norberg, K. Gudmundsson, Textural and thermal conductivity properties of a low density mesoporous silica material, Energy Build. 75 (2014) 210–215, https://doi.org/10.1016/j.enbuild.2014.02.012.
[159] N. Bheekhun, A. Talib, A. Rahim, M.R. Hassan, Aerogels in aerospace: an overview, Adv. Mater. Sci. Eng. 2013 (2013).
[160] A. Emmerling, R. Petricevic, A. Beck, P. Wang, H. Scheller, J. Fricke, Relationship between optical transparency and nanostructural features of silica aerogels, J. Non. Cryst. Solids 185 (3) (1995) 240–248.
[161] P. Wang, W. Körner, A. Emmerling, A. Beck, J. Kuhn, J. Fricke, Optical investigations of silica aerogels, J. Non. Cryst. Solids 145 (1992) 141–145.
[162] K. Athmuri, V. Marinov, Optically transparent and structurally sound silica aerogels: insights from a process study, Adv. Mater. Sci. 12 (1) (2012) 5–16, https://doi.org/10.2478/v10077-012-0001-8.
[163] M. Tabata, I. Adachi, Y. Ishii, H. Kawai, T. Sumiyoshi, H. Yokogawa, Development of transparent silica aerogel over a wide range of densities, Nucl. Instruments Methods Phys. Res. Sect. A Accel. Spectrometers, Detect. Assoc. Equip. 623 (1) (2010) 339–341.
[164] M. Tabata, P. Allison, J.J. Beatty, et al., Developing a silica aerogel radiator for the HELIX ring-imaging Cherenkov system, Nucl. Instruments Methods Phys. Res. Sect. A Accel. Spectrometers, Detect. Assoc. Equip. (2020), https://doi.org/10.1016/j.nima.2019.02.006.
[165] M. Tabata, I. Adachi, Y. Hatakeyama, H. Kawai, T. Morita, T. Sumiyoshi, Large-area silica aerogel for use as Cherenkov radiators with high refractive index, developed by supercritical carbon dioxide drying, J. Supercrit. Fluids (2016), https://doi.org/10.1016/j.supflu.2015.11.022.
[166] T.A. Birks, M.D.W. Grogan, L.M. Xiao, M.D. Rollings, R. England, W.J. Wadsworth, Silica aerogel in optical fibre devices, in: *2010 12th International Conference on Transparent Optical Networks*, 2010, pp. 1–4, https://doi.org/10.1109/ICTON.2010.5549052.
[167] M. Dowson, I. Pegg, D. Harrison, Z. Dehouche, Predicted and in situ performance of a solar air collector incorporating a translucent granular aerogel cover, Energy Build. 49 (2012) 173–187, https://doi.org/10.1016/j.enbuild.2012.02.007.
[168] K. Duer, S. Svendsen, Monolithic silica aerogel in superinsulating glazings, Sol. Energy 63 (4) (1998) 259–267, https://doi.org/10.1016/S0038-092X(98)00063-2.
[169] M.V. Khedkar, S.B. Somvanshi, A.V. Humbe, K.M. Jadhav, Surface modified sodium silicate based superhydrophobic silica aerogels prepared via ambient pressure drying process, J. Non. Cryst. Solids 511 (2019) 140–146, https://doi.org/10.1016/j.jnoncrysol.2019.02.004.
[170] L. Zhao, S. Yang, B. Bhatia, E. Strobach, E.N. Wang, Modeling silica aerogel optical performance by determining its radiative properties, AIP Adv. 6 (2) (Feb. 2016) 25123, https://doi.org/10.1063/1.4943215.
[171] T. Fu, J. Tang, K. Chen, F. Zhang, Visible, near-infrared and infrared optical properties of silica aerogels, Infrared Phys. Technol. 71 (2015) 121–126, https://doi.org/10.1016/j.infrared.2015.03.004.
[172] A. Venkateswara Rao, G.M. Pajonk, Effect of methyltrimethoxysilane as a co-precursor on the optical properties of silica aerogels, J. Non. Cryst. Solids 285 (1) (2001) 202–209, https://doi.org/10.1016/S0022-3093(01)00454-9.
[173] A. Sedova, B. Višić, V. Vega-Mayoral, D. Vella, C. Gadermaier, H. Dodiuk, S. Kenig, R. Tenne, R. Gvishi, G. Bar, Silica aerogels as hosting matrices for WS2 nanotubes and their optical characterization, J. Mater. Sci. 55 (18) (2020) 7612–7623, https://doi.org/10.1007/s10853-020-04562-1.
[174] F. Merli, A.M. Anderson, M.K. Carroll, C. Buratti, Acoustic measurements on monolithic aerogel samples and application of the selected solutions to standard window systems, Appl. Acoust. (2018), https://doi.org/10.1016/j.apacoust.2018.08.008.
[175] ISO 12354, "Building acoustics–Estimation of acoustic performance of buildings from the performance of elements–Part 1: Airborne sound insulation between rooms, Part 2: Impact sound insulation between rooms, Part 3: Airborne sound insulation against outdoor sound." Part, 2017.
[176] ASTM E90-09, "Standard Test Method for Laboratory Measurement of Airborne Sound Transmission Loss of Building Partitions and Elements," West Conshohocken, PA, 2009. 10.1520/E0090-09.
[177] W. Dong, T. Faltens, M. Pantell, D. Simon, T. Thompson, W. Dong, "Acoustic Properties of Organic/Inorganic Composite Aerogels," MRS Proc., vol. 1188, pp. 1188-LL07-02, Jan. 2009, 10.1557/PROC-1188-LL07-02.
[178] L. Forest, V. Gibiat, T. Woignier, Evolution of the acoustical properties of silica alcogels during their formation, Ultrasonics 36 (1–5) (1998) 477–481, https://doi.org/10.1016/S0041-624X(97)00149-2.
[179] S. Caponi, A. Fontana, M. Montagna, O. Pilla, F. Rossi, F. Terki, T. Woignier, Acoustic attenuation in silica porous systems, J. Non. Cryst. Solids 322 (1) (2003) 29–34, https://doi.org/10.1016/S0022-3093(03)00167-4.
[180] E. Moretti, F. Merli, E. Cuce, C. Buratti, Thermal and acoustic properties of aerogels: preliminary investigation of the influence of granule size, Energy Procedia 111 (2017) 472–480.
[181] X. Li, Z. Yang, K. Li, S. Zhao, Z. Fei, Z. Zhang, A flexible silica aerogel with good thermal and acoustic insulation prepared via water solvent system, J. Sol-Gel Sci. Technol. 92 (3) (2019) 652–661, https://doi.org/10.1007/s10971-019-05107-y.
[182] J. Gross, G. Reichenauer, J. Fricke, Mechanical properties of SiO2 aerogels, J. Phys. D. Appl. Phys. 21 (9) (1988) 1447.
[183] J. Gross, J. Fricke, R.W. Pekala, L.W. Hrubesh, Elastic nonlinearity of aerogels, Phys. Rev. B 45 (22) (1992) 12774.
[184] J. Gross, J. Fricke, L.W. Hrubesh, Sound propagation in SiO2 aerogels, J. Acoust. Soc. Am. 91 (4) (1992) 2004–2006.
[185] ISO 10534-2, "Acoustics-Determination of sound absorption coefficient and impedance in impedance tubes-Part 2: Transfer-function method." Oct, 2001.
[186] L. Feng, Modified impedance tube measurements and energy dissipation inside absorptive materials, Appl. Acoust. 74 (12) (2013) 1480–1485, https://doi.org/10.1016/j.apacoust.2013.06.013.
[187] M. Sachithanadam, S.C. Joshi, Effect of granule sizes on acoustic properties of protein-based silica aerogel composites via novel inferential transmission loss method, Gels (Basel, Switzerland) 2 (1) (2016) 11, https://doi.org/10.3390/gels2010011.
[188] T. Sato, T. Shimosato, and D. M. Klinman, "Silicosis and lung cancer: current perspectives, Lung Cancer (Auckland, N.Z.), vol. 9, pp. 91–101, Oct. 2018, 10.2147/LCTT.S156376.
[189] R. Merget, T. Bauer, H. Küpper, S. Philippou, H. Bauer, R. Breitstadt, T. Bruening, Health hazards due to the inhalation of amorphous silica, Arch. Toxicol. 75 (11–12) (2002) 625–634.
[190] I. A. for R. on C. (IARC), "Arsenic, metals, fibres and dusts.," IARC Monogr. Eval. Carcinog. risks to humans, 2012.
[191] I. A. for R. on C. (IARC), "Silica, some silicates, coal dust and para-Aramid fibrils," IARC Monogr. Eval. Carcinog. risks to humans, 1997.
[192] P. Santos, C. Martins, L. Simões da Silva, Thermal performance of lightweight steel-framed construction systems, Metall. Res. Technol. 111 (6) (2014) 329–338, https://doi.org/10.1051/metal/2014035.
[193] S. Ng, B.P. Jelle, L.I.C. Sandberg, T. Gao, Ó.H. Wallevik, Experimental investigations of aerogel-incorporated ultra-high performance concrete, Constr. Build. Mater. 77 (2015) 307–316, https://doi.org/10.1016/j.conbuildmat.2014.12.064.
[194] C. Buratti, E. Moretti, E. Belloni, M. Zinzi, Experimental and numerical energy assessment of a monolithic aerogel glazing unit for building applications, Appl. Sci. 9 (24) (2019) 5473.
[195] C. Buratti, E. Moretti, Glazing systems with silica aerogel for energy savings in buildings, Appl. Energy 98 (2012) 396–403, https://doi.org/10.1016/j.apenergy.2012.03.062.
[196] U. Berardi, Development of glazing systems with silica aerogel, Energy Procedia 78 (2015) 394–399.
[197] C. Garnier, T. Muneer, L. McCauley, Super insulated aerogel windows: Impact on daylighting and thermal performance, Build. Environ. 94 (2015) 231–238.
[198] T. Gao, B.P. Jelle, A. Gustavsen, Building integration of aerogel glazings, Procedia Eng. 145 (2016) 723–728, https://doi.org/10.1016/j.proeng.2016.04.090.
[199] W. Kurdowski, Cement and Concrete Chemistry, Springer Science & Business, 2014.
[200] F.S. Merritt, J.T. Ricketts, Building Design and Construction Handbook, vol. 13, McGraw-Hill New York, NY, USA, 2001.
[201] A. Reichel, A. Hochberg, C. Köpke, Plaster, Render, Paint and Coatings: Details, Products, Case Studies, Walter de Gruyter, 2012.
[202] R.B. Holland, K.E. Kurtis, L.F. Kahn, "7 – Effect of different concrete materials on the corrosion of the embedded reinforcing steel," A. B. T.-C. of S. in C. S. Poursaee, Ed. Oxford: Woodhead Publishing, 2016, pp. 131–147.
[203] P. Mangat, P. Lambert, "18 – Sustainability of alkali-activated cementitious materials and geopolymers," in Woodhead Publishing Series in Civil and

Structural Engineering, J. M. B. T.-S. of C. M. (Second E. Khatib, Ed. Woodhead Publishing, 2016, pp. 459–476.
[204] R.H. Nosrati, U. Berardi, Hygrothermal characteristics of aerogel-enhanced insulating materials under different humidity and temperature conditions, Energy Build. 158 (2018) 698–711.
[205] K. Chen, A. Neugebauer, T. Goutierre, A. Tang, L. Glicksman, L.J. Gibson, Mechanical and thermal performance of aerogel-filled sandwich panels for building insulation, Energy Build. (2014), https://doi.org/10.1016/j.enbuild.2014.02.041.
[206] Y. Liang, H. Wu, G. Huang, J. Yang, H. Wang, Thermal performance and service life of vacuum insulation panels with aerogel composite cores, Energy Build. 154 (2017) 606–617, https://doi.org/10.1016/j.enbuild.2017.08.085.
[207] J. Yuying Liang, Huijun Wu, Gongsheng Huang, Y.D. Yang, ''Prediction and Optimization of Thermal Conductivity of Vacuum." pp. 2588–2562, 2017.
[208] J. Yang, H. Wu, X. Xu, G. Huang, T. Xu, S. Guo, Y. Liang, Numerical and experimental study on the thermal performance of aerogel insulating panels for building energy efficiency, Renew. Energy (2019), https://doi.org/10.1016/j.renene.2019.01.120.
[209] M. Joly, P. Bourdoukan, M. Ibrahim, M. Stipetic, S. Dantz, K. Nocentini, M. Aulagnier, F.G. Caiazzo, B. Fiorentino, Competitive high performance aerogel-based composite material for the European insulation market, Energy Procedia 122 (2017) 859–864, https://doi.org/10.1016/j.egypro.2017.07.450.
[210] A. Hoseini, A. Malekian, M. Bahrami, Deformation and thermal resistance study of aerogel blanket insulation material under uniaxial compression, Energy Build. 130 (2016) 228–237.
[211] A. Hoseini, M. Bahrami, Effects of humidity on thermal performance of aerogel insulation blankets, J. Build. Eng. 13 (2017) 107–115.
[212] H. Guo, S. Cai, K. Li, Z. Liu, L. Xia, J. Xiong, Simultaneous test and visual identification of heat and moisture transport in several types of thermal insulation, Energy (2020), https://doi.org/10.1016/j.energy.2020.117137.
[213] Á. Lakatos, Stability investigations of the thermal insulating performance of aerogel blanket, Energy Build. (2019), https://doi.org/10.1016/j.enbuild.2018.12.029.
[214] U. Berardi, R.H. Nosrati, Long-term thermal conductivity of aerogel-enhanced insulating materials under different laboratory aging conditions, Energy 147 (2018) 1188–1202.
[215] H. Huang, Y. Zhou, R. Huang, H. Wu, Y. Sun, G. Huang, T. Xu, Optimum insulation thicknesses and energy conservation of building thermal insulation materials in Chinese zone of humid subtropical climate, Sustain. Cities Soc. (2020), https://doi.org/10.1016/j.scs.2019.101840.
[216] M. Ibrahim, K. Nocentini, M. Stipetic, S. Dantz, F.G. Caiazzo, H. Sayegh, L. Bianco, Multi-field and multi-scale characterization of novel super insulating panels/systems based on silica aerogels: Thermal, hydric, mechanical, acoustic, and fire performance, Build. Environ. 151 (2019) 30–42, https://doi.org/10.1016/J.BUILDENV.2019.01.019.
[217] U. Berardi, L. Ákos, Thermal bridges of metal fasteners for aerogel-enhanced blankets, Energy Build. (2019), https://doi.org/10.1016/j.enbuild.2018.12.041.
[218] J. Kosny, A.D. Fontanini, N. Shukla, A. Fallahi, A. Watts, R. Trifu, B. Ganapathysubramanian, Thermal performance analysis of residential attics containing high performance aerogel-based radiant barriers, Energy Build. 158 (2018) 1036–1048.
[219] EN 13162, ''Thermal insulation products for buildings – Factory made mineral wool (MW) products – Specification," Eur. Comm. Stand., 2012.
[220] A. Hanif, S. Diao, Z. Lu, T. Fan, Z. Li, Green lightweight cementitious composite incorporating aerogels and fly ash cenospheres – Mechanical and thermal insulating properties, Constr. Build. Mater. 116 (2016) 422–430, https://doi.org/10.1016/j.conbuildmat.2016.04.134.
[221] Q. Zeng, T. Mao, H. Li, Y. Peng, Thermally insulating lightweight cement-based composites incorporating glass beads and nano-silica aerogels for sustainably energy-saving buildings, Energy Build. (2018), https://doi.org/10.1016/j.enbuild.2018.06.031.
[222] J. Lu, J. Jiang, Z. Lu, J. Li, Y. Niu, Y. Yang, Pore structure and hardened properties of aerogel/cement composites based on nanosilica and surface modification, Constr. Build. Mater. (2020), https://doi.org/10.1016/j.conbuildmat.2020.118434.
[223] K. Sandin, ''Mortars for masonry and rendering choice and application," Build. Issues, Vol 7, 1995.
[224] S. Ng, B.P. Jelle, Y. Zhen, Ó.H. Wallevik, Effect of storage and curing conditions at elevated temperatures on aerogel-incorporated mortar samples based on UHPC recipe, Constr. Build. Mater. (2016), https://doi.org/10.1016/j.conbuildmat.2015.12.162.
[225] S. Ng, B.P. Jelle, T. Stæhli, Calcined clays as binder for thermal insulating and structural aerogel incorporated mortar, Cem. Concr. Compos. (2016), https://doi.org/10.1016/j.cemconcomp.2016.06.007.
[226] M.G. Gomes, I. Flores-Colen, L.M. Manga, A. Soares, J. De Brito, The influence of moisture content on the thermal conductivity of external thermal mortars, Constr. Build. Mater. 135 (2017) 279–286.
[227] M.G. Gomes, I. Flores-Colen, F. da Silva, M. Pedroso, Thermal conductivity measurement of thermal insulating mortars with EPS and silica aerogel by steady-state and transient methods, Constr. Build. Mater. (2018), https://doi.org/10.1016/j.conbuildmat.2018.03.162.
[228] P. Zhu, S. Brunner, S. Zhao, M. Griffa, A. Leemann, N. Toropovs, A. Malekos, M. M. Koebel, P. Lura, Study of physical properties and microstructure of aerogel-cement mortars for improving the fire safety of high-performance concrete linings in tunnels, Cem. Concr. Compos. 104 (2019) 103414.
[229] A.K.A. Al Zaidi, B. Demirel, C.D. Atis, Effect of different storage methods on thermal and mechanical properties of mortar containing aerogel, fly ash and nano-silica, Constr. Build. Mater. 199 (2019) 501–507.
[230] L. Bostanci, Synergistic effect of a small amount of silica aerogel powder and scrap rubber addition on properties of alkali-activated slag mortars, Constr. Build. Mater. (2020), https://doi.org/10.1016/j.conbuildmat.2020.118885.
[231] N. Abbas, H.R. Khalid, G. Ban, H.T. Kim, H.-K.K. Lee, Silica aerogel derived from rice husk: An aggregate replacer for lightweight and thermally insulating cement-based composites, Constr. Build. Mater. 195 (2019) 312–322, https://doi.org/10.1016/j.conbuildmat.2018.10.227.
[232] M. Pedroso, I. Flores-Colen, J.D. Silvestre, M.G. Gomes, L. Silva, L. Ilharco, Physical, mechanical, and microstructural characterisation of an innovative thermal insulating render incorporating silica aerogel, Energy Build. 211 (2020), https://doi.org/10.1016/j.enbuild.2020.109793.
[233] A. Ababneh, F. Matalkah, R. Aqel, Synthesis of kaolin-based alkali-activated cement: carbon footprint, cost and energy assessment, J. Mater. Res. Technol. 9 (4) (2020) 8367–8378, https://doi.org/10.1016/j.jmrt.2020.05.116.
[234] L.K. Turner, F.G. Collins, Carbon dioxide equivalent (CO2-e) emissions: A comparison between geopolymer and OPC cement concrete, Constr. Build. Mater. 43 (2013) 125–130, https://doi.org/10.1016/j.conbuildmat.2013.01.023.
[235] CEN EN 998-1:2010, ''Specification for Mortar for Masonry – Part 1: Rendering and Plastering Mortar." European Committee for Standardization, Brussels, Belgium, 2010.
[236] E. N. ISO, ''10456: 2007 Building materials and products–Hygrothermal properties–Tabulated design values and procedures for determining declared and design thermal values," Brussels CEN, 2007.
[237] ''REM-Tech." http://www.rem-tech.co.kr/.
[238] M. Pedroso, I. Flores-Colen, J.D. Silvestre, M.G. Gomes, L. Silva, P. Sequeira, J. de Brito, Characterisation of a multilayer external wall thermal insulation system. Application in a Mediterranean climate, J. Build. Eng. (2020), https://doi.org/10.1016/j.jobe.2020.101265.
[239] EOTA, ''ETAG 004, Guideline for European Technical Approval of External Thermal Insulation Composite Systems (ETICS) with Rendering," European Organisation for Technical Approvals. Brussels, Belgium, 2013.
[240] L. Binda, B. de Vekey, A. Acharhabi, G. Baronio, P. Bekker, G. Borchelt, N. Bright, F. Emrich, M. Forde, H. Gallegos, RILEM TC 127-MS: Tests for masonry materials and structures, Mater. Struct. 31 (205) (1998) 2–19.
[241] C. Buratti, F. Merli, E. Moretti, Aerogel-based materials for building applications: Influence of granule size on thermal and acoustic performance, Energy Build. 152 (2017) 472–482, https://doi.org/10.1016/j.enbuild.2017.07.071.
[242] P. Westgate, K. Paine, R.J. Ball, Physical and mechanical properties of plasters incorporating aerogel granules and polypropylene monofilament fibres, Constr. Build. Mater. 158 (2018) 472–480, https://doi.org/10.1016/j.conbuildmat.2017.09.177.
[243] M. Ibrahim, P.H. Biwole, P. Achard, E. Wurtz, G. Ansart, Building envelope with a new aerogel-based insulating rendering: Experimental and numerical study, cost analysis, and thickness optimization, Appl. Energy 159 (2015) 490–501.
[244] M. de Fátima Júlio, A. Soares, L.M. Ilharco, I. Flores-Colen, J. de Brito, Silica-based aerogels as aggregates for cement-based thermal renders, Cem. Concr. Compos. 72 (2016) 309–318.
[245] K.G. Wakili, C. Dworatzyk, M. Sanner, A. Sengespeick, M. Paronen, T. Stahl, Energy efficient retrofit of a prefabricated concrete panel building (Plattenbau) in Berlin by applying an aerogel based rendering to its façades, Energy Build. 165 (2018) 293–300.
[246] P. Achard, A. Rigacci, T. Echantillac, A. Bellet, M. Aulagnier, and A. Daubresse, ''Enduit isolant a base de xerogel de silice," WO 2011/083174 A1, 2011.
[247] S. Fickler, B. Milow, L. Ratke, M. Schnellenbach-Held, T. Welsch, Development of high performance aerogel concrete, Energy Procedia 78 (2015) 406–411.
[248] S. Liu, K. Zhu, S. Cui, X. Shen, G. Tan, A novel building material with low thermal conductivity: Rapid synthesis of foam concrete reinforced silica aerogel and energy performance simulation, Energy Build. 177 (2018) 385–393, https://doi.org/10.1016/j.enbuild.2018.08.014.
[249] P. Li, H. Wu, Y. Liu, J. Yang, Z. Fang, B. Lin, Preparation and optimization of ultra-light and thermal insulative aerogel foam concrete, Constr. Build. Mater. (2019), https://doi.org/10.1016/j.conbuildmat.2019.01.212.
[250] Y. Wang, J. Huang, D. Wang, Y. Liu, Z. Zhao, J. Liu, Experimental investigation on thermal conductivity of aerogel-incorporated concrete under various hygrothermal environment, Energy (2019), https://doi.org/10.1016/j.energy.2019.115999.
[251] H.S. Yoon, T.K. Lim, S.M. Jeong, K.H. Yang, Thermal transfer and moisture resistances of nano-aerogel-embedded foam concrete, Constr. Build. Mater. (2020), https://doi.org/10.1016/j.conbuildmat.2019.117575.
[252] T. Gao, T. Ihara, S. Grynning, B.P. Jelle, A.G. Lien, Perspective of aerogel glazings in energy efficient buildings, Build. Environ. 95 (2016) 405–413, https://doi.org/10.1016/j.buildenv.2015.10.001.
[253] D. Valachova, N. Zdrazilova, V. Panovec, and I. Skotnicova, ''Using of Aerogel to Improve Thermal Insulating Properties of Windows," Civ. Environ. Eng., vol. 14, no. 1, pp. 2–11, 10.2478/cee-2018-0001.
[254] T. Ihara, T. Gao, S. Grynning, B.P. Jelle, A. Gustavsen, Aerogel granulate glazing facades and their application potential from an energy saving perspective, Appl. Energy 142 (2015) 179–191, https://doi.org/10.1016/j.apenergy.2014.12.053.

[255] Y. Yang, H. Wu, L. Yang, T. Xu, Y. Ding, P. Fu, Thermal and day-lighting performance of aerogel glazing system in large atrium building under cooling-dominant climates, Energy Procedia 158 (2019) 6347–6357, https://doi.org/10.1016/j.egypro.2019.01.273.
[256] M.M.H. Bhuiya, A.M. Anderson, M.K. Carroll, B.A. Bruno, J.L. Ventrella, B. Silberman, B. Keramati, Preparation of monolithic silica aerogel for fenestration applications: scaling up, reducing cycle time, and improving performance, Ind. Eng. Chem. Res. 55 (25) (2016) 6971–6981.
[257] E. Moretti, M. Zinzi, E. Carnielo, F. Merli, Advanced polycarbonate transparent systems with aerogel: preliminary characterization of optical and thermal properties, Energy Procedia 113 (2017) 9–16, https://doi.org/10.1016/j.egypro.2017.04.003.
[258] M. Zinzi, G. Rossi, A.M. Anderson, M.K. Carroll, E. Moretti, C. Buratti, Optical and visual experimental characterization of a glazing system with monolithic silica aerogel, Sol. Energy 183 (2019) 30–39, https://doi.org/10.1016/j.solener.2019.03.013.
[259] D. Li, C. Zhang, Q. Li, C. Liu, M. Arıcı, Y. Wu, Thermal performance evaluation of glass window combining silica aerogels and phase change materials for cold climate of China, Appl. Therm. Eng. 165 (2020), https://doi.org/10.1016/j.applthermaleng.2019.114547 114547.
[260] B. Büttner, J. Nauschütz, U. Heinemann, G. Reichenauer, C. Scherdel, H. Weinläder, S. Weismann, D. Buck, A. Beck, Evacuated Glazing with Silica Aerogel Spacers (2018).
[261] D. Zheng, Y. Chen, Y. Liu, Y. Li, S. Zheng, B. Lu, Experimental comparisons on optical and thermal performance between aerogel glazed skylight and double glazed skylight under real climate condition, Energy Build. 222 (2020), https://doi.org/10.1016/j.enbuild.2020.110028 110028.
[262] A.E. Kabeel, T. Arunkumar, D.C. Denkenberger, R. Sathyamurthy, Performance enhancement of solar still through efficient heat exchange mechanism–a review, Appl. Therm. Eng. 114 (2017) 815–836.
[263] S. Grynning, F. Goia, B. Time, Dynamic thermal performance of a PCM window system: characterization using large scale measurements, Energy Procedia 78 (2015) 85–90, https://doi.org/10.1016/j.egypro.2015.11.119.
[264] S. Li, G. Sun, K. Zou, X. Zhang, Experimental research on the dynamic thermal performance of a novel triple-pane building window filled with PCM, Sustain. Cities Soc. 27 (2016) 15–22, https://doi.org/10.1016/j.scs.2016.08.014.
[265] T. Silva, R. Vicente, F. Rodrigues, Literature review on the use of phase change materials in glazing and shading solutions, Renew. Sustain. Energy Rev. 53 (2016) 515–535, https://doi.org/10.1016/j.rser.2015.07.201.
[266] M. Reim, A. Beck, W. Körner, R. Petricevic, M. Glora, M. Weth, T. Schliermann, J. Fricke, C. Schmidt, F.J. Pötter, Highly insulating aerogel glazing for solar energy usage, Sol. Energy 72 (1) (2002) 21–29, https://doi.org/10.1016/S0038-092X(01)00086-X.
[267] E. Strobach, B. Bhatia, S. Yang, L. Zhao, E.N. Wang, High temperature annealing for structural optimization of silica aerogels in solar thermal applications, J. Non. Cryst. Solids 462 (2017) 72–77, https://doi.org/10.1016/j.jnoncrysol.2017.02.009.
[268] L. Zhao, B. Bhatia, T. Cooper, E. Strobach, S. Yang, L.A. Weinstein, G. Chen, E.N. Wang, Intermediate Temperature Solar Thermal Collector Enabled by Non-Evacuated Transparent Aerogel and Non-Tracking Compound Parabolic Concentrator, International Heat Transfer Conference Digital Library (2018).
[269] L. Zhao, B. Bhatia, S. Yang, E. Strobach, L.A. Weinstein, T.A. Cooper, G. Chen, E. N. Wang, Harnessing heat beyond 200 C from unconcentrated sunlight with nonevacuated transparent aerogels, ACS Nano 13 (7) (2019) 7508–7516.
[270] Q. Li, Y. Zhang, Z.-X. Wen, Y. Qiu, An evacuated receiver partially insulated by a solar transparent aerogel for parabolic trough collector, Energy Convers. Manag. 214 (2020) 112911.
[271] G. Masera, K.G. Wakili, T. Stahl, S. Brunner, R. Galliano, C. Monticelli, S. Aliprandi, A. Zanelli, A. Elesawy, Development of a super-insulating, aerogel-based textile wallpaper for the indoor energy retrofit of existing residential buildings, Procedia Eng. 180 (2017) 1139–1149.
[272] G. Jia, Z. Li, P. Liu, Q. Jing, Preparation and characterization of aerogel/expanded perlite composite as building thermal insulation material, J. Non. Cryst. Solids 482 (2018) 192–202, https://doi.org/10.1016/j.jnoncrysol.2017.12.047.
[273] M.E. Li, S.X. Wang, L.X. Han, W.J. Yuan, J.B. Cheng, A.N. Zhang, H.B. Zhao, Y.Z. Wang, Hierarchically porous SiO2/polyurethane foam composites towards excellent thermal insulating, flame-retardant and smoke-suppressant performances, J. Hazard. Mater. (2019), https://doi.org/10.1016/j.jhazmat.2019.04.065.
[274] F. Stazi, C. Urlietti, C. Di Perna, G. Chiappini, M. Rossi, F. Tittarelli, Thermal and mechanical optimization of nano-foams for sprayed insulation, Constr. Build. Mater. (2019), https://doi.org/10.1016/j.conbuildmat.2018.12.177.
[275] F. Chen, Y. Zhang, J. Liu, X. Wang, P.K. Chu, B. Chu, N. Zhang, Fly ash based lightweight wall materials incorporating expanded perlite/SiO2 aerogel composite: Towards low thermal conductivity, Constr. Build. Mater. (2020), https://doi.org/10.1016/j.conbuildmat.2020.118728.